JAQUELINE NATIELE PEREIRA

DEPOSIÇÃO ATMOSFÉRICA TOTAL EM UMA REGIÃO AGRÍCOLA DO SUL DE MINAS GERAIS: AVALIAÇÃO DA COMPOSIÇÃO QUÍMICA E CONTRIBUIÇÃO DE FONTES

LAVRAS – MG
2022

JAQUELINE NATIELE PEREIRA

DEPOSIÇÃO ATMOSFÉRICA TOTAL EM UMA REGIÃO AGRÍCOLA DO SUL DE MINAS GERAIS: AVALIAÇÃO DA COMPOSIÇÃO QUÍMICA E CONTRIBUIÇÃO DE FONTES

Dissertação apresentada à Universidade Federal de Lavras, como parte das exigências do Programa de Pós-Graduação em Engenharia Ambiental, para obtenção do título de Mestre.

Prof. Dr. Marcelo Vieira da Silva Filho
(Orientador)

LAVRAS – MG
2022

Ficha catalográfica elaborada pelo Sistema de Geração de Ficha Catalográfica da Biblioteca Universitária da UFLA, com dados informados pelo(a) próprio(a) autor(a).

Pereira, Jaqueline Natiele.

Deposição atmosférica total em uma região agrícola do Sul de Minas Gerais : avaliação da composição química e contribuição de fontes / Jaqueline Natiele Pereira. - 2022.

93 p. : il.

Orientador(a): Marcelo Vieira-Filho.

Dissertação (mestrado acadêmico) - Universidade Federal de Lavras, 2022.

Bibliografia.

1. Deposição atmosférica total. 2. Composição química. 3. Contribuição de fontes. I. Vieira-Filho, Marcelo. II. Título.

JAQUELINE NATIELE PEREIRA

DEPOSIÇÃO ATMOSFÉRICA TOTAL EM UMA REGIÃO AGRÍCOLA DO SUL DE MINAS GERAIS: AVALIAÇÃO DA COMPOSIÇÃO QUÍMICA E CONTRIBUIÇÃO DE FONTES

BULK ATMOSPHERIC DEPOSITION IN AN AGRICULTURAL REGION IN THE SOUTH OF MINAS GERAIS: CHEMICAL COMPOSITION AND SOURCE APPORTIONMENT ASSESSMENT

Dissertação apresentada à Universidade Federal de Lavras, como parte das exigências do Programa de Pós-Graduação em Engenharia Ambiental, para obtenção do título de Mestre.

APROVADA em 14 de fevereiro de 2022.

Dr(a). Pamela Alejandra Dominutti USP
Dr(a). Simone Andréa Pozza UNICAMP

Prof. Dr. Marcelo Vieira da Silva Filho
(Orientador)

LAVRAS – MG
2022

Aos meus pais, Zaira e Odilon, e meus irmãos, Gustavo e Júlia,
pelo amor, carinho e compreensão.
Ao meu companheiro, Rafael, por todo incentivo e apoio durante minha jornada.
Dedico.

AGRADECIMENTOS

Em primeiro lugar a Deus, Anjos da Guarda, Universo ou Força Maior por sempre atender às minhas orações e iluminar o meu caminho.

Aos meus pais Odilon e Zaira por todo esforço que fizeram para que eu cumprisse essa árdua, enriquecedora e linda jornada. Também agradeço pelos valores ensinados e por todo amor, carinho, paciência e compreensão.

Aos meus irmãos, Júlia e Gustavo, pelo amor incondicional.

Ao meu namorado Rafael, pelo amor, companheirismo e incentivo.

Aos meus amigos, em especial, Letícia, Thays, Mateus, Gabriela, Marina A. e Lucas por todos os anos de amizade, inclusive os que estive ausente.

Aos meus colegas do laboratório, em especial, Larissa, Marina T. e Vanessa M., pela parceria, conhecimento e momentos de descontração compartilhados.

Ao meu orientador, Marcelo Vieira-Filho, exemplo de professor e sabedoria. Gostaria de agradecer imensamente pelos ensinamentos, conversas, incentivos, paciência e pela amizade. Foi, e continua sendo, um privilégio desenvolver pesquisa científica ao seu lado.

Ao Núcleo de Estudos em Poluição Urbana e Agroindustrial, que tenho enorme carinho e amor. Obrigada por todo conhecimento compartilhado.

Aos professores que me acompanharam durante a pós-graduação por proporcionar enorme conhecimento.

Aos técnicos Isael, Juliana e Rosana pelo profissionalismo e auxílios prestados para que este projeto pudesse ser realizado com qualidade.

À Universidade Federal de Lavras e à Universidade de São Paulo, pela oportunidade para a realização deste trabalho.

À CAPES pelo apoio à Pós-Graduação e concessão de bolsa que permitiu a dedicação exclusiva a este projeto.

Deixo meu agradecimento a todos aqueles que contribuíram direta ou indiretamente para a realização desse trabalho.

Por fim ressalto que o presente trabalho foi realizado com apoio da Coordenação de Aperfeiçoamento de Pessoal de Nível Superior – Brasil (CAPES) – Código de Financiamento 001.

"Em algum lugar, alguma coisa incrível está esperando para ser descoberta." (Carl Sagan)

RESUMO

A deposição atmosférica é um mecanismo chave para a ciclagem de compostos químicos entre os ecossistemas ambientais, uma vez que fornece informações úteis sobre a composição química da atmosfera, rotas reacionais e impactos ambientais, além de informações que alimentam modelos receptores para identificar a distribuição de fontes de poluição atmosférica. Diante dessa perspectiva, esse estudo avaliou a composição química da deposição atmosférica a fim de quantificar sua acidez, seus fluxos e impactos ecológicos e a contribuição de fontes naturais e antropogênicas, no município de Lavras, região Sul de Minas Gerais. Para isso, foi utilizado um coletor de deposição total que foi instalado no *campus* da Universidade Federal de Lavras (UFLA) e ficou exposto ao ar livre para coletas semanais de águas de chuva (deposição úmida) e material particulado (deposição seca). Uma série de 59 amostras foram coletadas no período entre março de 2018 e outubro de 2019, nas quais foram realizadas análises de pH, condutividade elétrica e cromatografia iônica para quantificação dos íons Ca^{2+}, Na^{+}, NH_4^{+}, Mg^{2+}, K^{+}, Cl^{-}, NO_3^{-} e SO_4^{2-}. Para melhor entendimento, os resultados obtidos nesse estudo foram discutidos em três artigos. O primeiro, intitulado *Atmospheric deposition chemistry in a Brazilian rural area: alkaline species behavior and agricultural inputs* mostrou que a maioria das amostras de deposição atmosférica foram alcalinas e que Ca^{2+} foi a espécie dominante, sendo o principal agente neutralizante das espécies ácidas. No segundo artigo, em que foi adotado o modelo EPA PMF 5.0 para investigar a contribuição de fontes para as espécies presentes na deposição atmosférica, foram encontradas três fontes: processos atmosféricos de neutralização, processos crustais e incêndios e produção e aplicação de fertilizantes. Por fim, o terceiro artigo, intitulado *Nitrogen Atmospheric Deposition Driven by Seasonal Processes in a Brazilian Region with Agricultural Background*, contou com a colaboração de pesquisadores do Programa de Pós-Graduação em Recursos Hídricos da UFLA, que forneceram dados de deposição úmida de nitrogênio total kjeldahl, permitindo quantificação dos fluxos de nitrogênio total dissolvido (NTD), nitrogênio orgânico e inorgânico dissolvido (NOD e NID, respectivamente). Esse artigo revelou que o fluxo de NOD foi dominante em relação ao NTD e que o fluxo de NID apresentou potencial de causar acidificação e eutrofização em ecossistemas ambientais. De forma geral, os resultados discutidos nos três artigos fornecem informações críticas para a formulação de políticas que visem à redução das emissões de poluentes na região de Lavras-MG.

Palavras-chave: Deposição Atmosférica Total. Composição Química. Contribuição de Fontes. Impactos Ambientais.

ABSTRACT

Atmospheric deposition is a key mechanism for the chemical compounds cycling between environmental ecosystems, since provides useful information about the atmosphere chemical composition, reaction pathways and environmental impacts, as well as information that feeds receptor models to identify the sources apportionment. Given this perspective, this study evaluated the chemical composition of atmospheric deposition in order to quantify its acidity, its fluxes and ecological impacts and natural and anthropogenic sources contribution, in the Lavras city, Southern Region of Minas Gerais. Bulk atmospheric deposition collector was used, which was installed on the Universidade Federal de Lavras campus (UFLA) and was exposed to open field for weekly collections of rainwater (wet deposition) and particulate matter (dry deposition). A dataset of 59 samples was collected between March 2018 and October 2019, in which we performed pH, electrical conductivity and ion chromatography analyzes to quantify Ca^{2+}, Na^{+}, NH_4^{+}, Mg^{2+}, K^{+}, Cl^{-}, NO_3^{-} e SO_4^{2-}. For better understanding, the results obtained in this study were discussed in three articles. The first one, entitled Atmospheric deposition chemistry in a Brazilian rural area: alkaline species behavior and agricultural inputs, showed that most of atmospheric deposition samples were alkaline, Ca^{2+} was the dominant species and the main neutralizing agent of acidic species. In the second article, we applied the EPA PMF 5.0 model to investigate the sources contribution to the atmospheric deposition species and we found three sources: neutralization atmospheric processes, crustal processes and fires, and fertilizers production and application. The third article, entitled Nitrogen Atmospheric Deposition Driven by Seasonal Processes in a Brazilian Region with Agricultural Background, had the collaboration of researchers from the Programa de Pós-Graduação em Recursos Hídricos at UFLA, who provided data on wet deposition of total kjeldahl nitrogen, allowing quantification of total dissolved nitrogen (TDN), dissolved organic and inorganic nitrogen fluxes (DON and DIN, respectively). This article revealed a dominant DON flux and that DIN flux had the potential to cause acidification and eutrophication in environmental ecosystems. In general, the results presented in the three articles provide critical information for the policies formulation aimed at reducing pollutant emissions in the region of Lavras-MG.

Keywords: Bulk Atmospheric Deposition. Chemical Composition. Source Contribution. Environmental Impacts.

SUMÁRIO

PRIMEIRA PARTE

1. INTRODUÇÃO

A intensificação das atividades humanas no último século, como combustão de combustíveis fósseis, exaustão automobilística e atividades agrícolas, como uso de fertilizantes e criação de animais, têm aumentado cada vez mais as emissões de poluentes atmosféricos. Esses poluentes (aerossóis e gases) podem sofrer reações foto(químicas), ser transportados, diluídos e arrastados por meio dos processos de deposição atmosférica úmida ou seca. Assim, a deposição atmosférica se constitui como uma fonte difusa e uma rota de entrada direta de nutrientes e poluentes para os ecossistemas terrestres e aquáticos (MIGLIAVACCA et al., 2005; SEINFELD; PANDIS, 1998).

Uma compreensão mais aprofundada da química da deposição atmosférica pode fornecer informações sobre a poluição do ar e também ajudar a diferenciar influências naturais e antropogênicas (AKPO et al., 2015). Nessa perspectiva, os métodos estatísticos e matemáticos vêm sendo amplamente utilizados para a interpretação e análise da composição iônica da deposição atmosférica, devido a sua utilidade de identificar fontes potenciais de poluentes (MOLDAN; VESELY; BARTOŇOVÁ, 1987; ZHANG et al., 2014).

As propriedades químicas dos íons solúveis na deposição atmosférica bem como suas fontes têm sido extensivamente investigadas na Ásia, Europa e América do Norte através de redes de monitoramento, como a *Acid Deposition Monitoring Network in East Asia*, *European Monitoring and Evaluation Programme* e *National Atmospheric Deposition Program*, respectivamente (XU et al., 2020). Por outro lado, dados disponíveis para muitos países em desenvolvimento do hemisfério sul, como o Brasil, são escassos ou inexistentes. Ressalta-se que essa ausência de dados empobrece a análise global dos processos químicos, antrópicos e atmosféricos causadores das variações na composição química da deposição atmosférica.

Com base nessa perspectiva, esse estudo pretende avaliar a composição química da deposição atmosférica total na região Sul de Minas Gerais, Brasil, a fim de quantificar sua acidez, seus fluxos e impactos ecológicos e a contribuição de fontes naturais e antropogênicas. Vale a pena mencionar que o Sul de Minas Gerais se constitui como uma importante região econômica, a qual é responsável por 21,8% das commodities agrícolas

(principalmente das regiões produtoras de café) e também responde por cerca de 12% do Produto Interno Bruto do estado (ALMEIDA et al., 2017).

2. REFERENCIAL TEÓRICO

2.1 Composição da Atmosfera Terrestre

A atmosfera da Terra é composta por espécies gasosas e particuladas que podem ser emitidas diretamente de fontes naturais e antropogênicas (origem primária), ou podem ser formadas na atmosfera a partir de transformações físico-químicas (origem secundária) (BRAGA et al., 2005; OLIVEIRA, 2007).

Com relação à fase gasosa, a atmosfera é composta principalmente pelos gases nitrogênio (N_2 = 78,084%), oxigênio (O_2 = 20,946%) e argônio (Ar = 0,934%) cujas abundâncias são controladas em escalas de tempo geológicas pela biosfera, captação e liberação de material crustal e desgaseificação do interior do planeta. Dióxido de carbono (CO_2 ~ 0,035%) e vapor de água ($H_2O_{(v)}$ ~ até 3%) também são constituintes da atmosfera, cujas concentrações são variáveis. Destaca-se que a quantidade de vapor d'água é controlada por processos de evaporação e precipitação (LENZI; FAVERO, 2019).

Também existem na atmosfera os gases-traço, em geral na ordem de partes por milhão e partes por bilhão, que correspondem a menos de 1% da massa total atmosférica. Dentre eles podem ser citados por exemplo compostos inorgânicos como monóxido de carbono (CO), óxidos de nitrogênio (NO_x), amônia gasosa (NH_3), sulfeto de hidrogênio (H_2S), dióxido de enxofre (SO_2), e compostos orgânicos como alcanos, alcenos, arilas, carbonilas, nitratos orgânicos, entre outros. Esses gases residuais têm a abundância controlada por processos biogênicos, reações fotoquímicas, atividades vulcânicas e descargas elétricas e desempenham um papel crucial nas propriedades químicas da atmosfera (LENZI; FAVERO, 2019).

Além da fase gasosa, na atmosfera também se encontram os aerossóis, que são particulados sólidos e/ou líquidos, que se apresentam dispersos na atmosfera com dimensões variando de 100 μm a 0,002 μm. Os aerossóis são classificados quanto a seu diâmetro aerodinâmico, em que partículas grossas compreendem aquelas com diâmetro aerodinâmico maior que 2,5 μm e as partículas finas apresentam diâmetro aerodinâmico menor que 2,5 μm. Destaca-se que entre estes particulados encontram-se corpos abióticos inorgânicos e

orgânicos (poeira atmosférica contendo alumínio e cálcio, spray marinho contendo sódio e cloreto, emissões de incêndios espontâneos contendo particulados policíclicos orgânicos) e os bioaerossois que são corpos bióticos (pólen, bactérias, vírus, entre outros) (TRIADÓ-MARGARIT et al., 2019; WALLACE; HOBBS, 2005).

Destaca-se que aproximadamente 85 a 90% de toda a massa atmosférica encontra-se na troposfera, que é camada mais próxima da superfície da Terra, se estendendo do nível do mar, 0 km, a 16-20 km de altitude. Essa camada é uma região de turbulência incessante e mistura, onde acontecem os fenômenos atmosféricos. No topo da troposfera encontra-se a tropopausa, caracterizada pela baixa temperatura (–56^{o}C), que serve de barreira para quase a totalidade dos constituintes atmosféricos e principalmente para o vapor d'água, o qual se condensa e solidifica, não alcançando, portanto, altitudes maiores (SEINFELD; PANDIS, 1998).

É importante mencionar que, nas últimas décadas, o esforço das populações em crescimento em garantir alimentos e energia e ao mesmo tempo estimular o desenvolvimento econômico, levou a um aumento nas emissões desses gases e partículas. Assim, a entrada em excesso desses compostos na atmosfera têm modificado sua composição química e causado poluição, uma vez que esses compostos se acumulam em concentrações suficientemente altas para causar danos à saúde pública e aos ecossistemas (FOWLER et al., 2009; MONKS et al., 2009).

2.1.1 Compostos de Enxofre

O elemento enxofre (S) pode ser encontrado em rochas vulcânicas da crosta terrestre, em minerais como a pirita (FeS_2) e também nos seres vivos, onde pode estar na forma iônica e como éster, aminoácidos, proteínas, coenzimas e vitaminas (BRAGA et al., 2005).

Dentre os processos que liberam $SO_{2(g)}$ para a atmosfera se encontram a atividade vulcânica e todos os processos de combustão que utilizam tanto matéria orgânica de biomassa (lenha, carvão vegetal) quanto material fóssil (petróleo, carvão de pedra), seja de forma controlada (fornos, aquecimento industrial, aquecimento domiciliar, combustão interna de veículos) ou de forma descontrolada (incêndios) (ZHONG et al., 2020).

Além da liberação direta, o SO_2 também pode ser formado na atmosfera por meio de reações fotoquímicas envolvendo o ácido sulfídrico (H_2S). O H_2S pode ser liberado para atmosfera a partir de processos em refinarias de petróleo, por meio da mineralização da

matéria orgânica (processo que também libera SO_4^{2-}), e também pode ser produzido na própria atmosfera pela oxidação do sulfeto de carbono (CS_2). O $H_2S_{(g)}$ ao entrar na troposfera reage com o radical hidroxila ($HO^{\bullet}_{(g)}$) produzindo o $SO_{2(g)}$ (AGUILAR-DODIER et al., 2020).

Na troposfera o $SO_{2(g)}$ reage por meio de processos de fase gasosa e aquosa e também é removido fisicamente por deposição seca e úmida. Nessa perspectiva, o SO_2 pode reagir com a água formando ácido sulfuroso (R-1), que por sua vez pode reagir com amônia (R-2), óxidos de cálcio (R-3) ou com agente oxidantes como ozônio (R-4) e peróxido de hidrogênio (R-5) levando à formação de sulfato (SO_4^{2-}) (EATOUGH; CAKA; FARBER, 1994).

$$SO_2 + H_2O \leftrightarrow H_2SO_{3\,(part)} \text{ (R-1)}$$

$$H_2SO_{3(aq)} + 2NH_{3(g)} \leftrightarrow (NH_4)_2SO_{3\,(part)} \text{ (R-2)}$$

$$H_2SO_{3(aq)} + CaO_{(part)} \leftrightarrow CaSO_{3\,(s)} + H_2O_{\,liq} \text{(R-3)}$$

$$H_2SO_{3(aq)} + O_{3(g)} \leftrightarrow SO_{4\,(aq)}^{2-} + 2H^+_{(aq)} + O_{2(g)} \text{ (R-4)}$$

$$H_2SO_{3(aq)} + H_2O_{\,2(g)} \leftrightarrow SO_{4\,(aq)}^{2-} + 2H^+_{(aq)} + H_2O_{\,liq} \text{ (R-5)}$$

Com relação à reação em fase gasosa, a reação com o radical $OH^{\bullet}_{(g)}$ é dominante, levando à formação de ácido sulfúrico (R-6 a R-9) (EATOUGH; CAKA; FARBER, 1994).

$$SO_{2(g)} + HO^{\cdot}_{(g)} \rightarrow HSO^{\cdot}_{3\,(g)} \text{ (R-6)}$$

$$HSO^{\cdot}_{3\,(g)} + O_{2(g)} \rightarrow HSO^{\cdot}_{5\,(g)} \text{ (R-7)}$$

$$HSO^{\cdot}_{5\,(g)} \rightarrow HOO^{\cdot}_{(g)} + SO_{3(g)} \text{ (R-8)}$$

$$SO_{3(g)} + H_2O_{(g)} \rightarrow H_2SO_{4(part)} \text{ (R-9)}$$

É importante observar que, a partir das reações, são formados na atmosfera o ácido sulfuroso e quase sempre o ácido sulfúrico.

Atualmente, a emissão global de SO_2, desconsiderando emissões vulcânicas, foi estimada em 105,4 $Tg.ano^{-1}$, com uma contribuição predominante de fontes antropogênicas (98%), das quais 43% corresponde a usinas de energia, 35% a fontes industriais e 16% a transporte marítimo (ZHONG et al., 2020). Com relação ao Brasil, Zhong et al. (2020) estimaram que as principais emissões são provenientes de fontes industriais e da queima de biomassa a céu aberto. Nesse sentido, Kawashima et al. (2020) encontraram que no Brasil, as emissões de

fontes industriais foram de 1,51 $Tg.ano^{-1}$, e, segundo Ren et al. (2021a), as emissões de queima de biomassa, incluindo incêndios florestais e agrícolas, corresponderam a 0,35 $Tg.ano^{-1}$. Ressalta-se que as emissões de fontes veiculares foram insignificantes (0,005 $Tg.ano^{-1}$) (KAWASHIMA et al., 2020).

2.1.2 Compostos de Nitrogênio

Dentre os principais compostos inorgânicos nitrogenados que são liberados para a atmosfera, seja de forma natural ou devido à ação antrópica, encontram-se o N_2, N_2O, NH_3 e NO_x.

A concentração de $N_2O_{(g)}$ atmosférico aumentou em mais de 20%, de 270 ppb em 1750 para 331 ppb em 2018, com o crescimento mais rápido observado nas últimas cinco décadas (PRINN et al., 2018). A liberação de $N_2O_{(g)}$ para a atmosfera, naturalmente, é controlada pelos processos bioquímicos de nitrificação e desnitrificação dos ecossistemas oceânicos e dos solos de regiões tropicais. Durante a oxidação do NH_4^+ em NO_3^- em ambiente anaeróbio e durante a redução do NO_3^- a $N_{2(g)}$ em ambiente aeróbio, ocorre a formação do $N_2O_{(g)}$ como um subproduto (BAIRD; CANN, 2011). Destaca-se que esses processos bioquímicos são regulados por fatores como a temperatura, níveis de água e oxigênio, acidez, disponibilidade de substrato (uso de fertilizantes nitrogenados e resíduos animais) e reciclagem. Nesse sentido, as emissões antropogênicas globais de $N_2O_{(g)}$ são principalmente devido à adição de nitrogênio às plantações, atividade que aumentou em 30% as emissões de $N_2O_{(g)}$ nas últimas quatro décadas e, estão associadas especialmente às economias emergentes como Brasil, China e Índia (TIAN et al., 2020).

A $NH_{3(g)}$ é o gás alcalino predominante na atmosfera e ativamente envolvido na química atmosférica. As fontes naturais de $NH_{3(g)}$ têm sido associadas a processos de volatilização a partir dos solos e oceanos (ZENG; TIAN; PAN, 2018). Como exemplo, a fixação do nitrogênio pelos microrganismos que vivem em simbiose com algumas espécies de leguminosas no solo ou a mineralização do nitrogênio orgânico em NH_4^+, em ecossistemas terrestres ou marinhos com condições alcalinas (LENZI; FAVERO, 2019).

A agricultura é geralmente aceita como a maior fonte antropogênica de emissões de NH_3, incluindo perdas de fertilizantes nitrogenados e volatilização de dejetos animais (ANEJA et al., 2020). Com relação às perdas de fertilizantes aplicados no solo, aqueles que contêm NH_4^+ (soluções amoniacais, sulfato de amônio, nitrato de amônio e fosfatos de amônio), em um

ambiente alcalino e temperatura adequada (25-35^{o}C), podem liberar $NH_{3(g)}$ para a atmosfera. Fertilizantes como a ureia também levam à volatilização da $NH_{3(g),}$ visto que, quando aplicada ao solo forma carbonato de amônio, composto que, dependendo das condições do solo, pode provocar a perda de nitrogênio na forma de $NH_{3(g)}$ ou na forma de $N_{2(g)}$ (LENZI; FAVERO, 2019).

Outras fontes antropogênicas incluem atividades industriais. Um processo industrial importante, no que tange às fontes de $NH_{3(g)}$, é a produção de amônia sintética e a produção de fertilizantes a partir da síntese de $NH_{3(g)}$ por meio do processo de Claude[1]. Além disso, a produção de cal e cimento também propicia a volatilização de $NH_{3(g)}$ quando são aplicadas técnicas de remoção de NO_x aplicando reagentes como NH_3 ou ureia nos fornos (MENG et al., 2017). Dentre as técnicas mais adequadas podem ser citadas a Redução Seletiva Não Catalítica e Redução Seletiva Catalítica, nas quais fatores como alta redução de NO_x, temperatura inadequada e injeção imprecisa do reagente causam volatilização de $NH_{3(g)}$ (HAKKARAINEN, 2014).

Também é importante mencionar que os sistemas de exaustão de veículos podem atuar como uma fonte direta de $NH_{3(g)}$ em áreas urbanas, principalmente como um produto indesejável de redução de NO na superfície do conversor catalítico de três vias, de veículos leves. Nesse processo, a $NH_{3(g)}$ é formada a partir da degradação de hidrocarbonetos, ou via reação do NO com H_2 a partir de uma reação heterogênea entre o CO e vapor d'água (VIEIRA-FILHO et al., 2016).

Com relação aos óxidos de nitrogênio ($NO_x = NO + NO_2$), são gases quimicamente ativos que desempenham um papel crítico na regulação do equilíbrio oxidante da troposfera. Suas fontes mais importantes são a combustão de combustíveis fósseis (eletricidade e transporte), queima de biomassa e emissões de solos de ecossistemas terrestres (TIAN et al., 2020).

Durante um processo de combustão, que ocorre na presença de ar contendo 78% de N_2 e 21% de O_2 e na presença de um corpo catalisador como as paredes do forno ou do cilindro de um motor veicular, inicialmente ocorre dissociação das moléculas de N_2 e O_2 e em seguida ocorre a síntese do NO_x (LENZI; FAVERO, 2019).

Em solos, o NO_x resulta do balanço líquido de processos microbianos de nitrificação e desnitrificação e processos abióticos de quimiodesnitrificação (redução do NO_3^- no solo sob condições de elevada acidez (pH < 5,0)), os quais são controlados por fatores do solo como

[1]Processo em que há combinação de hidrogênio (H_2) com oxigênio (N_2), sob alta pressão na presença de um catalizador, para formar NH_3.

disponibilidade de nitrogênio e carbono, umidade, temperatura, pH e práticas de gestão (MOLINA-HERRERA et al., 2017; VELDKAMP; KELLER, 1997). Assim, é importante mencionar que as emissões biogênicas de NO_x aumentam quando fertilizantes nitrogenados são aplicados ao solo (ALMARAZ et al., 2018).

Desde a revolução industrial, tem sido assumido que a queima de combustíveis fósseis dominam as crescentes emissões de NO_x (SONG et al., 2021). No entanto, como as fontes de combustão são geralmente localizadas nos grandes centros urbanos, a emissão proveniente do solo é significativa especialmente nas áreas rurais do mundo ocidental, durante os períodos de primavera e verão, onde há um alto uso de fertilizantes inorgânicos em solos de ecossistemas agrícolas (MOLINA-HERRERA et al., 2017; SHEPHERD; BARZETTI; HASTIE, 1991).

As estimativas globais mais recentes das emissões de NH_3 e NO_x estão compiladas no inventário *Emissions Database for Global Atmospheric Research (EDGAR v5.0 air pollutants*, https://edgar.jrc.ec.europa.eu/overview.php?v=50_AP). Segundo o inventário, a estimativa global de emissão de NH_3 é de 49,0 $Tg.ano^{-1}$, dos quais 54% correspondem a emissões do solo, especialmente solos agrícolas, e 23% são provenientes do processamento de estrume animal. O Brasil é o quarto país que mais emite NH_3 no mundo (2,97 $Tg.ano^{-1}$) e a distribuição de fontes é semelhante ao padrão mundial (63% de emissões do solo e 18% de emissões do processamento de estrume). Com relação ao NO_x, a estimativa global de emissão é de 124 $Tg.ano^{-1}$ e são oriundas principalmente do transporte rodoviário (27%), produção de energia (25%) e indústrias de transformação e construção (17%). No Brasil, a emissão de NO_x é de cerca de 4,10 $Tg.ano^{-1}$ e o padrão de distribuição de fontes difere do padrão mundial, uma vez que o transporte rodoviário é a principal fonte (42%) seguido pelas indústrias de transformação e construção (21%), queima de biomassa (11%), produção de energia (10%) e emissões do solo (5%).

Uma vez na atmosfera, o N_2 é extremamente estável quimicamente e não está envolvido na química da troposfera ou estratosfera. Comportamento semelhante é observado para o N_2O, o qual é inerte na troposfera e seu principal sumidouro atmosférico é a fotodissociação na estratosfera (cerca de 90%) (SEINFELD; PANDIS, 1998). Em contrapartida, o óxido nítrico (NO) é um gás quimicamente ativo de vida curta e um componente chave na fotoquímica da troposfera. Nesse sentido, pode reagir com compostos oxidantes, como

ozônio, radical hidroperoxilo, radical hidroxilo, entre outros, levando à formação do ácido nítrico (Figura 1) (LENZI; FAVERO, 2019).

Figura 1. Possíveis reações do NO_x na atmosfera

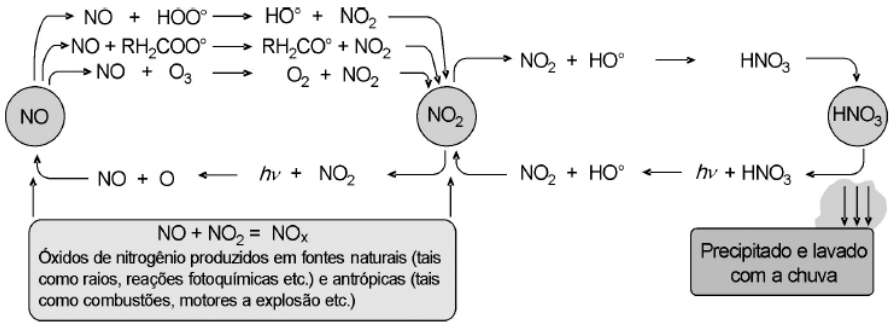

Fonte: Adaptado de Lenzi e Favero (2019)

A amônia é o gás básico primário na atmosfera e, devido à essa propriedade alcalina, as reações com os ácidos e óxidos de caráter ácido na troposfera geram sais de amônio. Como exemplo, pode reagir com o HNO3 (R-10) ou com o H2SO4 (R-11), formando compostos particulados (CHEN; ZHAO; ZHANG, 2018).

$$NH_{3(g\ ou\ aq)} + HNO_{3(part)} \leftrightarrow NH_4NO_{3(part)} \text{ (R-10)}$$

$$2NH_{3(g\ ou\ aq)} + H_2SO_{4(part)} \leftrightarrow (NH_4)_2SO_{4(part)} \text{ (R-11)}$$

Além de reações que levam à formação de sais de amônio, a NH3 pode reagir com o radical hidroxila formando o radical H2N•(g) (R-12). Esse por sua vez pode reagir com gases componentes da troposfera, como O2 (R-13), formando compostos ácidos e mais radicais livres.

$$2NH_{3(g\ ou\ aq)} + HO^{\cdot}_{(g)} \leftrightarrow H_2N^{\cdot} + H_2O_{(v)} \text{ (R-12)}$$

$$H_2N^{\cdot} + O_{2(g)} \leftrightarrow HO^{\cdot} + HNO \text{ (R-13)}$$

2.1.3 Compostos Particulados (Aerossóis)

Conforme visto anteriormente, os aerossóis são caracterizados devido ao seu tamanho, assim, a distinção entre as partículas de acordo com seu diâmetro é fundamental para

compreender suas origens, características químicas, rotas reacionais e seus processos de remoção (ZHANG et al., 2017).

As partículas grossas têm velocidades de sedimentação suficientemente grandes, se fixando na atmosfera em um tempo razoavelmente curto, e são geralmente produzidas por processos mecânicos. Dentre eles podem ser citados a ruptura de bolhas do oceano e a rebentação das ondas do mar que levam à atmosfera partículas de água líquida que contêm sais dissolvidos (Cl^-, Na^+, SO_4^{2-}, Mg^{2+}, Ca^{2+}, K^+, HCO_3^-) (COCHRAN et al., 2017), emissão de cinza vulcânica contendo SiO_2, Al_2O_3, FeO, MgO, CaO, Na_2O, K_2O (VOGEL et al., 2017), ressuspensão de partículas do solo contendo Ca^{2+}, Mg^{2+}, CO_3^{2-} (GONÇALVES et al., 2017; KARANASIOU et al., 2011; UPADHYAY et al., 2015) e a dispersão de pólens das flores das plantas, esporos de fungos e bactérias.

A emissão de partículas grossas também pode ser atribuída às atividades humanas, como a emissão de partículas de Ca, Al e Fe oriundos da indústria de processamento de pedra; emissão de partículas contendo Ca, SO_4^{2-} e K^+ provenientes da produção de cimento; emissão de partículas de Al, K e Mg da indústria de cerâmica; poeiras de construção que emitem partículas de Fe, Al e NO_3^-; poeiras de terras agrícolas que levam para a atmosfera partículas de Fe, Al, SO_4^{2-} e NH_4^+; e ressuspensão de poeiras de estradas contendo Al, Fe e Zn (LI et al., 2013).

Embora a maior parte das partículas grossas sejam primárias, existem alguns sulfatos e nitratos secundários, os quais são formados na atmosfera a partir da reação dos compostos HNO_3, SO_2 ou H_2SO_4 com NaCl em aerossóis de sal marinho (R-14 e R-15), ou com carbonatos aquosos, como $CaCO_3$ e $MgCO_3$, dissolvidos em partículas grosseiras de solo (R-16 e R-17) (PÉREZ et al., 2016; ZHUANG et al., 1999).

$$HNO_{3(aq)} + NaCl_{(aq,s)} \rightarrow NaNO_{3(aq,s)} + HCl_{(g)} \text{ (R-14)}$$

$$H_2SO_{4(aq)} + 2NaCl_{(aq,s)} \rightarrow Na_2SO_{4(aq,s)} + 2HCl_{(g)} \text{ (R-15)}$$

$$2HNO_{3(g)} + CaCO_{3(s)} \rightarrow Ca(NO_3)_{2(s)} + H_2O + CO_{2(g)} \text{ (R-16)}$$

$$H_2SO_{4(aq,g)} + CaCO_{3(s)} \rightarrow CaSO_{4(s)} + H_2O + CO_{2(g)} \text{ (R-17)}$$

As partículas finas possuem maior tempo de residência na atmosfera, e são uma mistura de emissões primárias e de material secundário formado por mecanismos de conversão de gás em partículas.

Dentre as emissões primárias destacam-se a queima de biomassa e os incêndios florestais que emitem para atmosfera partículas ricas em K^+, SO_4^{2-}, Cl^- e compostos orgânicos (PIO et al., 2008; REN et al., 2021b; YAMASOE et al., 2000), tráfego rodoviário e marítimo que emitem particulados contendo carbono orgânico, carbono negro (*black carbon*), SO_4^{2-} e Na^+ (ALLEN et al., 2001; AMIL et al., 2016; VIEIRA-FILHO; PEDROTTI; FORNARO, 2013), e combustão nas indústrias de energia e manufatura que emitem partículas contendo Pb, Cd, Cr, Ni, Ti, entre outras (CAGGIANO; MACCHIATO; TRIPPETTA, 2010).

Com relação às partículas finas secundárias, são formadas na atmosfera por meio de transformações químicas de precursores gasosos, como SO_2, NO_x e NH_3 (SU et al., 2021). O SO_2 pode adsorver a umidade do ambiente e reagir formando o ácido sulfuroso, o qual absorve mais água formando fumaças esbranquiçadas visíveis (R-1), ou o $SO_{2(g)}$ pode ser oxidado a $SO_{3(g)}$, o qual reage com a água formando o ácido sulfúrico H_2SO_4 aquoso ou particulado (R-6 a R-9). O $NO_{(g)}$, pode ser oxidado a $NO_{2(g)}$, que na presença do radical $HO^{\bullet}$ forma o ácido nítrico, HNO_3 (Reações da figura 1). Além disso, o HNO_3 também pode ser formado a partir da hidrólise do N_2O_5. Tanto o ácido sulfúrico quanto o ácido nítrico formados na atmosfera podem reagir com outros particulados ou serem neutralizados pela NH_3, único precursor de NH_4^+, formando partículas de NO_3^-, NH_4^+ e SO_4^{2-} conforme reações R-10 e R-11.

Um resumo dos principais compostos presentes nos aerossóis e suas respectivas fontes pode ser observado na tabela 1.

Tabela 1. Composição Química dos Aerossóis

	Partículas Finas	Partículas Grossas
Vias de Formação	Reações químicas, Nucleação, Condensação Coagulação, Processamento em nuvem / nevoeiro	Interrupção mecânica, Suspensão de poeira
Composição	Sulfato	Poeira ressuspensa
	Nitrato	Cinzas volantes de carvão e óleo
	Amônio	Elemento crustal (Si, Al, Ti,
	Íon hidrogênio	Fe)
	Carbono elementar (CE)	$CaCO_3$, NaCl
	Compostos orgânicos	Pólen, mofo, esporos

Fonte	Água	Planta, restos de animais
	Metais (Pb, Cd, V, Ni, Cu, Zn, Mn, Fe, etc.)	Resíduos de desgaste de pneus
	Combustão (carvão, petróleo, gasolina, diesel, madeira)	Ressuspensão de poeira e solo industrial
	Conversão gás-partícula de NO_x, SO_3 e COVs	Suspensão do solo (agricultura, mineração, estradas não pavimentadas)
	Fundições, moinhos, etc.	Fontes biológicas, Construção, Spray oceânico

Fonte: Adaptado de Seinfeld e Pandis (1998)

As emissões globais totais anuais de partículas grossas e finas foram estimadas no estudo desenvolvido por Huang et al. (2014) para o ano base de 2007, e apresentaram valores de 99,0 e 78,0 $Tg.ano^{-1}$, respectivamente. No total, a queima de biomassa, incluindo incêndios florestais, combustíveis residenciais e resíduos agrícolas, foi responsável por 60% das partículas grossas e 68% das partículas finas, enquanto a geração de energia contribuiu com 10 e 6% das partículas grossas e finas, respectivamente. Destaca-se que as emissões oriundas dos veículos motorizados foram insignificantes (0,8 e 1,4%). Além disso, esse mesmo estudo estimou que a emissão de partículas finas no Brasil foi em torno de 0,81 $Tg.ano^{-1}$, dos quais 57% foram provenientes de áreas rurais (HUANG et al., 2014).

2.2 Processos de Remoção de Poluentes Atmosféricos

Os poluentes (aerossóis e gases) caracterizam-se por sua fonte, mecanismos de transporte, e suas variações, reações químicas, interações e seus sumidouros. Ressalta-se que qualquer aerossol ou gás-traço presente na atmosfera será arrastado para a superfície pelos processos de deposição total (somatório das deposições úmida e seca) (Figura 2), visto que a perda de poluentes para a estratosfera é praticamente desprezível em comparação ao total encontrado na troposfera (TOSITTI et al., 2018; VIEIRA-FILHO, 2011).

Figura 2. Processos que envolvem os poluentes atmosféricos

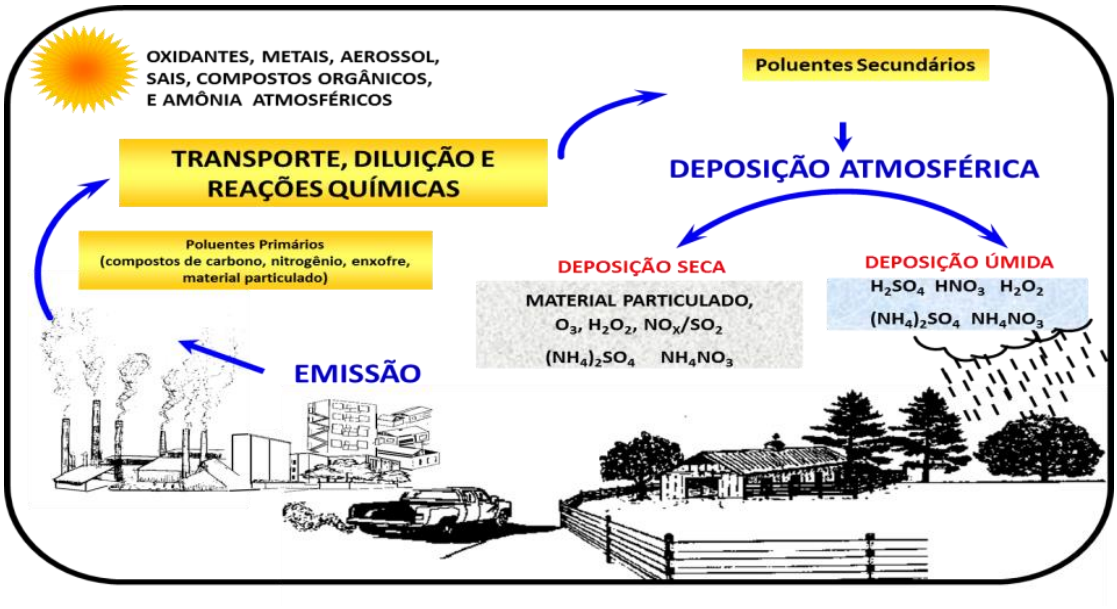

Fonte: Adaptado de Fornaro (2006)

2.2.1 Deposição Úmida

A deposição úmida pode ser definida como o processo natural em que ocorre eliminação de aerossóis e gases pelos hidrometeoros atmosféricos (gotas de nuvens e nevoeiro, chuva, neve) e, consequentemente, deposição na superfície da Terra (SEINFELD; PANDIS, 1998). Essa remoção úmida é o resultado de muitos processos individuais, envolvendo remoção dentro da nuvem (*in-cloud scavenging*) e abaixo da nuvem (*below-cloud scavenging*) (Figura 3).

Figura 3. Modelo do processo de deposição úmida

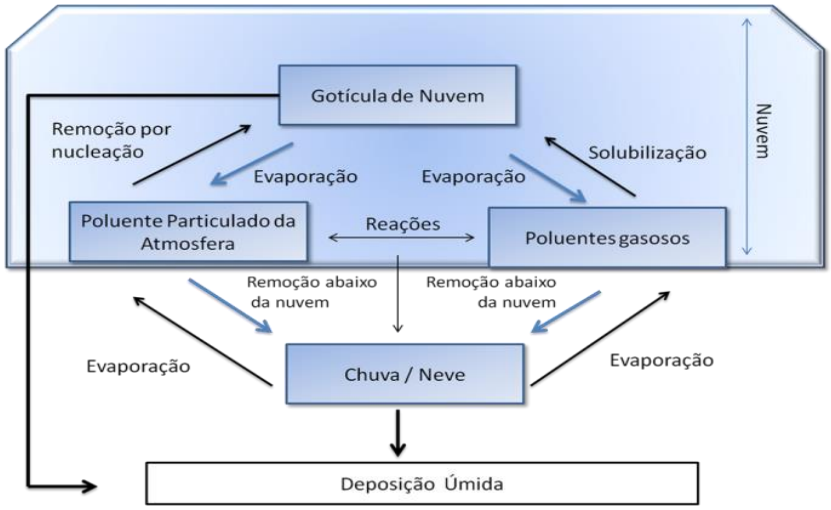

Fonte: Adaptado de Seinfeld e Pandis (1998)

No processo de remoção dentro da nuvem as espécies (gás ou aerossol) são levadas à presença de água condensada e são eliminadas pelos hidrometeoros (CHATTERJEE et al., 2010). Para os aerossóis, primeiro ocorre a remoção por nucleação, em que uma fração da população de aerossóis, que servem como núcleos de condensação de nuvens (NCC), tornam-se ativados e crescem livremente por difusão de vapor d'água, formando gotículas de névoa ou nuvem de 10 μm ou mais de diâmetro, em uma dada supersaturação (WALLACE; HOBBS, 2005). Destaca-se que a capacidade de uma partícula servir como NCC depende de seu tamanho, composição química e supersaturação local. Por exemplo, partículas maiores que 0,5 μm possuem maiores eficiências de remoção por nucleação em comparação com as partículas mais finas (MUKHERJEE et al., 2021). A fração dos aerossóis restantes, permanece como partículas intersticiais e podem ser removidas ao colidirem com as gotículas de nuvem (CELLE-JEANTON et al., 2009). É importante mencionar que essa coleta de aerossol intersticial por gotículas de nuvem é um processo lento e elimina uma fração insignificante da massa do aerossol intersticial (SEINFELD; PANDIS, 1998).

Com relação aos gases, compostos como HNO_3, NH_3 e SO_2 podem ser removidos por solubilização nas gotas de nuvem. De acordo com a Lei de Henry, o equilíbrio da espécie *A* entre a fase gasosa e aquosa pode ser representada por $A_{(g)} \leftrightarrow A_{(aq)}$, e o equilíbrio entre *A* gasoso e dissolvido é geralmente expresso pelo chamado coeficiente da Lei de Henry (H_A) dada a equação 1.

$$[A_{(aq)}] = H_A p_A \quad (1)$$

Em que p_A é a pressão parcial de A na fase gasosa (atm) e [A (aq)] é a concentração da fase aquosa de *A* (molL^{-1}) em equilíbrio com *pA*. O coeficiente da lei de Henry H_A é dado em molL^{-1}atm^{-1}, indicando que quanto maior o coeficiente da Lei de Henry, maior a solubilidade do gás. Além disso, a concentração da fase aquosa de *A* não depende da quantidade de água líquida disponível ou do tamanho da gota. Também cabe mencionar que o coeficiente da Lei de Henry geralmente aumenta conforme a temperatura diminui, refletindo uma maior solubilidade do gás em temperaturas mais baixas (SANDER, 2015; SEINFELD; PANDIS, 1998).

A tabela 2 fornece os valores dos coeficientes de Henry para alguns compostos gasosos em água liquida a 298K. Dentre as espécies apresentadas na tabela 2, destaca-se como gás mais solúvel o HNO_3, seguido de gases menos solúveis como SO_2 e NH_3. Para O_3, NO, NO_2

e os hidrocarbonetos, menos de 1% de sua massa é dissolvido na fase aquosa dentro de uma nuvem, portanto são considerados relativamente insolúveis para aplicações atmosféricas. Destaca-se que para gases menos solúveis como SO_2 e NH_3, a absorção é uma função complexa não apenas das propriedades das espécies, mas também de outras espécies que podem participar de reações de fase aquosa ou controlar o pH da gota de nuvem (DE SOUZA et al., 2017).

Tabela 2. Coeficiente da Lei de Henry (solubilidade dos gases).

Espécie	H_A ($molL^{-1}$ atm^{-1}) at 298 K
NO	1.9×10^{-3}
NO_2	1.0×10^{-2}
O_3	1.1×10^{-2}
H_2S	1.0×10^{-1}
HCl	1.1×10^{0}
SO_2	1.2×10^{0}
NH_3	6.2×10^{1}
HNO_3	2.1×10^{5}

Fonte: Adaptada de Seinfeld e Pandis (1998)

Após a remoção dentro da nuvem, pode ocorrer a remoção abaixo da nuvem (*below-cloud scavenging*) durante a precipitação. Uma nuvem gera precipitação quando algumas gotas crescem até um tamanho precipitável, em torno de 1 mm, por meio de mecanismos como condensação de mais vapor d'água e coalescência de gotículas. Esse último se refere ao processo em que gotículas maiores caem mais rápido que gotículas menores, resultando nas gotas maiores ultrapassando as gotas menores, colidindo e coalescendo com elas. Quando ocorre a precipitação, as gotas de chuva colidem com partículas transportadas pelo ar e as coleta (ANDRONACHE, 2003). Além disso, espécies gasosas solúveis que existem abaixo das nuvens se dissolvem nas gotas de chuva e são removidos da atmosfera. Destaca-se que a eficiência de eliminação dos compostos gasosos depende do diâmetro da gota de chuva, uma vez que gotas pequenas caem mais lentamente e portanto são eficientes na eliminação de gases solúveis, enquanto que a eficiência de eliminação das partículas também depende do tamanho da partícula e de sua localização relativa à localização da gota de chuva (CELLE-JEANTON et al., 2009).

É importante mencionar que os compostos gasosos e particulados podem sofrer transformações químicas durante cada uma das etapas de remoção. Reações em fase aquosa podem ocorrer dentro de uma gotícula de água suspensa na atmosfera (Figura 4), geralmente resultando em uma aceleração do processo de eliminação. Além disso, quase todos os processos são reversíveis. Como exemplo, essas gotículas de água suspensas na atmosfera podem evaporar quando passam por um ambiente subsaturado, produzindo novos aerossóis (Figura 3). Nessa perspectiva, cabe mencionar que nuvens se formam e evaporam repetidamente, de forma que apenas cerca de 10% das nuvens geram precipitação, e mesmo nos casos em que ocorre precipitação, as gotas de chuva geralmente evaporam ao cair no ar (LENZI; FAVERO, 2019; SEINFELD; PANDIS, 1998). Dessa forma, nota-se que as vias de remoção úmida dependem de processos múltiplos e compostos, envolvem várias fases físicas e são influenciadas por fenômenos em uma variedade de escalas físicas, tornando a deposição úmida um dos processos atmosféricos mais complexos.

Figura 4. Representação de algumas reações em fase aquosa que ocorrem dentro de uma gotícula de água suspensa na atmosfera

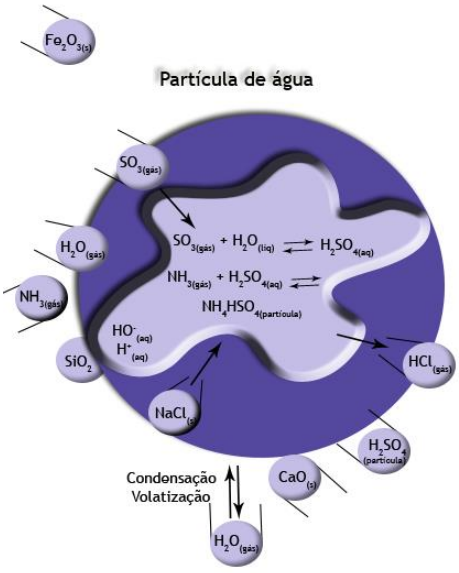

Fonte: Adaptada de Lenzi e Favero (2019)

2.2.2 Deposição Seca

A deposição seca é o transporte de espécies gasosas e particuladas da atmosfera para as superfícies na ausência de precipitação. É influenciada principalmente pelo nível de

turbulência atmosférica, pelas propriedades químicas das espécies depositantes e pela natureza da própria superfície (WESELY; HICKS, 2000). O primeiro rege a taxa na qual as espécies são depositadas à superfície, especialmente na camada mais próxima do solo. Com relação à propriedade química das espécies, destaca-se que absorção e captura pela superfície é determinada pela solubilidade e a reatividade química dos gases e pelo tamanho, densidade e forma das partículas, respectivamente. Além disso, superfícies não reativas podem impedir a absorção ou adsorção de certos gases, superfícies lisas podem levar ao retorno das partículas para a atmosfera e superfícies naturais, como vegetação, geralmente promovem a deposição seca (SEINFELD; PANDIS, 1998).

O processo de deposição seca de gases e partículas consiste de três etapas (MOHAN, 2016):

1. Transporte aerodinâmico de gases e partículas através da camada superficial atmosférica até uma camada muito fina de ar estagnado (subcamada quase laminar), adjacente à superfície;
2. Transporte molecular (para gases) ou browniano (para partículas) através da subcamada quase laminar, para a própria superfície;
3. Captação na superfície.

Cabe mencionar que partículas maiores também podem ser depositadas por sedimentação tanto na etapa 1 quanto na etapa 2. Com relação à captação, é influenciada pela umidade da superfície e por sua viscosidade. Por exemplo, para gases moderadamente solúveis, como SO_2 e O_3, a presença de umidade na superfície irá determinar se o gás será realmente removido, enquanto para gases altamente solúveis e quimicamente reativos, como o HNO_3, a deposição é rápida e irreversível em qualquer superfície. Além disso, partículas sólidas podem ricochetear em uma superfície lisa e as partículas líquidas têm maior probabilidade de aderir ao contato (SEINFELD; PANDIS, 1998).

2.2.3 Deposição Total

A deposição total é definida como a contribuição conjunta das deposições úmida (precipitação) e seca (gases e partículas), podendo ser obtida pela soma dessas duas parcelas individualmente ou pelo intermédio do uso de um coletor de deposição total (DE SOUZA et al., 2017). Esse tipo de coletor permanece continuamente aberto durante eventos chuvosos e períodos secos, e portanto, coleta a contribuição conjunta da deposição seca e úmida, não

permitindo a diferenciação entre ambas as frações. Além disso, os coletores de deposição total são susceptíveis à evaporação de água e de componentes voláteis da amostra, particularmente sob condições de temperaturas elevadas ou longos períodos de exposição, o que torna a análise da deposição atmosférica total uma tarefa bastante complexa e desafiadora. No entanto, esse coletor tem sido usado como um substituto ao coletor automático de deposição úmida (*wet-only*), visto que não requer uma fonte de energia elétrica, permitindo uma operação estável a longo prazo, além de ser mais econômico (IMAMURA et al., 2018). Também vale a pena mencionar que estudos que avaliaram a usabilidade de um coletor total em comparação com um coletor somente úmido verificaram por meio de testes estatísticos que a quantidade de precipitação coletada por ambos os coletores não foi significativamente diferente ($p<0,05$) (CHANTARA; CHUNSUK, 2008).

2.2.4 Composição Química do Produto da Deposição Atmosférica

Dentre as espécies que são eliminadas da atmosfera pelos processos de deposição úmida e seca, podem ser encontradas frações solúveis e insolúveis de espécies inorgânicas e orgânicas. A concentração da fração solúvel é comumente obtida por meio de análises de cromatografia iônica que permitem a quantificação de íons como SO_4^{2-}, NO_3^-, Cl^-, Na^+, K^+, Mg^{2+}, Ca^{2+}, NH_4^+, acetato, formiato, oxalato, entre outros. Com relação à fração insolúvel, é possível obter as concentrações de elementos como Al, Ba, Ca, Cu, Fe, K, Mg, Mn, Na, Ni, P, Pb, Sr, Ti, V e Zn por meio de análises de espectrometria de massa com fonte de plasma (CERRO et al., 2020; XING et al., 2017).

A acidez, definida como pH, também é um componente central na química da deposição atmosférica. O grau de acidez ou alcalinidade de uma solução pode ser quantificado com base na concentração dos íons de hidrogênio dissolvidos (H^+), que é comumente reportado como uma quantidade adimensional conhecida como pH (equação 2) (PYE et al., 2020).

$$pH = -log_{10}[H^+] \quad (2)$$

É importante destacar que o pH de uma solução é determinado pelo equilíbrio entre ácidos e bases em solução. Nessa perspectiva, a absorção de dióxido de carbono gasoso é um fator importante que governa o pH da água de chuva, especialmente em ambientes remotos. O equilíbrio de uma gota de água pura com os níveis atuais de CO2 atmosférico a 298 K resulta em um pH de aproximadamente 5,60, que geralmente é referido como o pH da chuva

natural. Portanto, os valores de pH acima ou abaixo de 5,60 são frequentemente chamados de alcalinos ou ácidos, respectivamente (PYE et al., 2020; SEINFELD; PANDIS, 1998).

Estudos sobre a composição química da deposição atmosférica, realizados no Brasil na década de 1990, reportaram eventos de deposição ácida. De Mello (2001) analisou amostras de deposição úmida na Região Metropolitana do Rio de Janeiro e encontrou um valor de pH médio de 4,77 e concentrações majoritárias de H^+ (17,0 $\mu molL^{-1}$). Williams, Fisher e Melack (1997) também encontraram baixos valores de pH (4,70) e concentrações iônicas majoritárias de H^+ (17,0 $\mu molL^{-1}$), seguido de Cl^- (4,60 $\mu molL^{-1}$) e NO_3^- (4,20 $\mu molL^{-1}$), para amostras de deposição atmosférica úmida coletadas em Lago Calado, Amazonas. Esse comportamento ácido da deposição atmosférica foi associado a elevadas emissões de precursores ácidos como NO_x e SO_2.

Nas décadas seguintes foi observada uma tendência de redução dessa acidez nas amostras de deposição atmosférica devido ao incremento espécies neutralizantes. Nessa perspectiva, Fornaro e Gutz (2006), analisando amostras de deposição atmosférica úmida na cidade de São Paulo, entre 1983 e 2003, mostraram que não foram observados valores de pH médio abaixo de 4,50 e que houve uma redução de 42% nas concentrações de sulfato entre 1990 e 2003. Além disso, esse mesmo estudo apontou para o aumento das concentrações de NH_4^+, que alcançou valores médios de 47,0 $\mu molL^{-1}$ no início da década de 2000, indicando a contribuição de NH_3 na neutralização da acidez da chuva.

Essa tendência de redução da acidez e aumento de alcalinidade é observada atualmente em várias regiões do Brasil. Como exemplo, Martins et al. (2019) encontraram um valor médio de pH de 5,60 e concentrações dominantes de NH_4^+ (34,4 $\mu molL^{-1}$) e Ca^{2+} (27,4 $\mu molL^{-1}$), em amostras de deposição úmida coletadas na região urbana de Limeira – SP. Comportamento similar foi observado no estudo de Alves et al. (2018), na Região Sul do Brasil, onde amostras de deposição úmida apresentaram pH médio de 5,96 e altas concentrações de NH_4^+ (15,7 $\mu molL^{-1}$) e Ca^{2+} (18,8 $\mu molL^{-1}$) quando comparadas às concentrações de SO_4^{2-} (10,3 $\mu molL^{-1}$) e NO_3^- (7,00 $\mu molL^{-1}$).

2.2.5 Estimativas Globais de Deposição Atmosférica

Uma avaliação global e regional das estimativas de deposição atmosférica total de enxofre, nitrogênio, cátions básicos (Ca2+, Mg2+, Na+ e K+), entre outros compostos, estão reunidas no estudo conduzido por Vet et al. (2014).

A deposição atmosférica total de enxofre, medida como $S\text{-}SO_4^{2-}$, apresentou os valores mais elevados (20 – 50 $kgha^{-1}ano^{-1}$) para a Ásia e Europa, seguido de deposições na faixa de 4,0 a 23 $kgha^{-1}ano^{-1}$ para América do Norte. No Brasil, a deposição de S variou de 0,2 para regiões remotas na Amazônia a 4,0 $kgha^{-1}ano^{-1}$ em regiões densamente urbanizadas no sudeste do país.

Com relação ao nitrogênio, também foram encontrados altos níveis de deposição (20 – 38 $kgha^{-1}ano^{-1}$) na Ásia e Europa e valores entre 10 a 20 $kgha^{-1}ano^{-1}$ para algumas regiões da América do Norte. No Brasil, pequenas áreas remotas na Amazônia recebem de 2,0 a 4,0 $kgha^{-1}ano^{-1}$ e uma pequena área no Sul do país recebe fluxos de deposição de nitrogênio na faixa de 10 a 20 $kgha^{-1}ano^{-1}$. Mas ressalta-se que a maior área do país recebe fluxos de deposição na faixa de 4,0 a 10 $kgha^{-1}ano^{-1}$.

Nesse mesmo estudo de Vet et al. (2014), foram avaliadas as estimativas de deposição atmosférica úmida dos cátions básicos, como a soma equivalente dos cátions Ca^{2+}, Mg^{2+}, Na^{+} e K^{+}, uma vez que os dados de deposição seca não estavam disponíveis. Globalmente, a deposição úmida da soma de cátions de base variou largamente, de 0,01 a 8,5 $keqha^{-1}ano^{-1}$, devido à variabilidade na distribuição das fontes dessas espécies. Nessa perspectiva, a maioria dos locais de alta deposição (>1 $keqha^{-1}ano^{-1}$) estão localizados em zonas costeiras, refletindo a importância do Na^{+} de sal marinho, enquanto a influência de fontes terrestres de cátions de base aumenta com a distância da costa para o interior. No Brasil, a deposição úmida desses cátions alcalinos varia entre 0,6 e 1,0 $keqha^{-1}ano^{-1}$, refletindo a influência tanto do sal marinho quanto da poeira do solo em diferentes regiões.

2.2.6 Impactos Ambientais da Deposição Atmosférica

Embora a deposição atmosférica seja um processo natural em que ocorre a limpeza da atmosfera, seu resultado final é a transferência de nutrientes e contaminantes do ar para os ecossistemas ambientais (DUAN et al., 2016).

É bem reconhecido que a deposição de espécies de SO_4^{2-} e de NO_3^{-} estão relacionadas à acidificação dos solos e das águas superficiais, causando perda de peixes e danos à biota. Além disso, a deposição de NH_4^{+} também pode causar acidificação, principalmente em

ecossistemas saturados de nitrogênio, devido ao processo de nitrificação e posterior lixiviação de NO_3^- (DUAN et al., 2016). Destaca-se que o efeito acidificante da deposição de nitrogênio pode ser mais importante do que a deposição de enxofre em solos tropicais e subtropicais bem drenados devido ao alto teor de adsorção de SO_4^{2-} nesses solos (VUORENMAA et al., 2018).

Além da acidificação, a adição de nitrogênio via deposição atmosférica também pode aumentar a produção de biomassa em comunidades de plantas e consequentemente alterar sua composição (STEVENS; DAVID; STORKEY, 2018). Em ecossistemas aquáticos, o excesso de entrada de nitrogênio também pode conduzir processos de eutrofização, que pode ser observado por meio de mudanças na dinâmica do nitrogênio, no crescimento de algas ou na alteração da biodiversidade (LEPORI; KECK, 2012).

Com relação à deposição de compostos alcalinos, contendo cálcio, magnésio e potássio por exemplo, estes podem reduzir o risco de acidificação do solo e também contribuir para a fertilidade, repondo nutrientes essenciais às plantas (Ca^{2+}, K^+ e Mg^{2+}) que foram lixiviados devido à acidez do solo (FENN et al., 2015). Por outro lado, especialmente em solos alcalinos, a deposição atmosférica de Ca^{2+}, K^+ e Mg^{2+} pode provocar acúmulo desses compostos no solo e consequentemente diminuir a disponibilidade de micronutrientes como manganês, zinco, ferro, entre outros.

A deposição atmosférica também oferece riscos à saúde pública, uma vez que pode ser uma fonte de contaminantes em sistemas de captação de águas pluviais. Nesse sentido, em regiões de escassez de água, a água da chuva se torna uma fonte alternativa ao abastecimento de água potável. No entanto, o consumo da água da chuva, ou seja deposição úmida, com alta concentração de contaminantes como Pb, Cu, Zn, pode acarretar em efeitos graves à saúde, especialmente em crianças devido aos efeitos neurológicos permanentes no desenvolvimento (HUSTON et al., 2009; TAFFERE et al., 2016). Além disso, a deposição atmosférica de espécies orgânicas também pode contribuir para a formação de subprodutos de desinfecção quando é realizada a desinfecção das águas pluviais para consumo (SHI et al., 2021).

2.2.7 Fatores Meteorológicos

É importante lembrar que, além da influência das fontes de emissão de poluentes atmosféricos, fatores meteorológicos como vento, temperatura, umidade relativa, intensidade

da radiação solar, pressão, percurso e altitude das nuvens, intensidade da chuva e tamanho das gotas interferem nos processos de transformação, dispersão e remoção de poluentes atmosféricos. Essas condições meteorológicas afetam tanto as variações sazonais quanto a variabilidade de curto prazo na concentração dos principais poluentes atmosféricos, como NO_x, SO_2, CO, O_3, partículas em suspensão, bem como a deposição de sulfato (SO_4^{-2}), nitrato (NO_3^-), amônio (NH_4^+), sódio (Na^+), cálcio (Ca^{2+}), entre outros (PLEIJEL et al., 2016).

A avaliação das condições meteorológicas e suas relações com a composição química da deposição atmosférica permite identificar as possíveis origens das espécies químicas. Nesse sentido, o conhecimento sobre os padrões de vento (velocidade e direção) é de suma importância para a compreensão dos processos que influenciam a deposição atmosférica, uma vez que o vento pode transportar nutrientes e poluentes de diversas fontes de emissão para a região de monitoramento. Gao et al. (2018) analisaram a deposição atmosférica úmida de nitrogênio no grande lago africano, Lago Tanganyika, e descobriram que os maiores valores de deposição de nitrogênio ocorreram quando 76% dos ventos foram de leste, soprando da terra para o lago. Além disso, outro estudo conduzido na Cidade do México associou altos níveis de deposição úmida de amônio com ventos predominantes provenientes de nordeste, região onde a agricultura constitui a principal atividade e o uso de fertilizantes poderia explicar os níveis de amônio encontrados (BRETÓN et al., 2014). Dessa forma, nota-se que o conhecimento sobre o padrão de ventos pode auxiliar a identificar os padrões de transporte atmosférico de compostos químicos na região de monitoramento.

2.4 Técnicas Estatísticas Multivariadas

A análise multivariada é uma ferramenta que permite a avaliação de uma base de dados que possui várias variáveis relacionadas simultaneamente (MANLY, 2008). Dentre os métodos multivariados mais utilizados em estudos de poluição do ar, Análise de Componentes Principais (ACP), Análises de Fatores (AF) e mais recentemente a Fatoração de Matriz Positiva (FMP), são comumente empregados para identificação de fontes poluidoras.

2.4.1 Análise de Componentes Principais

A Análise de Componentes Principais (ACP) é uma técnica de análise multivariada cujo objetivo é reduzir a dimensionalidade de um conjunto de dados no qual existe muitas

variáveis inter-relacionadas, mantendo ao máximo a variação do conjunto de dados. Essa redução é alcançada transformando-se em um novo conjunto de variáveis, os chamados componentes principais (CPs), os quais são combinações lineares das variáveis originais, não são correlacionados entre si, e são ordenados para que os primeiros retenham a maior parte da variação presente em todas as variáveis originais. Assim, as variáveis originais que são correlacionadas entre si irão contribuir fortemente para o mesmo componente principal (JOLLIFFE, 2010).

A computação dos componentes principais baseia-se em autovalores e correspondentes autovetores de uma matriz de variância-covariância ou de correlação entre as variáveis. Um autovetor é uma direção e o autovalor corresponde a uma variância calculada na matriz, ou seja, o autovalor informa a quantidade de variação existentes nos dados na direção dada pelo autovetor. Cada componente principal possui um autovalor, o qual é extraído da matriz em ordem decrescente de magnitude. Assim, o autovetor com o maior autovalor será o primeiro componente principal (HENRIQUES, 2009).

De forma geral, a ACP permite identificar quais amostras são similares uma a outra e quais são muito diferentes. Nessa perspectiva, diversos estudos têm aplicado essa técnica multivariada para identificar as fontes dos compostos iônicos presentes na deposição atmosférica (KARA et al., 2014; MARTINS et al., 2019; TAFFERE et al., 2016), visto que diferentes fontes tendem a formar diferentes componentes principais, pois elementos pertencentes à mesma fonte variam ao mesmo tempo (ALMEIDA, 2001).

2.4.2 Análise de Fatores

A Análise de Fatores (AF), semelhante à ACP, tem como objetivo estudar a variação em uma quantidade de variáveis originais usando menos variáveis índices ou fatores. Assume-se que cada variável original possa ser expressa como uma combinação linear desses fatores. Entretanto, as duas análises diferem visto que a análise de fatores é baseada em um modelo particular para os dados, apresentando um termo residual que reflete o quanto uma variável é independente das outras variáveis (VIEIRA-FILHO, 2011).

Um tipo de AF começa tomando alguns poucos primeiros componentes principais como os fatores nos dados a serem considerados. O número de fatores será o número de autovalores maiores do que a unidade na matriz de correlações dos *score* do teste. Esses fatores iniciais

são então modificados por um processo especial de transformação chamado rotação fatorial, a fim de torná-las mais fáceis de serem interpretados (MANLY, 2008).

A rotação de fatores pode ser ortogonal (os novos fatores serão não correlacionados) ou oblíqua (os novos fatores serão correlacionados). Independentemente do tipo de rotação aplicada, é desejável que as cargas de fator para os novos fatores sejam próximas de zero ou muito diferentes de zero. Uma carga de fator próxima de zero indica que a variável original não é fortemente relacionada ao fator, enquanto um grande valor positivo ou negativo indica que a variável original, é determinada em grande parte pelo fator. Dessa forma, se cada *score* de teste é fortemente relacionado com alguns fatores, mas não relacionado com outros, a identificação dos fatores se torna mais fácil (MANLY, 2008).

Dentre os métodos de rotação ortogonal, o mais utilizado é a rotação Varimax. Esse método se concentra na máxima simplificação das colunas da matriz fatorial através da maximização da soma de variâncias dos quadrados dos *scores* exigidos da matriz fatorial. Vale ressaltar que normalizar as cargas de fator antes de maximizar as variâncias de seus quadrados fornece melhores resultados (KAISER, 1958). Nessa perspectiva, alguns estudos têm aplicado a AF com rotação Varimax e normalização de Kaiser para identificação de fontes dos íons presentes na deposição atmosférica (ANIL; ALAGHA; KARACA, 2017; SUNDRIYAL et al., 2018; ZHANG; ZHANG; LIU, 2007).

2.4.3 Fatoração de Matriz Positiva

A Fatoração de Matriz Positiva (FMP) ou *Positive Matrix Factorization* (PMF) é um recente aprimoramento das técnicas de análise multivariada, em que o problema fundamental é resolver as identidades e contribuições dos componentes em uma mistura desconhecida. Nessa perspectiva, a FMP pode ser considerada um aperfeiçoamento da aplicação da ACP e da Análise de Fatores à identificação de fontes de poluição atmosférica (REFF; EBERLY; BHAVE, 2007).

Embora possua princípios básicos semelhantes à AF, a FMP incorpora vínculos físicos ao problema estatístico, como a não-negatividade e a ponderação dos pesos das variáveis de acordo com suas incertezas. Assim, o modelo não permite que haja ocorrência de fontes negativas, corroborando com o fato de que não pode haver uma quantidade negativa de um constituinte básico em nenhuma amostra. Além disso, os pesos das medidas para a análise são influenciados pelas suas incertezas, ou seja, valores abaixo do limite de detecção, *outliers*

e valores perdidos têm incertezas maiores que os demais dados de concentração e portanto exercem menor influência na classificação das fontes (MACHADO, 2012).

De forma geral, o objetivo da FMP é identificar o número de fatores (fontes) e a variabilidade destes para cada evento amostrado. Para isso, diferente da ACP que utiliza matrizes de correlação e covariância, a FMP utiliza um ajuste de mínimos quadrados ponderados, em que os pesos das variáveis são baseados em seus desvios padrão. Dessa forma, esse modelo é mais quantitativo e mais adequado para as ciências físicas, químicas e ambientais do que os modelos baseados na ACP (PAATERO, 1997; PAATERO; TAPPER, 1994). Alves et al. (2018) e Mehr, Keshavarzi e Sorooshian (2019) aplicaram a análise FMP para identificar as possíveis fontes dos íons da deposição atmosférica e também quantificar suas contribuições relativas.

3. REFERÊNCIAS

AGUILAR-DODIER, L. C. et al. Spatial and temporal evaluation of H_2S, SO_2 and NH_3 concentrations near Cerro Prieto geothermal power plant in Mexico. **Atmospheric Pollution Research**, v. 11, n. 1, p. 94–104, 2020.

AKPO, A. B. et al. Precipitation chemistry and wet deposition in a remote wet savanna site in West Africa: Djougou (Benin). **Atmospheric Environment**, v. 115, p. 110–123, 2015.

ALLEN, J. O. et al. Emissions of size-segregated aerosols from on-road vehicles in the Caldecott Tunnel. **Environmental Science and Technology**, v. 35, n. 21, p. 4189–4197, 2001.

ALMARAZ, M. et al. Erratum: Agriculture is a major source of NO_x pollution in California. **Science Advances**, v. 4, n. 6, p. 1–9, 2018.

ALMEIDA, M. D. DE. **Identificação dos principais fatores de controle do aporte atmosférico de substâncias inorgânicas no Maciço do Itatiaia – RJ**. [s.l.] Universidade Federal Fluminense, 2001.

ALMEIDA, G. L. M. D. et al. **Estudo sobre as regiões de planejamento de Minas Gerais: Sul de Minas Gerais**. Belo Horizonte: [s.n.]. Disponível em: <https://www.fecomerciomg.org.br/wp-content/uploads/2018/05/Projeto-Estadual-Sul-de-Minas.pdf>.

ALVES, D. D. et al. Chemical composition of rainwater in the Sinos River Basin, Southern Brazil: a source apportionment study. **Environmental Science and Pollution Research**, v. 25, n. 24, p. 24150–24161, 2018.

AMIL, N. et al. Seasonal variability of $PM_{2.5}$ composition and sources in the Klang Valley urban-industrial environment. **Atmospheric Chemistry and Physics**, v. 16, n. 8, p. 5357–5381, 2016.

ANDRONACHE, C. Estimated variability of below-cloud aerosol removal by rainfall for observed aerosol size distributions. **Atmospheric Chemistry and Physics**, v. 3, n. 1, p. 131–143, 2003.

ANEJA, V. P. et al. Characterization of the Global Sources of Atmospheric Ammonia from Agricultural Soils. **Journal of Geophysical Research: Atmospheres**, v. 125, n. 3, p. 1–13, 2020.

ANIL, I.; ALAGHA, O.; KARACA, F. Effects of transport patterns on chemical composition of sequential rain samples: trajectory clustering and principal component analysis approach. **Air Quality, Atmosphere and Health**, v. 10, n. 10, 2017.

BAIRD, C.; CANN, M. **Química Ambiental**. 4. ed. Porto Alegre: Bookman, 2011.

BRAGA, B. et al. **Introdução à Engenharia Ambiental**. 2. ed. São Paulo: Pearson Prentice Hall, 2005.

BRETÓN, R. M. C. et al. Wet Deposition Fluxes and Related Atmospheric Chemistry at Three Sites in Mexico. **Open Journal of Air Pollution**, v. 03, n. 01, p. 1–9, 2014.

CAGGIANO, R.; MACCHIATO, M.; TRIPPETTA, S. Levels, chemical composition and sources of fine aerosol particles (PM1) in an area of the Mediterranean basin. **Science of the Total Environment**, v. 408, n. 4, p. 884–895, 2010.

CELLE-JEANTON, H. et al. Rainwater chemistry at a Mediterranean inland station (Avignon, France): Local contribution versus long-range supply. **Atmospheric Research**, v. 91, n. 1, p. 118–126, 2009.

CERRO, J. C. et al. Chemistry of dry and wet atmospheric deposition over the Balearic Islands, NW Mediterranean: Source apportionment and African dust areas. **Science of the Total Environment**, v. 747, p. 141187, 2020.

CHANTARA, S.; CHUNSUK, N. Comparison of wet-only and bulk deposition at Chiang Mai (Thailand) based on rainwater chemical composition. **Atmospheric Environment**, v. 42, n. 22, p. 5511–5518, 2008.

CHATTERJEE, A. et al. In-cloud and below-cloud scavenging of aerosol ionic species over a tropical rural atmosphere in India. **Journal of Atmospheric Chemistry**, v. 66, p. 27–40, 2010.

CHEN, S.; ZHAO, Y.; ZHANG, R. Formation Mechanism of Atmospheric Ammonium Bisulfate: Hydrogen-Bond-Promoted Nearly Barrierless Reactions of SO_3 with NH_3 and H_2O. **ChemPhysChem**, v. 19, n. 8, p. 967–972, 2018.

COCHRAN, R. E. et al. Sea spray aerosol: The chemical link between the oceans, atmosphere, and climate. **Accounts of Chemical Research**, v. 50, n. 3, p. 599–604, 2017.

DE MELLO, W. Z. Precipitation chemistry in the coast of the Metropolitan Region of Rio de Janeiro, Brazil. **Environmental Pollution**, v. 114, n. 2, p. 235–242, 2001.

DE SOUZA, P. A. et al. Deposições Atmosféricas Úmida, Seca e Total de Nitrogênio Inorgânico Dissolvido no Estado do Rio de Janeiro de. **Revista Virtual de Quimica**, v. 9, n. 5, p. 2052–2066, 2017.

DUAN, L. et al. Atmospheric S and N deposition relates to increasing riverine transport of S and N in southwest China: Implications for soil acidification. **Environmental Pollution**, v. 218, p. 1191–1199, 2016.

EATOUGH, D. J.; CAKA, F. M.; FARBER, R. J. The Conversion of SO_2 to Sulfate in the Atmosphere. **Israel Journal of Chemistry**, v. 34, n. 3–4, p. 301–314, 1994.

FENN, M. E. et al. Atmospheric deposition of nitrogen, sulfur and base cations in jack pine stands in the Athabasca Oil Sands Region, Alberta, Canada. **Environmental Pollution**, v. 196, p. 497–510, 2015.

FORNARO, A. Águas de chuva: conceitos e breve histórico. Há chuva ácida no Brasil? **Revista USP**, v. 70, p. 78–87, 2006.

FORNARO, A.; GUTZ, I. G. R. Wet deposition and related atmospheric chemistry in the São Paulo metropolis, Brazil: Part 3. Trends in precipitation chemistry during 1983 – 2003. **Atmospheric Environment**, v. 40, p. 5893–5901, 2006.

FOWLER, D. et al. Atmospheric composition change: Ecosystems-Atmosphere interactions.

Atmospheric Environment, v. 43, n. 33, p. 5193–5267, 2009.

GAO, Q. et al. Wet deposition of atmospheric nitrogen contributes to nitrogen loading in the surface waters of Lake Tanganyika, East Africa: a case study of the Kigoma region. **Environmental Science and Pollution Research**, v. 25, n. 12, p. 11646–11660, 2018.

GONÇALVES, C. et al. Size-segregated aerosol chemical composition from an agro-industrial region of São Paulo state, Brazil. **Air Quality, Atmosphere and Health**, v. 10, n. 4, p. 483–496, 2017.

HAKKARAINEN, T. **Reduction of nitrogen oxide emissions in lime kiln**. [s.l.] Lappeenranta University of Technology, 2014.

HENRIQUES, R. V. D. H. **Aporte atmosférico de nitrogênio inorgânico e orgânico nas proximidades de Maceió (AL) - Potencial impacto da atividade canavieira**. [s.l.] Universidade Federal Fluminense, 2009.

HUANG, Y. et al. Quantification of global primary emissions of $PM_{2.5}$, PM_{10}, and TSP from combustion and industrial process sources. **Environmental Science and Technology**, v. 48, n. 23, p. 13834–13843, 2014.

HUSTON, R. et al. Characterisation of atmospheric deposition as a source of contaminants in urban rainwater tanks. **Water Research**, v. 43, n. 6, p. 1630–1640, 2009.

IMAMURA, N. et al. A comparison between wet-only and bulk deposition at two forest sites in Japan. **Asian Journal of Atmospheric Environment**, v. 12, n. 1, p. 67–77, 2018.

JOLLIFFE, I. T. **Principal Components Analysis**. 2ª ed. [s.l.] Springer, 2010.

KAISER, H. F. The varimax criterion for analytic rotation in factor analysis. **Psychometrika**, v. 23, n. 3, p. 187–200, 1958.

KARA, M. et al. Seasonal and spatial variations of atmospheric trace elemental deposition in the Aliaga industrial region, Turkey. **Atmospheric Research**, v. 149, p. 204–216, 2014.

KARANASIOU, A. et al. On the quantification of atmospheric carbonate carbon by thermal/optical analysis protocols. **Atmospheric Measurement Techniques**, v. 4, n. 11, p. 2409–2419, 2011.

KAWASHIMA, A. B. et al. Development of a spatialized atmospheric emission inventory for the main industrial sources in Brazil. **Environmental Science and Pollution Research**, v. 27, n. 29, p. 35941–35951, 2020.

LENZI, E.; FAVERO, L. O. B. **Introdução à Química da Atmosfera - Ciência, Vida e Sobrevivência**. 2. ed. Rio de Janeiro: Grupo Gen, 2019.

LEPORI, F.; KECK, F. Effects of atmospheric nitrogen deposition on remote freshwater ecosystems. **Ambio**, v. 41, n. 3, p. 235–246, 2012.

LI, T. C. et al. Diurnal variation and chemical characteristics of atmospheric aerosol particles and their source fingerprints at Xiamen Bay. **Aerosol and Air Quality Research**, v. 13, n. 2, p. 596–607, 2013.

MACHADO, V. B. **Identificação das fontes de Material Particulado Fino (MP2,5) de Porto Alegre**. [s.l.] USP, 2012.

MANLY, B. F. J. **Métodos Estatísticos Multivariados: Uma Introdução**. 3ª ed. Porto Alegre: Bookman, 2008.

MARIRAJ MOHAN, S. An overview of particulate dry deposition: measuring methods, deposition velocity and controlling factors. **International Journal of Environmental Science and Technology**, v. 13, n. 1, p. 387–402, 2016.

MARTINS, E. H. et al. Chemical composition of rainwater in an urban area of the southeast of Brazil. **Atmospheric Pollution Research**, v. 10, n. 2, p. 520–530, 2019.

MEHR, M. R.; KESHAVARZI, B.; SOROOSHIAN, A. Influence of natural and urban emissions on rainwater chemistry at a southwestern Iran coastal site. **Science of the Total Environment**, v. 668, p. 1213–1221, 2019.

MENG, W. et al. Improvement of a Global High-Resolution Ammonia Emission Inventory for Combustion and Industrial Sources with New Data from the Residential and Transportation Sectors. **Environmental Science and Technology**, v. 51, n. 5, p. 2821–2829, 2017.

MIGLIAVACCA, D. et al. Evaluation of the atmospheric deposition in an urban region in south Brazil. **Water, Air, and Soil Pollution**, v. 167, n. 1–4, p. 91–110, 2005.

MOLDAN, B.; VESELY, M.; BARTOŇOVÁ, A. Chemical composition of atmospheric precipitation in Czechoslovakia, 1976-1984-I. Monthly samples. **Atmospheric Environment (1967)**, v. 21, n. 11, p. 2383–2395, 1987.

MOLINA-HERRERA, S. et al. Importance of soil NO emissions for the total atmospheric NOxbudget of Saxony, Germany. **Atmospheric Environment**, v. 152, p. 61–76, 2017.

MONKS, P. S. et al. Atmospheric composition change - global and regional air quality. **Atmospheric Environment**, v. 43, n. 33, p. 5268–5350, 2009.

MUKHERJEE, S. et al. Investigation of physico-chemical characteristics and associated CCN activation for different combustion sources through Chamber experiment approach. **Atmospheric Environment**, v. 266, n. September, p. 118726, 2021.

OLIVEIRA, M. G. L. **Evolução Das Distribuições De Tamanho Em Massa E Número Do Aerossol Atmosférico Em São Paulo**. [s.l.] Universidade de São Paulo, 2007.

PAATERO, P. Least squares formulation of robust non-negative factor analysis. **Chemometrics and Intelligent Laboratory Systems**, v. 37, n. 1, p. 23–35, 1997.

PAATERO, P.; TAPPER, U. Positive matrix factorization: A non-negative factor model with optimal utilization of error estimates of data values. **Environmetrics**, v. 5, n. 2, p. 111–126, 1994.

PÉREZ, N. et al. Impact of harbour emissions on ambient PM_{10} and $PM_{2.5}$ in Barcelona (Spain): Evidences of secondary aerosol formation within the urban area. **Science of the Total Environment**, v. 571, p. 237–250, 2016.

PIO, C. A. et al. Chemical composition of atmospheric aerosols during the 2003 summer intense forest fire period. **Atmospheric Environment**, v. 42, n. 32, p. 7530–7543, 2008.

PLEIJEL, H. et al. A method to assess the inter-annual weather-dependent variability in air pollution concentration and deposition based on weather typing. **Atmospheric Environment**, v. 126, n. 2, p. 200–210, 2016.

PRINN, R. G. et al. History of chemically and radiatively important atmospheric gases from the Advanced Global Atmospheric Gases Experiment (AGAGE). **Earth System Science Data**, v. 10, n. 2, p. 985–1018, 2018.

PYE, H. O. T. et al. The Acidity of Atmospheric Particles and Clouds. **Atmospheric Chemistry and Physics**, v. 20, p. 4809–4888, 2020.

REFF, A.; EBERLY, S. I.; BHAVE, P. V. Receptor modeling of ambient particulate matter data using positive matrix factorization: Review of existing methods. **Journal of the Air and Waste Management Association**, v. 57, n. 2, p. 146–154, 2007.

REN, Y. et al. Contributions of biomass burning to global and regional SO_2 emissions. **Atmospheric Research**, v. 260, n. March, p. 105709, 2021a.

REN, Y. Q. et al. Chemical composition of fine organic aerosols during a moderate pollution event in summertime in Beijing: Combined effect of primary emission and secondary formation. **Atmospheric Environment**, v. 246, n. December 2020, p. 118167, 2021b.

SANDER, R. Compilation of Henry's law constants (version 4.0) for water as solvent. **Atmospheric Chemistry and Physics**, v. 15, n. 8, p. 4399–4981, 2015.

SEINFELD, J. H.; PANDIS, S. N. **Atmospheric Chemistry and Physics: From Air Pollution to Climate Change**. 2. ed. Hoboken, New Jersey: John Wiley & Sons, Inc., 1998. v. 51

SHEPHERD, M. F.; BARZETTI, S.; HASTIE, D. R. The production of atmospheric NOx and N2O from a fertilized agricultural soil. **Atmospheric Environment Part A, General Topics**, v. 25, n. 9, p. 1961–1969, 1991.

SHI, M. et al. Influence of atmospheric deposition on surface water quality and DBP formation potential as well as control technology of rainwater DBPs: a review. **Environmental Science: Water Research & Technology**, n. 12, 2021.

SONG, W. et al. Important contributions of non-fossil fuel nitrogen oxides emissions. **Nature Communications**, v. 12, n. 1, p. 1–8, 2021.

STEVENS, C. J.; DAVID, T. I.; STORKEY, J. Atmospheric nitrogen deposition in terrestrial ecosystems: Its impact on plant communities and consequences across trophic levels. **Functional Ecology**, v. 32, n. 7, p. 1757–1769, 2018.

SU, J. et al. Insights into measurements of water-soluble ions in $PM_{2.5}$ and their gaseous precursors in Beijing. **Journal of Environmental Sciences (China)**, v. 102, p. 123–137, 2021.

SUNDRIYAL, S. et al. Deposition of atmospheric pollutant and their chemical characterization in snow pit profile at Dokriani Glacier, Central Himalaya. **Journal of**

Mountain Science, v. 15, n. 10, p. 2236–2246, 2018.

TAFFERE, G. R. et al. Characterization of Atmospheric Bulk Deposition: Implications on the Quality of Rainwater Harvesting Systems in the Semi-Arid City of Mekelle, Northern Ethiopia. **Environmental Processes**, v. 3, n. 1, p. 247–261, 2016.

TIAN, H. et al. A comprehensive quantification of global nitrous oxide sources and sinks. **Nature**, v. 586, n. 7828, p. 248–256, 2020.

TOSITTI, L. et al. Chemical characteristics of atmospheric bulk deposition in a semi-rural area of the Po Valley (Italy). **Journal of Atmospheric Chemistry**, v. 75, n. 1, p. 97–121, 2018.

TRIADÓ-MARGARIT, X. et al. High similarity in bacterial bioaerosol compositions between the free troposphere and atmospheric depositions collected at high-elevation mountains. **Atmospheric Environment**, v. 203, p. 79–86, 2019.

UPADHYAY, N. et al. Size-differentiated chemical composition of re-suspended soil dust from the Desert Southwest United States. **Aerosol and Air Quality Research**, v. 15, n. 2, p. 387–398, 2015.

VELDKAMP, E.; KELLER, M. Fertilizer-induced nitric oxide emissions from agricultural soils. **Nutrient Cycling in Agroecosystems**, v. 48, n. 1–2, p. 69–77, 1997.

VET, R. et al. A global assessment of precipitation chemistry and deposition of sulfur, nitrogen, sea salt, base cations, organic acids, acidity and pH, and phosphorus. **Atmospheric Environment**, v. 93, p. 3–100, 2014.

VIEIRA-FILHO, M. **Avaliação dos efeitos locais na composição química de águas de chuva na cidade de São Paulo e Cubatão**. [s.l.] Universidade de São Paulo, 2011.

VIEIRA-FILHO, M. S. et al. Gas-phase ammonia and water-soluble ions in particulate matter analysis in an urban vehicular tunnel. **Environmental Science and Pollution Research**, v. 23, n. 19, p. 19876–19886, 2016.

VIEIRA-FILHO, M. S.; PEDROTTI, J. J.; FORNARO, A. Contribution of long and mid-range transport on the sodium and potassium concentrations in rainwater samples, São Paulo megacity, Brazil. **Atmospheric Environment**, v. 79, p. 299–307, 2013.

VOGEL, A. et al. Reference data set of volcanic ash physicochemical and optical properties. **Journal of Geophysical Research: Atmospheres**, v. 122, n. 17, p. 9485–9514, 2017.

VUORENMAA, J. et al. Long-term changes (1990–2015) in the atmospheric deposition and runoff water chemistry of sulphate, inorganic nitrogen and acidity for forested catchments in Europe in relation to changes in emissions and hydrometeorological conditions. **Science of the Total Environment**, v. 625, p. 1129–1145, 2018.

WALLACE, J. M.; HOBBS, P. V. **Atmospheric Science: An Introductory Survey**. 2. ed. Washington, D.C.: Elsevier, 2005.

WESELY, M. L.; HICKS, B. B. A review of the current status of knowledge on dry deposition. **Atmospheric Environment**, v. 34, n. 12–14, p. 2261–2282, 2000.

WILLIAMS, M. R.; FISHER, T. R.; MELACK, J. M. Chemical composition and deposition of rain in the central Amazon, Brazil. **Atmospheric Environment**, v. 31, n. 2, p. 207–217, 1997.

XING, J. et al. Fluxes, seasonal patterns and sources of various nutrient species (nitrogen, phosphorus and silicon) in atmospheric wet deposition and their ecological effects on Jiaozhou Bay, North China. **Science of the Total Environment**, v. 576, n. 7, p. 617–627, 2017.

XU, W. et al. Precipitation chemistry and atmospheric nitrogen deposition at a rural site in Beijing, China. **Atmospheric Environment**, v. 223, n. July 2019, p. 117253, 2020.

YAMASOE, M. A. et al. Chemical composition of aerosol particles from direct emissions of vegetation fires in the Amazon Basin: Water-soluble species and trace elements. **Atmospheric Environment**, v. 34, n. 10, p. 1641–1653, 2000.

ZENG, Y.; TIAN, S.; PAN, Y. Revealing the Sources of Atmospheric Ammonia: a Review. **Current Pollution Reports**, v. 4, n. 3, p. 189–197, 2018.

ZHANG, G. S.; ZHANG, J.; LIU, S. M. Chemical composition of atmospheric wet depositions from the Yellow Sea and East China Sea. **Atmospheric Research**, v. 85, n. 1, p. 84–97, 2007.

ZHANG, J. et al. Chemical composition, source, and process of urban aerosols during winter haze formation in Northeast China. **Environmental Pollution**, v. 231, p. 357–366, 2017.

ZHANG, N. et al. Chemical composition of rainwater at Lijiang on the Southeast Tibetan Plateau: Influences from various air mass sources. **Journal of Atmospheric Chemistry**, v. 71, n. 2, p. 157–174, 2014.

ZHONG, Q. et al. Global Sulfur Dioxide Emissions and the Driving Forces. **Environmental Science and Technology**, v. 54, n. 11, p. 6508–6517, 2020.

ZHUANG, H. et al. Formation of nitrate and non-sea-salt sulfate on coarse particles. **Atmospheric Environment**, v. 33, n. 26, p. 4223–4233, 1999.

SEGUNDA PARTE

1. ARTIGO I - ATMOSPHERIC DEPOSITION CHEMISTRY IN A BRAZILIAN RURAL AREA: ALKALINE SPECIES BEHAVIOR AND AGRICULTURAL INPUTS

Environmental Science and Pollution Research
https://doi.org/10.1007/s11356-020-12317-3

RESEARCH ARTICLE

Atmospheric deposition chemistry in a Brazilian rural area: alkaline species behavior and agricultural inputs

Jaqueline Natiele Pereira [1] & Adalgiza Fornaro[2] & Marcelo Vieira-Filho[1*]

1 Departamento de Engenharia Ambiental (DAM), Universidade Federal de Lavras (UFLA), Campus da UFLA, 37200-000, Lavras, Minas Gerais, Brazil

2 Departamento de Ciências Atmosféricas, Instituto de Astronomia, Geofísica e Ciências (IAG), Atmosféricas da Universidade de São Paulo (USP), Rua do Matão, 1226, 05508-090, Cidade, Universitária, São Paulo, SP, Brazil

*e-mail marcelo.filho@ufla.br, phone: (+55)11-9 8598 6567

Responsible Editor: Philippe Garrigues

Received: 4 June 2020 / Accepted: 30 December 2020

Abstract

Since 2000s, several studies have been reporting an increase of alkaline species in atmospheric deposition worldwide. This study aims to evaluate and give a better understanding about atmospheric deposition chemistry collected in Lavras, a Brazilian city with rural background. Bulk atmospheric deposition samples were collected from March 2018 to February 2019 and major ionic species were quantified. The pH values ranged from 5.52 to 8.29, with an average of 5.92 and most deposition samples (~ 94%) were alkaline (pH > 5.60). For the whole sampling campaign, the ions profile in volume weighted mean (VWM) was described as follows Ca^{2+} (35.02) > NH_4^+ (11.26) > Cl^- (11.19) > Mg^{2+} (9.04) > NO_3^- (8.57) > Na^+ (5.65) > K^+ (2.61) > SO_4^{2-} (2.43) > H^+ (0.94) $\mu molL^{-1}$. We identified Ca^{2+} and NH_4^+ as the most predominant species accounting for 53% of the total ionic species distribution. In addition, all samples showed neutralization factor (NF) index greater than 1, with mean value of 6.4. Regarding regression analysis, acidity neutralization precursors such as calcium and ammonia accounted for 50% and 4%, respectively. In addition, samples alkaline pattern was mainly due to agricultural sources, including fertilizer production and application, and cement manufacturing inside the county air basin.

Keywords Atmospheric deposition chemistry · Bulk atmospheric deposition · Alkaline species · Neutralization factor · Agricultural sources · Brazil

Introduction

Air pollution is closely related to both human emissions and meteorological factors, influencing the emissions rate from local sources, (photo)chemical activity, dispersion and deposition in the atmosphere (Avila and Alarco 1999; Pleijel et al. 2016; Cheng et al. 2019). In addition, such air pollution processes are considerably modified by long-range transport of the air masses, enriching the complex interactions among air pollutants and their environmental fate (Mahapatra et al. 2018). Such atmospheric pollutants are subjected to atmospheric recirculation processes and may be redistributed at local, regional and global scale through atmospheric deposition (Tositti et al. 2018). Thus, understanding pollutants physicochemical processes in the atmospheric system provides an important tool for identifying chemical composition, emission processes, public health impacts and their environment fate (Zhang et al. 2016; Deusdará et al. 2017; Mo et al. 2018).

Atmospheric deposition exerts a key role in terrestrial and aquatic biogeochemical processes, since it is a main cycling pathway for both primary chemical species (Cl^-, Na^+, K^+, Mg^{2+}, Ca^{2+}), as well as secondary chemical species (SO_4^{2-}, NO_3^-, NH_4^+) (De Souza et al. 2006; Araujo et al. 2015; Xing et al. 2017). Primary species derive directly from aerosols, mainly from sea spray and soil dust, while the secondary species originate from gaseous emissions and subsequent reactions into the atmosphere (Seinfeld and Pandis 1998). These nutrients and pollutants may carried out into environmental compartments causing significant impacts, such as eutrophication and soil acidity due to atmospheric deposition (Duan et al. 2016; Zhan et al. 2017). Ti et al. (2018) showed that nitrogen atmospheric deposition contributed with 33.3% of the nitrogen total loading in Taihu Lake, China, highlighting the importance of atmospheric deposition as surface water pollutant.

The chemical composition of the atmospheric deposition has been widely studied, since it elucidates the chemical transformation processes, reaction routes and also feeds several receptor techniques to untangle source apportionment (Vieira-Filho et al. 2015; Lenzi and Favero 2019; Meng et al. 2019). Regarding the major ions species in atmospheric deposition, some of them may modify the acid-base

conditions on both dry (particulate matter) and wet deposition (rainwater, snow, fog, clouds) (Pye et al. 2020). Also, some early studies conducted in the São Paulo city, in the 1980s, showed discussions about the role of H_2SO_4 and HNO_3 as responsible for rainwater acidification (Fornaro 1991). Moreover, the carboxylic acids (measured as rainwater ions: CHO_2^-, $C_2O_4^{2-}$ and$C_2H_3O_2^-$) may also represent significant part of atmospheric acidity in both urban and rural areas (Leal et al. 2004; Niu et al. 2018). Sun et al. (2016) verified that the rainwater presented 17.7% of acidity from carboxylic acids in the Mount Lu, South China, suggesting the major role of weak organic acids in atmospheric acidity.

Several studies highlighted the close link between vehicular fleet and deleterious air quality episodes (Massambani and Andrade 1994; Grosjean et al. 1999). However, due to vehicles and fuels technological innovations, as well as the electronic injection and catalytic converters use, this acidity was reduced in the decades that followed (Fornaro and Gutz 2006; Carvalho et al. 2015). In addition, Vet et al. (2014) showed that there has been an increase of atmospheric deposition of reduced nitrogen (NH_3-N) worldwide. Alkaline behavior tendency was observed in dry and wet deposition samples in the last decade, due to the emissions reductions of atmospheric acids, increasing the effects of the neutralization species such as ammonia (NH_3) and calcium carbonate ($CaCO_3$) (Vieira-Filho et al. 2016; Zeng et al. 2020).

Despite several atmospheric pollution studies (IEMA 2014; Carvalho et al. 2015), there are no federal monitoring networks for atmospheric deposition in Brazil. Moreover, in the Southeast region such studies are mainly performed in São Paulo and Rio de Janeiro states (Lara et al. 2001; De Mello and De Almeida 2004; Vieira-Filho et al. 2015; De Souza et al. 2017; Martins et al. 2019), however there are a few reports in Minas Gerais state (Mimura et al., 2016). Therefore, a study was carried out in the Southern Region of Minas Gerais, which is an important economic region responsible for 21.8% of agricultural commodities (mainly from coffee producing regions), and also accounts for about 12% of the state's Gross Domestic Product (Almeida et al. 2017). Given this perspective, we evaluated and quantified the acidity and its processes through atmospheric deposition in Lavras city, Southern Region of Minas Gerais

state.

METHODOLOGY

Sampling Site

Lavras is located in the Southern Minas Gerais state (21° 13' 45,3"S and 44° 58' 32,4"W), Brazil, 241 km from the Atlantic Ocean (in a straight line), with an area of 564.744 km² and altitude of 919m (Fig.1).Its population of 102,728 inhabitants occupies fifth place among the most populous city in Southern Minas Gerais (IBGE 2018).

Lavras has undergone the influence of several anthropogenic activities including transport, farming, biomass burning and industrial activities such as agroindustrial and cement plants (Almeida et al. 2017). Coffee plantations (~0.1km to northeast), lime mining companies (~ 5km to northwest), cement and limestone industries (~10km to northeast) and mining companies that produces spodumene concentrate, tantalum, tin in ingots and feldspar (~67km to east) are located around the sampling point. The vehicle fleet in Lavras is about 15 years old on average and categorically made up of 62% of passenger cars produced before 2010 and 14% before 1990 (DENATRAN 2018). In addition, the vehicular fleet has about 50 thousand light-duty vehicles, comprising of 54% automobiles and 26% motorcycles both burning gasohol (73% gasoline + 27% anhydrous ethanol or 100% hydrated ethanol), being the other remaining 20% heavy-duty vehicles, buses and trucks, both burning diesel with 7% of biodiesel (soya).

Regarding climatological conditions (1981-2010), Lavras presents average temperatures of 20.3ºC, more specifically with a minimum average in July (16.9ºC) and a maximum average in February (22.8ºC). The annual climatological rainfall is 1461.8 mm, mainly divided in two separate periods: (i) rainy season from October to March (covering 85% of total rainfall); and (ii) dry season from April to September (INMET 2019a).

Sampling Procedures

A set of 39 bulk deposition samples were collected at *Universidade Federal de Lavras (UFLA)* campus in Lavras city (Fig. 1), between March 2018 and February 2019. The bulk collector was composed of a high-density polyethylene bucket (NALGON) of 10L with a collecting area of 439cm^2, protected by a

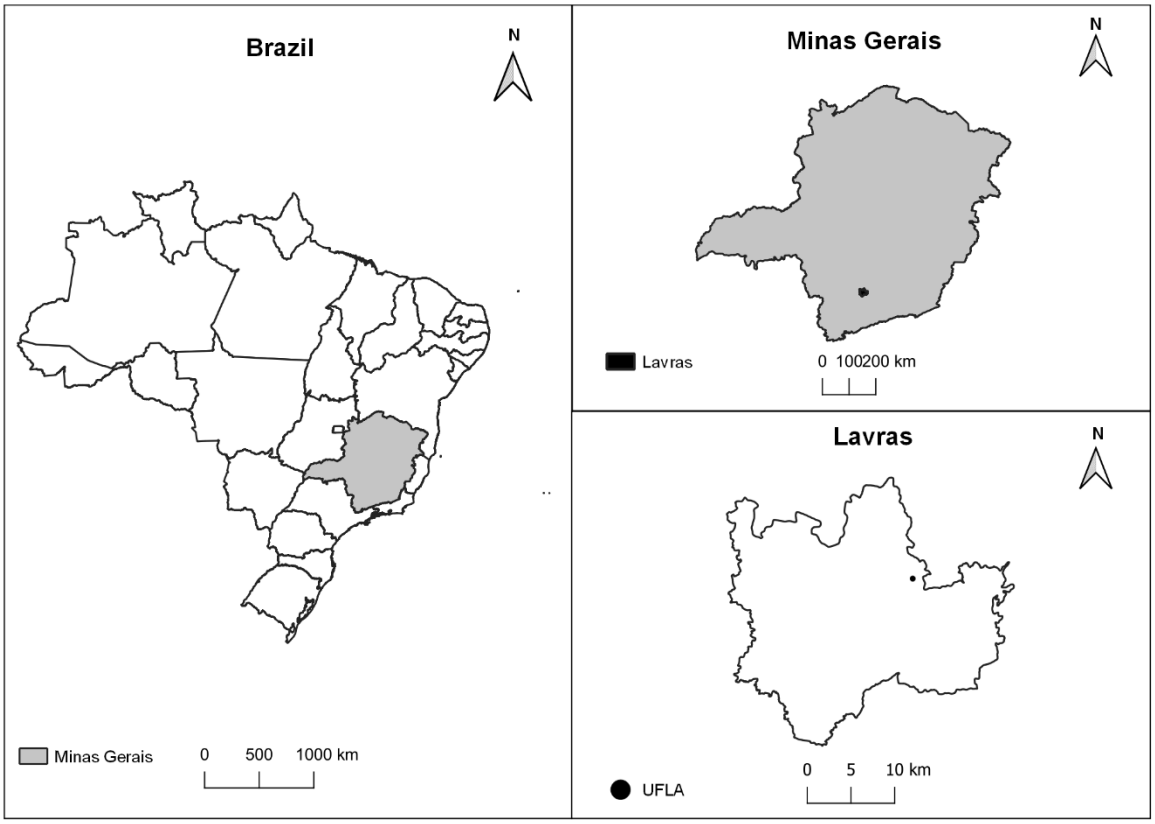

Fig.1 Geographical location of sampling site (UFLA) in Lavras city, Southern Minas Gerais state, Brazil

sun-protective PVC structure. To reduce litter fall in samples, the collector was covered with a nylon mesh and also fixed on a support at 1.5m above the ground level (WMO 2004). In order to follow GAW´s sampling procedures, the sampling set was rinsed with deionized water (18MΩ) several times during operations.

The sampling period was around 7 days, but longer sampling times were collected during rainfall events. The pH measurements were obtained by using pHmeter (AKSO AK model 151), calibrated with buffer solutions (pH 4.0 and 7.0), and conductivity measurements were performed by using a conductivity meter (AKSO AK model 151), calibrated with a standard solution of 1413µScm^{-1} potassium chloride. Regarding dry atmospheric only samples, a 50mL of deionized water was added in order to analyze soluble species.

In addition, one sample aliquot was filtered with a membrane with 0.22µm pore diameter (Millex), stored in conditioned polyethylene bottles kept at -18ºC prior to ion chromatography (IC)

analysis (Metrohm model 851) with anionic column (Metrosep ASupp5 - 250 mm x 4 mm) and cationic column (Metrosep C2 150 - 150 x 4 mm). The species quantified by IC were calcium (Ca^{2+}), ammonium (NH_4^+), magnesium (Mg^{2+}), sodium (Na^+), potassium (K^+), nitrate (NO_3^-), chloride (Cl^-) and sulfate (SO_4^{2-}). Analytical quantification was performed by using an external calibration curve from the standard concentrations for each ion. Detection limits (DL) values were calculated from the parameters obtained from the analysis, by the method of the least squares, from the calibration curve ($y = a + bx$) and corresponded to the white sign (or linear coefficient) plus 3 times the standard deviation (sd) of the angular coefficient ($sd_{y/x}$), that is, $DL = a + 3\ sd_{y/x}$. The DL values for all species evaluated varied between 0.04 $\mu molL^{-1}$ for K^+ and 0.81 $\mu molL^{-1}$ for Ca^{2+}, being the quantification limit (QL) ten times the DL values.

In order to estimate the uncertainties aside from the detection limits, several blank sample analysis were carried out through the experimental campaign. The blank sample concentrations were quantified, reaching average concentrations lower than 0.8 $\mu molL^{-1}$, except for calcium (Ca^{2+}) and sodium (Na^+) which showed values of 3.9 and 9.0 $\mu molL^{-1}$, respectively, for some blanks. Considering the blank concentrations as the bias, we calculated the median percentage error for all the ions between 1.3% and 8.5%.

Regarding meteorological data, wind direction and speed were retrieved from INPE meteorological station 83687 located at the *Universidade Federal de Lavras*. The retrieved data was dispersed in 3 times per day interval resolution (12:00, 18:00 and 24:00 UTC) in the CPTEC database (INPE 2019) and comprise the study period between March 2018 and February 2019.

Statistical Analysis

Data processing was performed by programming in R language, based on data obtained from ionic chromatography, physical-chemical and weather analysis. We specifically applied the functions contained in the stats, openair and ggplot2 packages (Carslaw and Ropkins 2012; Wickham 2016; R Core Team 2019).

Validation and QA/QC Procedures

The internal consistency of the entire data set was analyzed through

Cooperative Programme for Monitoring and Evaluation of Long-Range Transmission of Air Pollutants in Europe (EMEP) guidelines for rainwater samples validation (WMO 2004). This method is based in the equations 1, 2 and 3:

$$IS = \sum_{cations} C_i + \sum_{anions} C_i \quad (1)$$

$$ID = \sum_{cations} C_i - \sum_{anions} C_i \quad (2)$$

$$IB = (ID/IS) * 10^2 \quad (3)$$

Where C_i is the concentration of ion type i in a specific sample, expressed in μeqL^{-1}. IS is the sum of all ion concentrations and ID is the difference between the sum of the cation concentrations and the sum of the anion concentrations. Both IS and ID are expressed in μeqL^{-1}. The ion balance, IB, expresses the difference, ID, in percent of the sum of all concentrations, IS.

Apart from the equations, the samples pH values were also considered in this validation process, in which critical pH value of 5.5 was also used. For samples with pH ≤ 5.5 and with IB value within ±10% were considered valid, while samples with IB between –20% and –10% or +10% and +20% although considered valid were flagged. Results from samples outside ±20% were considered invalid. Concerning the samples with pH> 5.5, an upper limit of +20% was set for valid samples. When IB was higher than +20%, the data were considered valid and flagged. For IB values negatives, the criterion was the same as that applied to samples with pH ≤ 5.5. In addition, when IS< $100 \mu eqL^{-1}$, the criteria were based in ID (in μeqL^{-1}) rather than IB, due to strong increase in IB with decreasing in IS (Alves et al., 2018).

It is noteworthy that, overall, a poor ion balance may indicate bad data quality; however, this is not necessarily true at high pH or at low conductivity. Thus, samples with a poor ion balance and high pH or low conductivity were valid but flagged rather than considered invalid (WMO 2004). Moreover, specific details are described elsewhere (Schaug et al. 1997).

Carbonate and Bicarbonate Estimates

We estimate HCO_3^- concentrations from theoretical relationship between pH and HCO_3^-(Eq. 4) (WMO 2004; Szép et al. 2017). According to Granat (1972) this equation could under estimate the concentrations of HCO_3^- at very high pH, when the calculated bicarbonate values are too high and do not match the ion balance. Also, tests where bicarbonate solutions were equilibrated with laboratory air gave

results that were in good agreement with calculated values. Concerning CO_3^{2-} we considered the same concentration of Ca^{2+} (WMO, 2004), since no direct method was applied for measuring these species.

$$[HCO_3^-] = 5.1/10^{6-pH} \quad (4)$$

Volume Weighted Mean and Neutralization Factor

We calculated the volume weighted mean (VWM) of the atmospheric deposition samples in order to consider the sample total volume. VWM was expressed through the relationship between the sum of the concentrations product of each species (X_i) found in the n samples by the respective volume (V_i) and the sum of all the samples volumes according to the equation 5 (Clarke et al. 2016).

$$VWM = \frac{\sum_{i=1}^{n}(X_i * V_i)}{\sum_{i=1}^{n} V_i} \quad (5)$$

For dry atmospheric deposition samples, which we added 50mL of deionized water due to precipitation absence, we considered that volume for calculations.

The neutralization factor (NF) or index was calculated using the equation 6 adapted from Huang et al.(2009) and Qiao et al. (2015):

$$NF = \frac{[NH_4^+]+2*[Ca^{2+}]}{[NO_3^-]+2*[SO_4^{2-}]} \quad (6)$$

where all the concentrations were used in $\mu molL^{-1}$.

RESULTS AND DISCUSSION

Validation and QA/QC Procedures

The total rainfall amount collected by bulk atmospheric deposition in the sampling period – March 2018 and February 2019 – reached 870 mm. Such precipitation value represents 67% of the rainfall volume obtained by the meteorological station from INMET (INMET 2019b). Moreover, such differences were associated with sample loss by evaporation and sampling period variation, which went from 7 to 14 days. Therefore, we can assume that most of the atmospheric processes were represented by the atmospheric deposition samples collected. Regarding weather conditions for the sampling period, we observed that from October to March (rainy season) a total precipitation of 1146.7mm; and from April to September (dry season) a total of 152.3mm were registered by INMET. Such values are below the climatological standard normal (1981 to 2010) by 8% and 30%, respectively. Thus, the sampling period showed drier conditions for Lavras

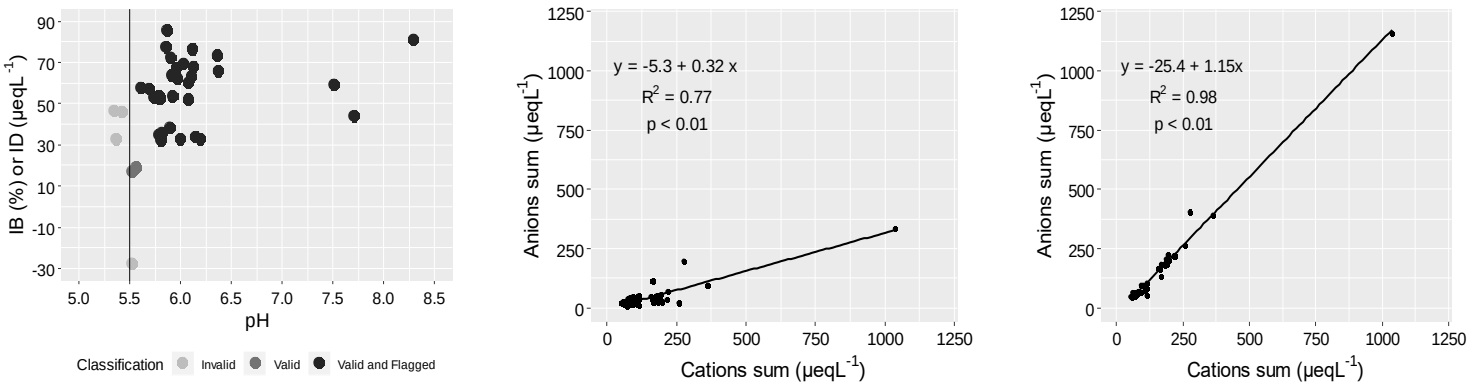

(a) (b) (c)

Fig.2 Ionic balance in bulk atmospheric deposition of Lavras city: (a) samples validation criteria from EMEP (n = 39) and the reference line represent a critical pH (5.5) value; (b) anions sum *vs*. cations sum (n = 34); (c) anions sum *vs.* cations sum considering the carbonate estimate (n = 34). Sampling period was between March 2018 and February 2019

city.

The pH values for the whole data set ranged from 5.34 to 8.29. Given the alkaline behavior of the samples, quality assurance and quality control (QA/QC) were verified applying the criteria from EMEP. Following the QA/QC, among the 39 atmospheric deposition events, 5 were invalid, 2 valid and 32 valid and flagged (Fig.2a). Only five invalid samples were rejected and not considered in the following discussion.

In order to verify the electroneutrality principle, the sum of anions *versus* cations plot was depicted in Fig.2b. In general, we observed a good and statistical significant linear fit (R^2 = 0.77 and p-value < 0.01) for the data set. In addition, the sum of cations was greater than the sum of anions, because the fitted line slope (value of 0.32 – Fig.2b) was lower than one. The anions deficit was expected in samples with pH values ranging from 5.5 to 6.0 (Schaug et al. 1997) and which could have been attributed to the lack of measurements of carbonate, bicarbonate and carboxylic acids concentration, such as acetic, formic and oxalic (Prathibha et al. 2010; Xu et al. 2011; Meng et al. 2019). In order to identify the carbonate deficit, an estimation of these species was carried out (WMO, 2004) and a new sum of cations *versus* anions plot was constructed (Fig.2c). It is noteworthy that adding the carbonate estimation to the sum of anions, the new angular coefficient presented a value closer tone with determination coefficient of 98% (p-value < 0.01). The bicarbonate estimation produced a poor

linear adjustment (slope = 0.04 andR^2 = -0.03 with p-value 0.92) and therefore we considered only the presence of carbonate in the bulk atmospheric deposition samples.

pH Distribution

The pH values distribution for the validated samples (n = 34), ranged from 5.52 (June/2019) to 8.29 (March/2019), with average of 5.92 (Fig.3). We considered 5.60 pH a critical value for rainwater acidity classification, due to the atmospheric CO_2 dissolution (Seinfeld and Pandis 1998; Zhao et al. 2013; Akpo et al. 2015). Therefore, most deposition samples (~94%) were alkaline, whereas, only 2 samples showed acidic behavior. Mixed behaviors regarding sample acidity were observed in Brazil. For instance, Alves et al. (2018) (n = 22) and Mimura et al.(2016) (n = 53) reported mean pH rainwater values of 5.94 and 6.56 in Campo Bom, Rio Grande do Sul and Juiz de Fora, Minas Gerais, respectively. These authors associated high pH values due to inputs of crustal aerosols in the atmosphere deposition, which contains a large fraction of carbonate and bicarbonate. In contrast, samples collected in São Paulo city (Leal et al. 2004) and Itabuna city (Araujo et al. 2015) registered slightly acidic pH values, 4.99 (n = 94) and 4.83 (n = 20), respectively.

Concerning the electrical conductivity (EC), the values ranged from 4.0 to 58.7μScm^{-1}, with an average of 14.5μScm^{-1}. The EC of bulk deposition was mainly attributed to the total soluble ionic components. Therefore, low EC values reflected a dilution of particulate matter and gases due to the increasing rainfall in the studied area (Zhang et al. 2007).

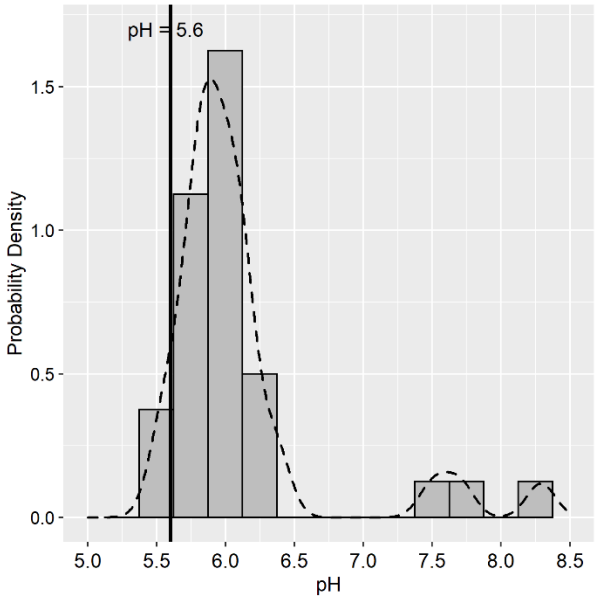

Fig.3 Histogram of the pH values of the 34 bulk atmospheric deposition samples in Lavras city, from March 2018 to February 2019. The vertical line refers to critical value for rainwater acidity classification (pH = 5.6) and the dotted line represents the probability density curve

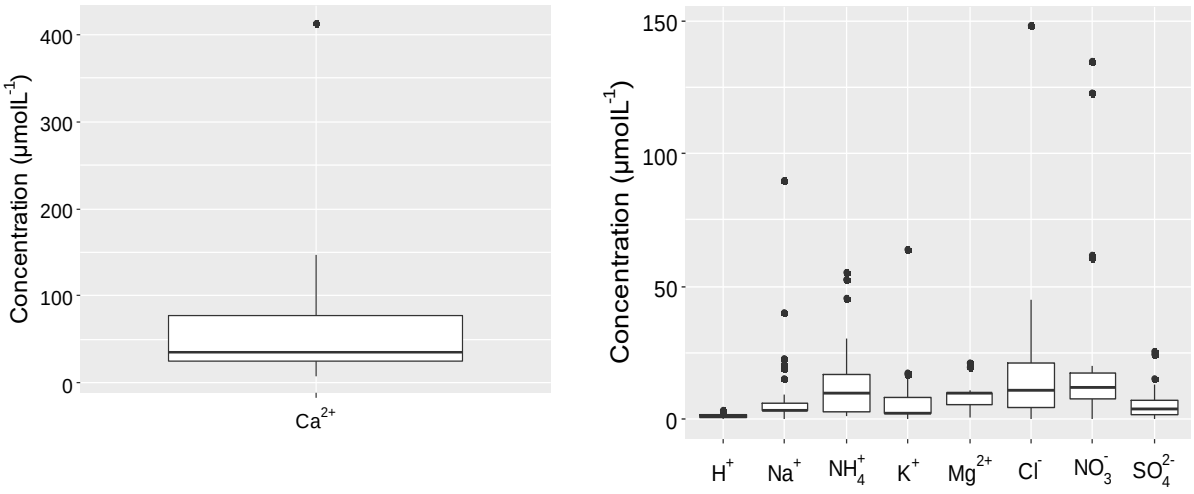

(a) (b)

Fig.4 Box and whisker plots for (a) calcium and (b) other ions identified and quantified in bulk atmospheric deposition in Lavras, from March 2018 to February 2019. Horizontal lines in the box represent the 25th, 50th and 75th percentile values

Ionic Chemical Composition

Among all the ions measured, Ca^{2+} was the dominant species, with greater variability (8.20 $\mu molL^{-1}$ – 413$\mu molL^{-1}$) (Fig.4a). The median value was 35.3 $\mu molL^{-1}$, almost four times higher than NH_4^+ (9.75$\mu molL^{-1}$), which was the second highest among the cations. Fig.4b shows the ions with lower concentrations. Regarding the anionic contribution, NO_3^- and Cl^- presented the highest concentrations, with medians of 12.0 and 10.8 $\mu molL^{-1}$, respectively. Also, some nitrate and chloride concentrations were around the range of calcium.

VWM concentrations were more amenable for comparisons and were calculated for all measured ions (Table 1).

Table 1. Seasonal VWM concentrations ($\mu molL^{-1}$) in bulk atmospheric deposition in Lavras, from March 2018 to February 2019

Season	N	Ca^{2+}	H^+	Na^+	NH_4^+	K^+	Mg^{2+}	Cl^-	NO_3^-	SO_4^{2-}
Autumn (MAM)	9	63.6	0.54	3.77	23.7	3.41	8.57	7.41	16.9	3.35
Winter (JJA)	5	46.5	1.52	6.60	5.23	8.91	8.31	16.3	11.4	11.7
Spring (SON)	11	35.2	0.92	9.13	10.7	2.56	8.63	13.8	8.25	1.97
Summer (DJF)	9	29.9	0.97	1.89	10.8	1.98	9.64	8.23	7.53	1.96
Annual	34	35.0	0.94	5.65	11.3	2.61	9.04	11.2	8.57	2.43

(MAM) = March, April, May; (JJA) = June, July, August; (SON) = September, October, November; (DJF) = December, January, February

For the whole sampling campaign, the ions profile in VWM (molar unit) are described in the following order: Ca^{2+} > NH_4^+ > Cl^- > Mg^{2+} > NO_3^- > Na^+ > K^+ > SO_4^{2-} > H^+. Ca^{2+} and NH_4^+ were the most abundant ions, representing ~53% of the total.

Regarding the ionic seasonality, Ca^{2+} had the highest VWM in all seasons, with an annual relative contribution of 40% (35.0μmolL^{-1}). In general, soil dust resuspension and cement manufacturing are considered the two major sources of Ca^{2+} to the atmosphere in urban areas (Da Conceição et al. 2011).This hypothesis is endorsed due to both Lavras' intense agricultural activity as well as soil properties, since calcium is a prominent constituent of soils correctives and fertilizers (Gomes et al. 2008). In addition, Lavras' industrial activities may influence the atmospheric deposition, specifically due to several cement plants across the county. Such influences may be perceived in the Table 1, where the Ca^{2+} concentrations were highest in the dry season (autumn and winter), with maximum value in autumn (63.6μmolL^{-1}).

NH_4^+ accounted for an annual relative contribution of 13% (11.3μmolL^{-1}). The presence of NH_4^+ can be directly attributed to an input of NH_3 in the atmosphere, mainly due to farming and agricultural sources (Losno et al. 1991; Araujo et al. 2015; Zeng et al. 2020). We observed that NH_4^+ concentrations were lower in the winter and this suggests a lower NH_3 emissions from agricultural activities during the dry season (Nogueira 1998).

K^+ presented very low concentrations (VWM = 2.61μmolL^{-1}). Celle-Jeanton et al. (2009) reported that concentrations of K^+ in atmospheric deposition could be due to either terrestrial potassium, marine aerosols or anthropogenic aerosols from biomass burning. From this perspective, we noted that K^+ showed VWM in winter (8.91μmolL^{-1}) ~3.4 times higher than VWM for entire studied period (2.61μmolL^{-1}), which may be attributed to the forest fires observed during the dry season.

An opposite behavior was observed for Mg^{2+}, which remained constant during the year. Its annual relative contribution was about 10% (9.04μmolL^{-1}), with maximum concentration in summer (9.64μmolL^{-1}). The ion Mg^{2+}has been considered originated mainly from the marine aerosols and/or crustal particles

sources (Vieira-Filho et al. 2015; Zhou et al. 2019), however given the distance from the ocean (~240km), such ion concentrations are likely to be from soil resuspension or cement industries sources.

Furthermore, Cl^- was the predominant water-soluble anion in bulk deposition, accounting for almost 13% (11.2 $\mu molL^{-1}$) of the total ions for the whole period. The average VWM concentration Na^+ was 5.65 $\mu molL^{-1}$, additionally, sea-salt composition is mainly related to the ions Cl^- and Na^+ (Niu et al. 2013). In the present study, the Cl^-/Na^+ ratio was 1.98, which was higher than the oceanic ratio (1.16), indicating a large excess of Cl^- and, therefore, suggesting an additional source of chlorine compounds in Lavras city. Also, considering the uncertainty given the high blank concentrations of Na^+, such Cl^- excess was substantial in the atmospheric samples.

Regarding atmospheric sulfur and nitrogen species, each ion showed different patterns. For instance, the SO_4^{2-} (2.43$\mu molL^{-1}$) showed small contribution compared to NO_3^- (8.57$\mu molL^{-1}$), which accounted for 3% and 10% of the total measured species, respectively. Their concentrations have been related to the large emissions of SO_2 and NO_x from the combustion of fossil fuel (Meng et al. 2019). Moreover, their low concentrations emphasize a low exhaust combustion emissions contribution by vehicle fleet, suggesting chemical processing and agricultural sources play a major role in Lavras city.

In order to identify the influence of local sources on the chemical composition of atmospheric deposition, an analysis of wind speed and direction during the study period was carried out (Fig.5). We observed persistent calm winds (<1.0 ms^{-1}) during entire study period (~24% - Fig.5a), with maximum percentages of calm events occurring in the summer (36.5%) and winter (29.6%) (Fig.5b). In addition, about 47% of winds come from the North-East (N-E) quadrant with average speed of 1.26 ms^{-1} (Fig.5a). All seasons showed similar profiles, indicating that the inter-seasonal variability of winds in the study region was insignificant (Fig.5b). Highlighted that most of industries are located in these N-E wind directions, such as mining companies that produces spodumene concentrate, tantalum, tin in ingots and feldspar (~67km to east), cement and limestone industries (~10km to northeast) and coffee plantations (~0.1km to northeast),

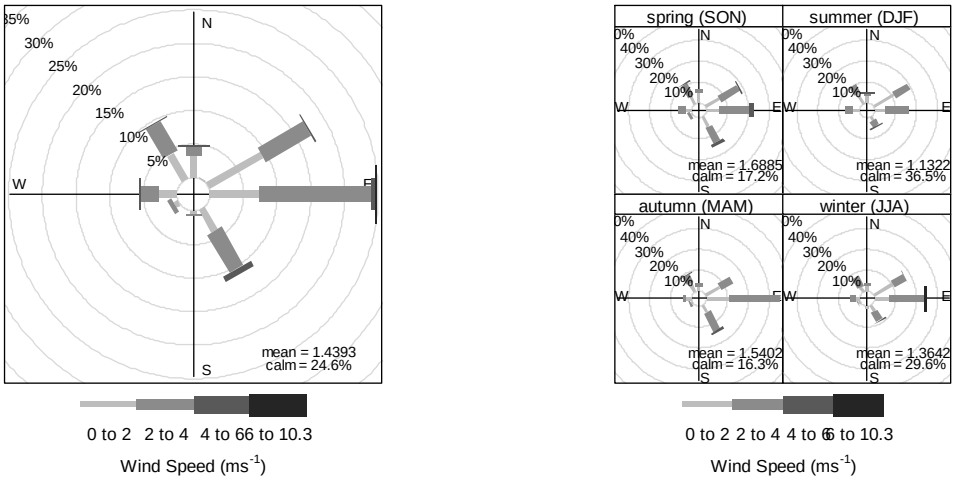

(a) (b)

Fig.5 Wind roses (a) for the entire study period and (b) for the seasons. The bars indicate the frequency (in %) of the wind for a given range of direction (in degrees), while the gray scale inside the bars describe the wind speed range (ms^{-1}). North, East, South and West are the cardinal directions that correspond to 0°/360°, 90°, 180° and 270°, respectively

suggesting that these sources may be contributing to the pollutants transport and deposition at the sampling point.

Acid Neutralization

We calculated the NF index in order to assess the influence of alkaline species in atmospheric samples. The NF values are shown in Table 2 segregated by seasons. The mean NF value was 6.4, no samples showed NF lower than 1 and only 2 samples were close to neutrality (NF = 1), implying that atmospheric samples were totally neutralized by carbonate and ammonia, measured in the samples such Ca^{2+} and NH_4^+, respectively. The overall seasonal NF pattern in samples was SON (spring) > MAM (autumn) > DJF (summer) > JJA (winter), from March 2018 to February 2019. The highest variation of NF values occurred in spring with interval of 1.1 and 25.3, such variation implies different atmospheric processes in this season. From September to November we reported 11 bulk deposition samples with a wide rain volume variability (~143mm), which hindered the neutralization reaction processes and led to inconstant NF values therein. Spring 2018 showed an anomalous rainfall amount of +28% in comparison with climatological data (1981 – 2010) in the region.

It is noteworthy that the sample with highest calcium concentration (413.2 $\mu molL^{-1}$ – Fig.4a) was collected in April

Table 2. Neutralization Factor (NF, represents the index average value) for all bulk deposition samples collected in Lavras city, Brazil, from March 2018 to February 2019

Season	N	NF	Maximum	Minimum	Standard Deviation
Autumn (MAM)	9	6.9	11	4.1	2.5
Winter (JJA)	5	3.4	4.7	1.3	1.6
Spring (SON)	11	7.8	25.3	1.1	6.8
Summer (DJF)	9	5.8	15.3	1.6	4.5
Annual	34	6.4	25.3	1.1	4.8

(MAM)=March, April, May; (JJA) = June, July, August; (SON) = September, October, November; (DJF) = December, January, February

(autumn), but the NF value was not so striking as expected (NF = 4.5). Therefore, this neutralization proxy is better suited for assessing the major chemical species interactions in rich alkaline atmosphere such as in Lavras city.

Figure 6 shows the linear regression analysis of acidity proxies (SO_4^{2-} and NO_3^-) and neutralizing species, Ca^{2+} (Fig.6a) and NH_4^+ (Fig.6b), for the bulk atmospheric deposition samples. As the application of the linear regression analysis suggests, Ca^{2+}precursor was the dominant neutralization substances in bulk atmospheric deposition, since its fitted line slope was higher than the unit (value of 2.6 – Fig.6a). However, we observed an opposite behavior in Fig.6b, in which slope value was 0.10, indicating that NH_4^+precursorwas insufficient to neutralize the major atmospheric acids. In addition, calcium carbonate was responsible for 54% of neutralization processes whereas ammonia for only 4%. Such observations are reasonable since the calcium presented the highest VWM for the entire period studied (Table 1). Similar phenomena have been observed in other sites in Brazil (Migliavacca et al. 2005; Alves et al. 2018) and worldwide (Singh et al. 2001; Herrera et al. 2009; Xiao 2016; Yatkin et al. 2016; Tositti et al. 2018). In contrast, some studies have been reporting the predominance of NH_4^+ (Zhang et al. 2007; Zeng et al. 2020)and Mg^{2+} (Deusdará et al. 2017) in the atmospheric neutralization process.

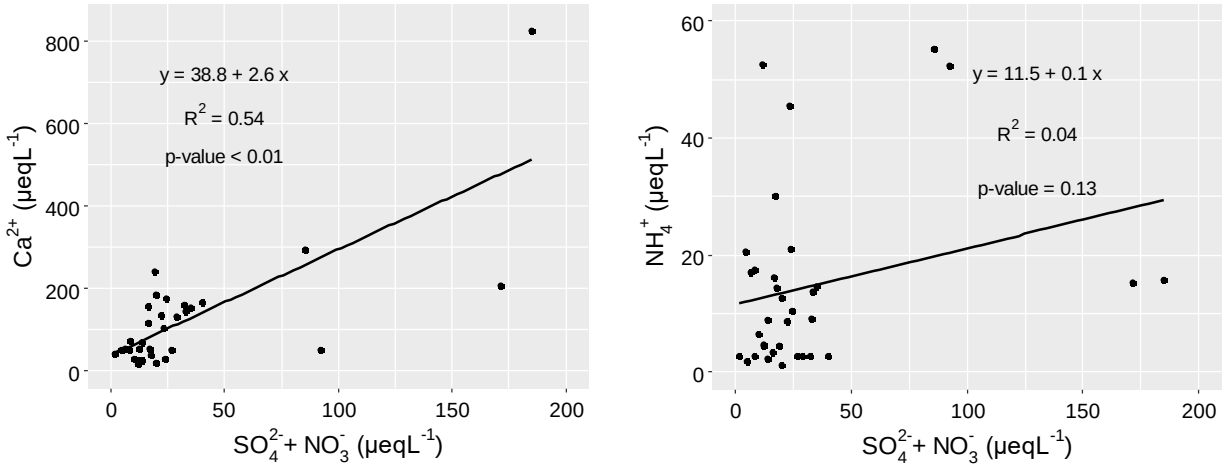

(a) (b)

Fig.6 Linear regression of acid precursors (SO_4^{2-} and NO_3^-) and neutralizing species precursors (a) Ca^{2+} and (b) NH_4^+ for bulk atmospheric deposition samples collected in Lavras city, Brazil, from March 2018 to February 2019

CONCLUSION

The systematic analysis of the atmospheric deposition is fundamental in the monitoring and evaluation of the chemical transformation processes and reaction routes, in the effort to improve identification and knowledge of the polluting sources. Bulk atmospheric deposition chemistry was assessed in a period with drier conditions in Lavras city, Southern Minas Gerais, Brazil, from March 2018 to February 2019. We highlighted the main characteristics of the bulk deposition below.

We observed that pH mean was 5.92 and most deposition samples (~94%) were alkaline (pH > 5.60). In addition, all samples showed NF higher than 1 and its mean value was 6.4.This may have been due to atmospheric inputs of crustal aerosols rich in calcium carbonate, neutralizing the samples acidity. This process was corroborated by the higher abundance of Ca^{2+} (40%) and NH_4^+ (13%) among all ions measured. Moreover, calcium precursor was accounted for 54% of neutralization processes, whereas ammonia was only 4%, indicating that neutralization of acidity in bulk deposition was much more related to $CaCO_3$ than to NH_3. Thus, the neutralizing pattern of the atmosphere in the study region suggested that bulk deposition chemical characteristic was controlled mainly by agricultural sources, including fertilizer production and application, and cement manufacturing across the county.

ACKNOWLEDGEMENTS

This study has been supported by *FAPEMIG*, *Fundação de Amparo à Pesquisa do Estado de Minas Gerais*.

REFERENCES

Akpo AB, Galy-Lacaux C, Laouali D, et al (2015) Precipitation chemistry and wet deposition in a remote wet savanna site in West Africa: Djougou (Benin). Atmos Environ 115:110–123. https://doi.org/10.1016/j.atmosenv.2015.04.064

Almeida GLMD, Ferreira EC da M, Mendes DJ da S, et al (2017) Estudo sobre as regiões de planejamento de Minas Gerais: Sul de Minas Gerais. Belo Horizonte

Alves DD, Backes E, Rocha-Uriartt L, et al (2018) Chemical composition of rainwater in the Sinos River Basin, Southern Brazil: a source apportionment study. Environ Sci Pollut Res 25:24150–24161. https://doi.org/10.1007/s11356-018-2505-1

Araujo TG, Souza MFL, De Mello WZ, Da Silva DML (2015) Bulk Atmospheric Deposition of Major Ions and Dissolved Organic Nitrogen in the Lower Course of a Tropical River Basin, Southern Bahia, Brazil. J Braz Chem Soc 26:1692–1701. https://doi.org/10.5935/0103-5053.20150143

Avila A, Alarco M (1999) Relationship between precipitation chemistry and meteorological situations at a rural site in NE Spain. Atmos Environ 33:1663–1677. https://doi.org/doi:10.1016/s1352-2310(98)00341-0

Carslaw DC, Ropkins K (2012) openair --- An R package for air quality data analysis. Environ Model Softw 27--28:52--61. https://doi.org/10.1016/j.envsoft.2011.09.008

Carvalho VSB, Freitas ED, Martins LD, et al (2015) Air quality status and trends over the Metropolitan Area of São Paulo, Brazil as a result of emission control policies. Environ Sci Policy 47:68–79. https://doi.org/10.1016/j.envsci.2014.11.001

Celle-Jeanton H, Travi Y, Loÿe-Pilot MD, et al (2009) Rainwater chemistry at a Mediterranean inland station (Avignon, France): Local contribution versus long-range supply. Atmos Res 91:118–126. https://doi.org/10.1016/j.atmosres.2008.06.003

Cheng N, Cheng B, Li S, Ning T (2019) Effects of meteorology and emission reduction measures on air pollution in Beijing during heating seasons. Atmos Pollut Res 10:971–979. https://doi.org/10.1016/j.apr.2019.01.005

Clarke N, Žlindra D, Ulrich E, et al (2016) Manual on methods and criteria for harmonized sampling, assessment, monitoring and analysis of the effects of air pollution on forests - Part XIV. Eberswalde, Germany

Da Conceição FT, Sardinha D de S, Navarro GRB, et al (2011) Composição química das águas pluviais e deposição atmosférica anual na bacia do alto sorocaba (SP). Quim Nova 34:610–616. https://doi.org/10.1590/S0100-40422011000400011

De Mello WZ, De Almeida MD (2004) Rainwater chemistry at the summit and southern flank of the Itatiaia massif, Southeastern Brazil. Environ Pollut 129:63–68. https://doi.org/10.1016/j.envpol.2003.09.026

De Souza PA, De Mello WZ, Da Silva JJN, et al (2017) Deposições Atmosféricas Úmida, Seca e Total de Nitrogênio Inorgânico Dissolvido no Estado do Rio de Janeiro de. Rev Virtual Quim 9:2052–2066. https://doi.org/10.21577/1984-6835.20170122

De Souza PA, De Mello WZ, Maldonado J, Evangelista H (2006) Composição química da chuva e aporte atmosférico na Ilha Grande, RJ. Quim Nova 29:471–476. https://doi.org/10.1590/S0100-40422006000300013

DENATRAN (2018) Frota de Veículos - 2018. In: Ministério da Infraestrutura.

https://www.gov.br/infraestrutura/pt-br/assuntos/transito/conteudo-denatran/frota-de-veiculos-2018. Accessed 1 Jun 2019

Deusdará KRL, Forti MC, Borma LS, et al (2017) Rainwater chemistry and bulk atmospheric deposition in a tropical semiarid ecosystem: the Brazilian Caatinga. J Atmos Chem 74:71–85. https://doi.org/10.1007/s10874-016-9341-9

Duan L, Chen X, Ma X, et al (2016) Atmospheric S and N deposition relates to increasing riverine transport of S and N in southwest China: Implications for soil acidification. Environ Pollut 218:1191–1199. https://doi.org/10.1016/j.envpol.2016.08.075

Fornaro A (1991) Chuva ácida em São Paulo: caracterização química de amostras integradas e sequenciais de deposição úmida. Universidade de São Paulo

Fornaro A, Gutz IGR (2006) Wet deposition and related atmospheric chemistry in the São Paulo metropolis, Brazil: Part 3. Trends in precipitation chemistry during 1983 – 2003. Atmos Environ 40:5893–5901. https://doi.org/10.1016/j.atmosenv.2005.12.007

Gomes MAF, Souza MD, Boeira RC, Toledo LG (2008) Nutrientes vegetais no meio ambiente: ciclos bioquímicos, fertilizantes e corretivos, 2nd edn. Ministério da Agricultura, Pecuária e Abastecimento, Jaguariúna, São Paulo

Granat L (1972) On the relation between pH and the chemical composition in atmospheric precipitation. Tellus, Ser B Chem Phys Meteorol 24:550–560. https://doi.org/http://dx.doi.org/10.3402/tellusa.v24i6.10682

Grosjean E, Rasmussen RA, Grosjean D (1999) Toxic air contaminants in Porto Alegre, Brazil. Environ Sci Technol 33:1970–1978. https://doi.org/10.1021/es980578x

Herrera J, Rodríguez S, Baéz AP (2009) Chemical composition of bulk precipitation in the metropolitan area of Costa Rica, Central America. Atmos Res 94:151–160. https://doi.org/10.1016/j.atmosres.2009.05.004

Huang DY, Xu YG, Peng P, et al (2009) Chemical composition and seasonal variation of acid deposition in Guangzhou, South China: Comparison with precipitation in other major Chinese cities. Environ Pollut 157:35–41. https://doi.org/10.1016/j.envpol.2008.08.001

IBGE (2018) Cidades e Estados: Lavras. https://cidades.ibge.gov.br/brasil/mg/lavras. Accessed 1 Jun 2019

IEMA (2014) 1º Diagnóstico da rede de monitoramento da qualidade do ar no Brasil. Cariacica - Espírito Santo

INMET (2019a) Normais Climatológicas do Brasil. In: Ministério da Agric. Pecuária e Abast. https://portal.inmet.gov.br/normais. Accessed 15 Sep 2019

INMET (2019b) Banco de Dados Meteorológicos para Ensino e Pesquisa. In: Ministério da Agric. Pecuária e Abast. https://bdmep.inmet.gov.br/. Accessed 2 May 2020

INPE (2019) Banco de Dados Meteorológicos. http://bancodedados.cptec.inpe.br/downloadBDM/. Accessed 15 Nov 2020

Lara LBLS, Artaxo P, Martinelli LA, et al (2001) Chemical composition of rainwater and anthropogenic influences in the Piracicaba River Basin, Southeast Brazil. Atmos Environ 35:4937–4945. https://doi.org/10.1016/S1352-2310(01)00198-4

Leal TFM, Fontenele APG, Pedrotti JJ, Fornaro A (2004) Composição iônica majoritária de águas de chuva no centro da cidade de São Paulo. Quim Nova 27:855–861. https://doi.org/10.1590/s0100-40422004000600003

Lenzi E, Favero LOB (2019) Introdução à Química da Atmosfera - Ciência, Vida e Sobrevivência, 2nd edn. Grupo Gen, Rio de Janeiro

Losno R, Bergametti G, Carlier P, Mouvier G (1991) Major ions in marine rainwater

with attention to sources of alkaline and acidic species. Atmos Environ Part A, Gen Top 25:763–770. https://doi.org/10.1016/0960-1686(91)90074-H

Mahapatra PS, Sinha PR, Boopathy R, et al (2018) Seasonal progression of atmospheric particulate matter over an urban coastal region in peninsular India: Role of local meteorology and long-range transport. Atmos Res 199:145–158. https://doi.org/10.1016/j.atmosres.2017.09.001

Martins EH, Nogarotto DC, Mortatti J, Pozza SA (2019) Chemical composition of rainwater in an urban area of the southeast of Brazil. Atmos Pollut Res 10:520–530. https://doi.org/10.1016/j.apr.2018.10.003

Massambani O, Andrade F (1994) Seasonal behavior of tropospheric ozone in the Sao Paulo (Brazil) metropolitan area. Atmos Environ 28:3165–3169. https://doi.org/10.1016/1352-2310(94)00152-B

Meng Y, Zhao Y, Li R, et al (2019) Characterization of inorganic ions in rainwater in the megacity of Shanghai: Spatiotemporal variations and source apportionment. Atmos Res 222:12–24. https://doi.org/10.1016/j.atmosres.2019.01.023

Migliavacca D, Teixeira EC, Wiegand F, et al (2005) Atmospheric precipitation and chemical composition of an urban site, Guaíba hydrographic basin, Brazil. Atmos Environ 39:1829–1844. https://doi.org/10.1016/j.atmosenv.2004.12.005

Mimura AMS, Almeida JM, Vaz FAS, et al (2016) Chemical composition monitoring of tropical rainwater during an atypical dry year. Atmos Res 169:391–399. https://doi.org/10.1016/j.atmosres.2015.11.001

Mo Z, Fu Q, Zhang L, et al (2018) Acute effects of air pollution on respiratory disease mortalities and outpatients in Southeastern China. Springer US

Niu H, He Y, Zhu G, et al (2013) Environmental implications of the snow chemistry from Mt. Yulong, southeastern Tibetan Plateau. Quat Int 313–314:168–178. https://doi.org/10.1016/j.quaint.2012.11.019

Niu Y, Li X, Pu J, Huang Z (2018) Organic acids contribute to rainwater acidity at a rural site in eastern China. Air Qual Atmos Heal 11:459–469. https://doi.org/10.1007/s11869-018-0553-9

Nogueira FAA (1998) A Cultura do Café no Sul de Minas Gerais. Universidade Federal de Santa Catarina

Pleijel H, Grundstrom M, Karlsson GP, et al (2016) A method to assess the inter-annual weather-dependent variability in air pollution concentration and deposition based on weather typing. Atmos Environ 126:200–210. https://doi.org/10.1016/j.atmosenv.2015.11.053

Prathibha P, Kothai P, Saradhi I V., et al (2010) Chemical characterization of precipitation at a coastal site in Trombay, Mumbai, India. Environ Monit Assess 168:45–53. https://doi.org/10.1007/s10661-009-1090-7

Pye HOT, Nenes A, Alexander B, et al (2020) The Acidity of Atmospheric Particles and Clouds. Atmos Chem Phys 20:4809–4888. https://doi.org/10.5194/acp-20-4809-2020

Qiao X, Xiao W, Jaffe D, et al (2015) Atmospheric wet deposition of sulfur and nitrogen in Jiuzhaigou National Nature Reserve, Sichuan Province, China. Sci Total Environ 511:28–36. https://doi.org/10.1016/j.scitotenv.2014.12.028

R Core Team (2019) R: A Language and Environment for Statistical Computing

Schaug J, Semb A, Hjellbrekke A-G, et al (1997) Data quality and quality assurance report. Kjeller, Norway

Seinfeld JH, Pandis SN (1998) Atmospheric Chemistry and Physics: From Air

Pollution to Climate Change, 2nd edn. John Wiley & Sons, Inc., Hoboken, New Jersey

Singh SP, Khare P, Satsangi GS, et al (2001) Rainwater composition at a regional representative site of a semi-arid region of India. Water Air Soil Pollut 127:93–108. https://doi.org/10.1023/A:1005295215338

Sun X, Wang Y, Li H, et al (2016) Organic acids in cloud water and rainwater at a mountain site in acid rain areas of South China. Environ Sci Pollut Res 23:9529–9539. https://doi.org/10.1007/s11356-016-6038-1

Szép R, Mateescu E, Nechifor AC, Keresztesi Á (2017) Chemical characteristics and source analysis on ionic composition of rainwater collected in the Carpathians "Cold Pole," Ciuc basin, Eastern Carpathians, Romania. Environ Sci Pollut Res 24:. https://doi.org/10.1007/s11356-017-0318-2

Ti C, Gao B, Luo Y, et al (2018) Dry deposition of N has a major impact on surface water quality in the Taihu Lake region in southeast China. Atmos Environ 190:1–9. https://doi.org/10.1016/j.atmosenv.2018.07.017

Tositti L, Pieri L, Brattich E, et al (2018) Chemical characteristics of atmospheric bulk deposition in a semi-rural area of the Po Valley (Italy). J Atmos Chem 75:97–121. https://doi.org/10.1007/s10874-017-9365-9

Vet R, Artz RS, Carou S, et al (2014) A global assessment of precipitation chemistry and deposition of sulfur, nitrogen, sea salt, base cations, organic acids, acidity and pH, and phosphorus. Atmos Environ 93:3–100. https://doi.org/10.1016/j.atmosenv.2013.10.060

Vieira-Filho M, Lehmann C, Fornaro A (2015) Influence of local sources and topography on air quality and rainwater composition in Cubatão and São Paulo, Brazil. Atmos Environ 101:200–208. https://doi.org/10.1016/j.atmosenv.2014.11.025

Vieira-Filho M, Pedrotti JJ, Fornaro A (2016) Water-soluble ions species of size-resolved aerosols: Implications for the atmospheric acidity in São Paulo megacity, Brazil. Atmos Res 181:281–287. https://doi.org/10.1016/j.atmosres.2016.07.006

Wickham H (2016) ggplot2: Elegant Graphics for Data Analysis

WMO (2004) Manual for the Gaw Precipitation Chemistry Programme: Guidelines, Data Quality Objectives and Standard Operating Procedures

Xiao J (2016) Chemical composition and source identification of rainwater constituents at an urban site in Xi'an. Environ Earth Sci 75:1–12. https://doi.org/10.1007/s12665-015-4997-z

Xing J, Song J, Yuan H, et al (2017) Fluxes, seasonal patterns and sources of various nutrient species (nitrogen, phosphorus and silicon) in atmospheric wet deposition and their ecological effects on Jiaozhou Bay, North China. Sci Total Environ 576:617–627. https://doi.org/10.1016/j.scitotenv.2016.10.134

Xu H, Bi XH, Feng YC, et al (2011) Chemical composition of precipitation and its sources in Hangzhou, China. Environ Monit Assess 183:581–592. https://doi.org/10.1007/s10661-011-1963-4

Yatkin S, Adali M, Bayram A (2016) A study on the precipitation in Izmir, Turkey: chemical composition and source apportionment by receptor models. J Atmos Chem 73:241–259. https://doi.org/10.1007/s10874-015-9325-1

Zeng J, Han G, Wu Q, Tang Y (2020) Effects of agricultural alkaline substances on reducing the rainwater acidification: Insight from chemical compositions and calcium isotopes in a karst forests area. Agric Ecosyst Environ 290:106782.

https://doi.org/10.1016/j.agee.2019.106782

Zhan X, Bo Y, Zhou F, et al (2017) Evidence for the Importance of Atmospheric Nitrogen Deposition to Eutrophic Lake Dianchi, China. Environ Sci Technol 51:6699–6708. https://doi.org/10.1021/acs.est.6b06135

Zhang M, Wang S, Wu F, et al (2007) Chemical compositions of wet precipitation and anthropogenic influences at a developing urban site in southeastern China. Atmos Res 84:311–322. https://doi.org/10.1016/j.atmosres.2006.09.003

Zhang Y, Ding A, Mao H, et al (2016) Impact of synoptic weather patterns and inter-decadal climate variability on air quality in the North China Plain during 1980–2013. Atmos Environ 124:119–128. https://doi.org/10.1016/J.ATMOSENV.2015.05.063

Zhao M, Li L, Liu Z, et al (2013) Chemical Composition and Sources of Rainwater Collected at a Semi-Rural Site in Ya'an, Southwestern China. Atmos Clim Sci 03:486–496. https://doi.org/10.4236/acs.2013.34051

Zhou X, Xu Z, Liu W, et al (2019) Chemical composition of precipitation in Shenzhen, a coastal mega-city in South China: Influence of urbanization and anthropogenic activities on acidity and ionic composition. Sci Total Environ 662:218–226. https://doi.org/10.1016/j.scitotenv.2019.01.096

2. ARTIGO II – SOURCE APPORTIONMENT OF ATMOSPHERIC DEPOSITION SPECIES IN AN AGRICULTURAL BRAZILIAN REGION USING POSITIVE MATRIX FACTORIZATION

Source apportionment of atmospheric deposition species in an agricultural Brazilian region using positive matrix factorization

Jaqueline Natiele Pereira [1] & Adalgiza Fornaro[2] & Marcelo Vieira-Filho[1*]

1 Departamento de Engenharia Ambiental (DAM), Universidade Federal de Lavras (UFLA), Campus da UFLA, 37200-000, Lavras, Minas Gerais, Brazil

2 Departamento de Ciências Atmosféricas, Instituto de Astronomia, Geofísica e Ciências (IAG), Atmosféricas da Universidade de São Paulo (USP), Rua do Matão, 1226, 05508-090, Cidade, Universitária, São Paulo, SP, Brazil

*e-mail marcelo.filho@ufla.br, phone: (+55)11-9 8598 6567

Abstract

We investigated the influence of natural and anthropogenic sources on bulk atmospheric deposition chemistry, from March 2018 until October 2019, in a Brazilian agricultural area. The pH mean value was 5.95 (5.52–8.29) and most deposition samples (~98%) were alkaline (pH > 5.60). The ions profile, as a volume weighted mean (VWM), was described as follows: Ca^{2+} (46.6) > Cl^- (21.6) > Na^+ (18.7) > NH_4^+ (13.6) > Mg^{2+} (13.3) > NO_3^- (9.76) > K^+ (5.93) > SO_4^{2-} (4.24) > H^+ (0.89) $\mu molL^{-1}$. Ca^{2+} was the predominant species, accounting for 35% of the total ionic species distribution. We applied the EPA PMF 5.0 model to quantify the measured ionic species sources and found an optimal 3-factor solution, which demonstrated the influence of anthropogenic and natural sources. The identified sources were neutralization processes, crustal processes and fires, and fertilizer production and application, which accounted for 44%, 34% and 17% of the total source's contribution.

Keywords Bulk Atmospheric Deposition; Source Apportionment; Positive Matrix Factorization; Brazil.

INTRODUCTION

Because of rapid economic development, increased energy consumption, anthropogenic activities, and industrialization over the last centuries, the atmospheric accumulation of several gases and aerosols was inevitable (Kamani and Hoseini, 2014). These pollutants move from the atmosphere to Earth's surface mainly by bulk deposition processes, which encompasses wet (in-cloud and below-cloud scavenging processes) and dry deposition (scavenging processes in the absence of precipitation) (Araujo et al., 2015). Therefore, atmospheric deposition exerts a key role in terrestrial and aquatic biogeochemical processes, since it is a main cycling pathway of nutrients and pollutants, which may enter into ecosystems causing significant impacts, such as eutrophication and soil acidity (Duan et al., 2016; Xing et al., 2017).

Atmospheric deposition chemistry has been widely studied in many areas worldwide and provides useful information that feeds several receptor models to identify anthropogenic and natural source apportionment (Deusdará et al., 2017; Sun et al., 2016; Szép et al., 2019; Zhou et al., 2019). Broadly, natural origin is related to marine salt and soil dust, while anthropogenic ones are mainly from fossil fuel combustion, industrial processes, and agricultural production (Rastegari Mehr et al., 2019). Moreda-Piñeiro et al. (2014) assessed rainwater samples in Spain and reported that Cl^-, Na^+, and Mg^{2+} were linked to sea salt, while SO_4^{2-} and Ca^{2+} were released from a terrestrial crustal source. Also, in this study, NH_4^+ and NO_3^- were mainly attributed to agricultural activity. On the other hand, (Garaga et al., 2020) investigated chemical components sources in rainwater samples collected in Guwahati, India, and found that Na^+, Cl^-, Ca^{2+} and K^+ characterized a marine source, and F^-, SO_4^{2-}, NO_3^- and Cl^- was associated with coal combustion.

Statistical techniques, such as Factor Analysis (FA), Principal Component Analysis (PCA), Chemical Mass Balance (CMB), and Positive Matrix Factorization (PMF), have been employed as receptor models for the identification of the main sources of pollutants (Anil et al., 2017; Kuzu and Saral, 2017; Zhang et al., 2014). According to Paatero (1997), PMF analysis is more quantitative and suitable for physical, chemical and environmental

sciences than models based on PCA or FA. In this perspective, PMF is commonly applied to airborne particles and atmospheric gases, but rarely to atmospheric deposition due to its complexity (Khan et al., 2016; Sofowote et al., 2015). Despite that, some studies obtained satisfactory results when applying PMF to assess source apportionment in atmospheric deposition samples (Qiao et al., 2015; Roy et al., 2016; Yatkin et al., 2016).

Considering the absence of an established network for routinely monitoring wet and dry deposition in Brazil (Alves et al., 2018; Lara et al., 2001), a study was carried out in the Southern region of Minas Gerais, which is an important economic region responsible for 21.8% of agricultural commodities (mainly from coffee-producing regions), and also accounts for about 12% of the state's Gross Domestic Product (Almeida et al., 2017). We investigated the influence of natural and anthropogenic sources on bulk atmospheric deposition chemistry in Lavras, a city in Southern Minas Gerais, using the receptor model PMF.

METHODS

Study Area

Lavras is located in the Southern Minas Gerais state (21°13′45.3″ S and 44°58′32.4″ W), Brazil, 241 km from the Atlantic Ocean (in a straight line), with an area of 564.744 km^2 and altitude of 919 m (Figure 1). Its population of 102,728 inhabitants occupies fifth place among the most populous city in Southern Minas Gerais (IBGE, 2018). Regarding weather conditions, the city has a mean annual (1981–2010) temperature of 20.3 °C, with minimum (16.9 °C) values in July and maximum (22.8 °C) in February. The annual rainfall of 1461.8 mm is mainly concentrated in two well-defined periods: (i) a rainy season from October to March (covering 85% of total rainfall), and (ii) a dry one from April to September (INMET, 2019a).

Lavras is generally known for its agricultural production, since about 19% (107 km^2) of its total area is associated with agricultural activities, mainly coffee production (42% of the planted area) (IBGE, 2019). From this perspective, the sampling point is specifically located within the Federal University of Lavras campus, where ~57% (2.71km^2) of the area is destined for agriculture and 100m northeast of the sampling point are coffee plantations. Furthermore, according to

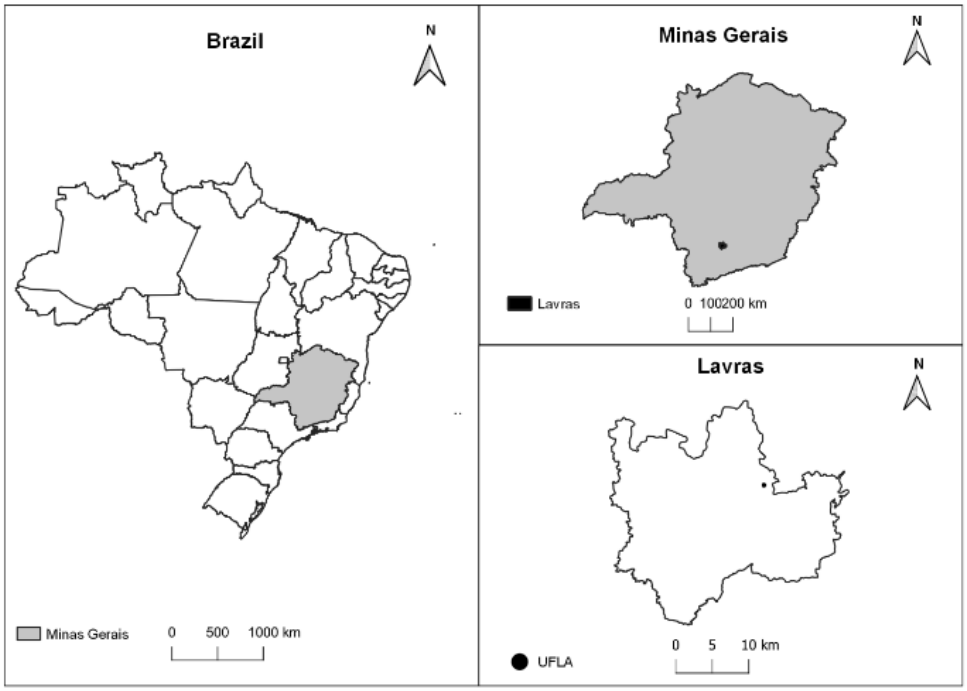

Figure 1. Geographical location of sampling site (UFLA) in Lavras, Southern Minas Gerais state, Brazil.

estimates made by the Brazilian Institute of Geography and Statistics, the average application rate of nitrogen, potassium and phosphate fertilizers in the region of Minas Gerais is around 110, 103 and 84.0 $kgha^{-1}year^{-1}$, respectively (IBGE, 2014). It is also important to note that Lavras' soil is predominantly classified as Dystrophic Red-Yellow Oxisol (RYOd1) and Eutrophic Red-Yellow Argisol (RYAe12). RYOd1 soils are suitable for tillage but are naturally acidic (EMBRAPA, 2006). Therefore, the liming process is common, in which lime is applied to correct soil acidity for agricultural purposes.

Lavras is also influenced by other anthropogenic activities, including industrial activities, transport, biomass burning mainly during the dry period and livestock. Regarding the industrial segments, among the most important and close to the sampling point are dairy products (~2km to the northwest), lime mining companies (~5km to the northwest), cement and limestone industries (~10km to the northeast), mining and fertilizer production (50km northeast) and mining companies producing spodumene concentrate, tantalum, tin ingots and feldspar (~67km east). In addition, small metallurgical and chemical industries are part of the industrial complex that operates in the Lavras city. The vehicle fleet in Lavras is

about 15 years old on average and categorically made up of 62% of passenger cars produced before 2010 and 14% before 1990 (DENATRAN, 2019). In addition, the vehicular fleet has about 50 thousand light-duty vehicles, comprising of 54% automobiles and 26% motorcycles both burning gasohol (73% gasoline + 27% anhydrous ethanol or 100% hydrated ethanol), being the other remaining 20% heavy-duty vehicles, busses and trucks, both burning diesel with 7% of biodiesel (soya) (DENATRAN, 2019).

Sample Collection and Analytical Procedures

A total of 59 bulk atmospheric deposition samples were collected for about one week periods, between March 2018 and October 2019, using a handmade collector composed of a high-density polyethylene bucket (NALGON) of 10 L with a collecting area of 439 cm^2. In order to attenuate the solar radiation effects, the collector lateral surface was protected by sun-protective PVC structure, and, to reduce litter fall in samples, the collector was covered with a nylon mesh and also fixed on a support at 1.5 m above the ground level (WMO, 2004). It is noteworthy that the entire collection device was installed on the Federal University of Lavras (UFLA) campus, close to the automatic weather station of Lavras, belonging to the National Institute of Meteorology (INMET), and remained continuously open to the field for dry and wet deposition collection. Regarding dry only atmospheric samples, a 50 mL of deionized water was added in order to analyze soluble species.

After each collection, the samples were divided into two parts. In a fraction of the samples, pH was measured using a pH meter (AKSO AK model 151), calibrated with buffer solutions (pH 4.0 and 7.0). The other sample aliquot was filtered with a 0.22 μm diameter membrane (Millex), stored in pre-cleaned polyethylene bottles kept at −18 °C prior to ion chromatography (IC) analysis (Metrohm model 851) with anionic column (Metrosep ASupp5–250 mm × 4 mm) and cationic column (Metrosep C2 150–150 × 4 mm). The species quantified by IC were calcium (Ca^{2+}), ammonium (NH_4^+), magnesium (Mg^{2+}), sodium (Na^+), potassium (K^+), nitrate (NO_3^-), chloride (Cl^-) and sulfate (SO_4^{2-}). Analytical quantification was performed by using an external calibration curve from the standard concentrations for each ion. Detection limits (DL) values were

calculated from the parameters obtained from the analysis, by the method of the least squares, from the calibration curve (y = a + bx) and corresponded to the white sign (or linear coefficient) plus 3 times the standard deviation (sd) of the angular coefficient ($sd_{y/x}$), that is, DL = a + 3 $sd_{y/x}$. The DL values for all species evaluated were 0.04, 0.05, 0.07, 0.09, 0.12, 0.15, 0.29, 0.81 $\mu molL^{-1}$ for K^+, Cl^-, NH_4^+, SO_4^{2-}, Na^+, NO_3^-, Mg^{2+} and Ca^{2+}, respectively, being the quantification limit (QL) ten times the DL values.

In order to estimate the uncertainties aside from the detection limits, blank sample analysis was carried out through the experimental campaign. The blank sample concentrations were quantified, reaching average concentrations lower than 0.8 $\mu molL^{-1}$, except for calcium (Ca^{2+}) and sodium (Na^+) which showed values of 3.9 and 9.0 $\mu molL^{-1}$, respectively, for some blanks. Considering the blank concentrations as the bias, we calculated the median percentage error for all the ions between 1.3 and 8.5%. Blank concentrations were subtracted from sample concentrations collected in the same period.

Data Set Validation

We applied the Cooperative Programme for Monitoring and Evaluation of Long-Range Transmission of Air Pollutants in Europe (EMEP) quality criteria, presented in the Manual for the GAW Precipitation Chemistry Programme (WMO, 2004) and the invalid samples were excluded. The criteria are suitable for samples with poor ion balances due to samples alkalinity and its specific details were previous described elsewhere (Pereira et al., 2021; Schaug et al., 1997; WMO, 2004).

In addition, we verified the principle of electroneutrality (charge balance) for the validate data set. The equivalent ionic ratio between the sum of anions to the sum of cations is expected to be close to unity, whether all the major ionic species present in the samples were analyzed (WMO, 2004). The charge balance was evaluated based on a ∑anions/∑cations ratio, in units of μeqL^{-1}, where $\sum cations = [H^+] + [NH_4^+] + [Na^+] + [K^+] + [Ca^{2+}] + [Mg^{2+}]$ and $\sum anions = [Cl^-] + [NO_3^-] + [SO_4^{2-}]$. It is noteworthy that H^+ values were obtained indirectly from the pH values.

Volume Weighted Mean

The volume weighted mean (VWM) was calculated as follows (Eq. 1):

$$VWM = \frac{\sum_{i=1}^{n}(X_i * V_i)}{\sum_{i=1}^{n} V_i} (1)$$

where Xi is the ionic concentration of individual chemical species (μmolL^{-1})and Vi and n are the amount of rainwater for each sample (L) and the total number of samples, respectively (Akpo et al., 2015). For dry atmospheric deposition samples, which we added 50 mL of deionized water due to precipitation absence, we considered that volume for calculations.

Positive Matrix Factorization

We identified the sources of pollutants and their relative contributions using Positive Matrix Factorization (PMF; version 5.0; US EPA Research, Durham – NC, USA) software made available by the United States Environmental Protection Agency (US EPA), which consists of a mathematical receptor model (US-EPA, 2018). The model software is available free at https://www.epa.gov/air-research/positive-matrix-factorization-model-environmental-data-analyses.

In general, a receptor model aims to solve the chemical mass balance between the species' measured concentrations and the source profiles (US-EPA, 2014). In this sense, the PMF model decomposes a matrix of sample data into one matrix of factor profiles (F) and another of factor contributions (G). Then, for a data matrix X of n samples by m chemical species, the model will identify the number of factors p, the species profile f_k of each factor k, and the amount of mass g_k contributed by each factor k to each individual sample, according to Equation (1):

$$X_{ij} = \sum_{k=1}^{p} g_{ik} f_{kj} + e_{ij} (1)$$

Where *i* and *j* are the rows and columns of *X*, g_{ik} is the contribution of the source *k* to the sample *i*, f_{kj} is the concentration of the species *j* from the source *k* and e_{ij} is the residual for each sample/species.

The factor contributions and profiles are simultaneously determined by the PMF model, using an iterative optimization technique that seeks to minimize the Q function (Equation (2)), with non-negativity constraints, i.e., $g_{ik} > 0$ and $f_{kj} > 0$ (Paatero, 1997; Paatero and Tapper, 1994).

$$Q = \sum_{i=1}^{n}\sum_{j=1}^{m}\left[\frac{e_{ij}}{u_{ij}}\right]^2 = \sum_{i=1}^{n}\sum_{j=1}^{m}\left[\frac{X_{ij} - \sum_{k=1}^{p} g_{ik} f_{kj}}{u_{ij}}\right]^2 (2)$$

where u_{ij} are uncertainties, which is a combination of measurement error and the variability in the source profile value, allowing each data value to be individually

weighted. The uncertainties (u_{ij}) for data with values below and above the DL were calculated according to Equations (3) and (4), respectively (Reff et al., 2007; US-EPA, 2014).

$$u_{ij} = 5\frac{DL_{ij}}{6} \quad (3)$$

$$u_{ij} = \sqrt{(Error\ Fraction * Concentração_{ij})^2 + (0.5 * DL_{ij})^2} \quad (4)$$

where the error fraction was estimated at 20% (Ye et al., 2018).

Input Data Quality

The quality of input data was assessed based on the signal-to-noise ratio (S/N; Eq.5), which analyze if the uncertainties are not too large in relation to the measurements of the chemical species. From S/N values the species were categorized as strong when S/N > 2.0 and as weak in the cases that S/N ranged from 0.2 to 2.0. Species with S/N < 0.2 or values below DL greater than 50% were categorized as bad in quality and were excluded from the PMF analysis. It is noteworthy that classifying a species as weak implies tripling its uncertainty (Rastegari Mehr et al., 2019).

$$\left(\frac{S}{N}\right)_j = \frac{\sum_{i=1}^{n}(x_{ij}-u_{ij})}{\sum_{i=1}^{n} {u_{ij}}^2} \quad (5)$$

In addition, the number of samples should be greater than the number of variables, suggested by (Arana, 2014) (Eq.6).

$$n > \left(\frac{m+3}{2}\right) \quad (6)$$

Output Data Quality

To find the optimal number of factors, the model was run with different numbers of factors (2 to 5) and different levels of extra modeling uncertainty (0 – 15%). For each run, the stability and reliability of the output were checked according to the Q value, determination coefficients between predicted and observed concentrations, scaled residual (e_{ij}/u_{ij}) analysis and physical meaningfulness of the factor profiles. Regarding Q values, the EPA PMF 5.0 model provides values of Q_{true}, which is calculated including all sampled points according to Eq.8, and Q_{robust}, which considers that outliers have been excluded. Solutions where the Q_{true} is greater than $1.5Q_{robust}$, indicates that extreme events may be disproportionately influencing the model (Arana, 2014). Moreover, we examined the $Q_{theoretical}$ values ($Q_{theoretical}$ = m x n), since it is an efficient way to understand the residuals of the PMF solution.

In addition, we assessed the factor uncertainties due to random errors and rotational ambiguity. Random errors were verified by Bootstrap analysis (BS), which is based on resampling the input dataset, fitting the parameters of the PMF model to this resampled dataset, and analysis of the correlation coefficient between bootstrapped-fit profiles and base solution factors profiles. Regarding rotational ambiguity, which can occur due to the existence of several solutions (G, F) with the same value of Q, was evaluated by the method of controlled displacement intervals of factor elements (DISP), which evaluates the lowering and majoring each species in every factor up to a given variation of the Q value ($dQ_{maximmum}$).

RESULTS AND DISCUSSION

Samples Representativeness

Precipitation recorded in Lavras during the sampling period, March 2018–October 2019, ranged between the minimum of 0.2 mm in July 2018 and the maximum of 323.2 mm in December 2018, with an accumulated total 1798.4 mm (INMET, 2019b). Of these, a representative amount, 1206 mm (67%), was collected by bulk atmospheric deposition and the differences were associated with sample loss by evaporation and sampling period variation. In addition, part of the study period was atypical, with lower levels of rainfall between March 2018 and February 2019 (1299 mm) in relation to annual climatological average (1461.8mm). On the other hand, a different behavior was observed for the following months (March to October 2019), which presented similar precipitation (499 mm) to the climatological average of the same months (501 mm).

Quality Assurance and Data Flagging Procedures

Following the quality criteria from EMEP, a data set containing 52 samples (88% of the original data set) was established, of which 3 were valid and 49 were valid and flagged. Only seven samples were invalid and excluded in the following discussion.

In order to assess the completeness of measured ions major, we calculated the ∑anions/∑cations equivalence ratio and founded a value of 0.28. The ∑anions/∑cations ratio lower than the unity suggest an anions deficit, which may be attributed to the lack of measurements of carbonate, according to showed by Pereira et al. (2021). In addition, a good and statistical significant linear association was obtained for the relationship between

anions and cations (R^2 = 0.87; p-value < 0.01).

Chemical Characterization

The statistical results of pH and major ionic concentrations in bulk atmospheric deposition are listed in Table 1.

The pH values ranged between 5.52 and 8.29, and most of the samples (90%) are within the range of 5.6–6.6, with a mean of 5.95. Only 2% of the samples have pH less than 5.6 (pH of natural rainwater in equilibrium with atmospheric CO_2), suggesting acid deposition events in this area were not serious and there are inputs of alkaline species into atmosphere, such as crustal elements (Ca^{2+}, Mg^{2+} and K^+). A similar behavior was also observed by Izquierdo and Avila (2012), analyzing the chemical composition of bulk deposition samples collected in North-Eastern Spain. Soil resuspension brings about an increase of Ca^{2+} and Mg^{2+} coupled with carbonates which provide further neutralization of aerosol-derived acidic species.

Broadly, the ionic species presented mean values higher than the median (Table 1), indicating that the frequency distributions were asymmetric and influenced by high concentrations. With the exception of Mg^{2+}, all the ion concentrations presented high dispersion around their arithmetic mean values according to the standard deviations (sd), which reveal great variability in the ionic samples composition levels. The same pattern was observed by comparing the median values with their respective interquartile ranges (iqr). In addition, among all cations, Ca^{2+} was the species with the greatest variability (8.20–455 $\mu molL^{-1}$), followed by Na^+ (0.03–179 $\mu molL^{-1}$). Regarding anionic species,

Table 1. Statistical summary of the pH and concentration of major ions in $\mu molL^{-1}$

	min	max	mean	std.dev	median	iqr	VWM
pH	5.52	8.29	5.95	0.51	5.96	0.30	6.05
Na^+	0.03	179	22.7	43.8	3.07	11.1	18.7
NH_4^+	0.30	115	23.3	27.5	14.1	21.5	13.6
K^+	0.15	120	14.2	21.5	5.51	13.4	5.93
Mg^{2+}	0.36	73.4	13.3	13.5	9.64	1.81	13.3
Ca_2^+	8.20	455	86.9	87.7	70.5	86.0	46.6
Cl^-	0.06	346	37.9	60.8	14.1	29.7	21.6
NO_3^-	0.12	213	24.7	37.4	13.6	11.4	9.76
SO_4^{2-}	0.00	90.3	9.23	14.1	4.22	10.1	4.25

Cl^- was the dominant compound with the largest variability (0.06–346 $\mu molL^{-1}$), followed by NO_3^- (0.11–213 $\mu molL^{-1}$).

The VWM were smaller than arithmetic means, indicating that the higher concentrations were usually associated with lower precipitations (Table 1).For the whole sampling campaign, the ions profile in VWM (molar unit) may be described in the following order: Ca^{2+} (46.6) > Cl^- (21.6) > Na^+ (18.7) > NH_4^+ (13.6) > Mg^{2+} (13.3) > NO_3^- (9.76) > K^+ (5.93) > SO_4^{2-} (4.24) > H^+ (0.89) $\mu molL^{-1}$. We identified Ca^{2+} as the most predominant specie accounting for 35%, which coupled with Na^+ and NH_4^+ represents 59% of the total ionic species distribution. Similar patterns were observed in Mbita, East Africa, which also is characterized as a tropical agricultural area (Bakayoko et al., 2021). It is also valuable to mention that Cl^- was the second largest ion with 16% of the total VWM concentration.

Source Identification Based on PMF Results

PMF was adopted to quantitatively analyze the emission sources of the measured ionic species in the bulk atmospheric deposition samples. All species presented S/N ratios greater than 2.0 and more than 95% of the data above the DL. Therefore, all species were categorized as strong (Table 2) and were included in the model without changing their uncertainties. In addition, according to equation 6, our database presented enough samples for the PMF application.

The PMF model was run 20 times and based on the evaluation of the stability and reliability criteria, we identified that three factors, combined with extra modeling uncertainty of 10%, were physically reasonable and could represent the major sources in the study region (Figure 2). The Q values of the base solution, Q_{robust} (651.459) and Q_{true} (651.458), were similar, with $Q_{true} < 1.5Q_{robust}$, indicating that the outlier concentrations of the species did not influence the model. Furthermore, both these Q values were close to the $Q_{theoretical}$ (52x8 = 416), suggesting that the data uncertainties were adequate.

Table 2 shows a summary of the input data characterization and of the base solution.

All species showed satisfactory coefficient of determination (R^2>0.70), except for NH_4^+, suggesting that most species were well fitted in the model and that some specific events may be influencing the NH_4^+ adjustment. In

addition, more than 90% of samples for all species showed scaled residuals within the 95% confidence interval (±3sd). Regarding the other 10%, the scaled residuals distribution presented values above 3sd, indicating that the uncertainties in these samples were very low. In general, the scaled residuals distribution suggested that the data uncertainties were suitable.

The factors profile and contribution are depicted in figure 2. The first factor identified accounted for 44% of the sum of measured ions and presented high loading values for Ca^{2+} (71%), NO_3^- (69%), and SO_4^- (62%). These species are involved in neutralizing atmospheric processes since $CaCO_3$ is an alkaline species that neutralizes the major atmospheric acids (H_2SO_4 and HNO_3). Thus, this factor was named as atmospheric neutralization processes. It should be noted that cement manufacturing and limestone mining were considered the two major sources of Ca^{2+} to the atmosphere in the study area. Although NO_3^- and SO_4^- have been related to the large emissions of SO_2 and NO_x from the combustion of fossil fuel in large urban areas (Meng et al., 2019), researches carried out in agricultural areas in California, United States, associated these species with agricultural soil emissions (Almaraz et al., 2018), which agrees with our study.

Table 2. Diagnosis of the base solution provided by the PMF model

Species	S/N[a]	R^{2b}	Residuals (%)[c]
Na^+	3.9	0.89	3.8
NH_4^+	4.0	0.30	5.7
K^+	4.0	0.88	0.0
Mg^{2+}	3.9	0.77	7.6
Ca_2^+	4.0	0.90	5.7
Cl^-	3.9	0.93	0.0
NO_3^-	3.9	0.78	0.0
SO_4^{2-}	3.8	0.92	1.9

a All species were classified as strong; b Determination coefficient between predicted and observed concentrations; c % Absolute frequency of the scaled residuals beyond 3 standard deviations (sd).

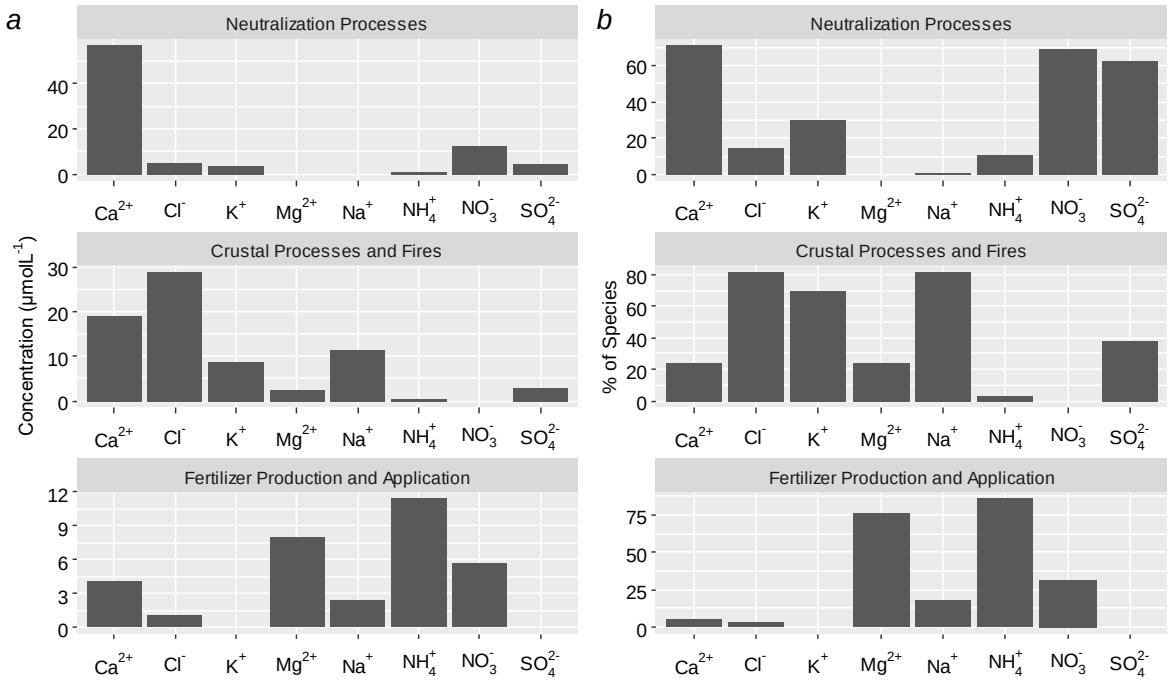

Figure 2. Source profiles for (a) concentration in µmolL^{-1} and (b) percentage of species (%) extracted by EPA PMF 5.0 model from 52 bulk deposition samples collected in Lavras in the period between March 2018 and October 2019.

The second factor explained 34% of the measured ions and was dominated by Na^+ (82%), K^+ (70%), and Cl^- (82%). These species generally originate from sea salt, crustal aerosols, and biomass burning (Niu et al., 2013). In the present study, the Cl^-/Na^+ ratio was 1.15, which was similar to the oceanic ratio (Cl^-/Na^+ = 1.17), indicating marine sources intrusion. However, the K^+/Na^+ ratio was 0.32, which was higher than the oceanic ratio (K^+/Na^+ = 0.022), suggesting a large excess of K^+ and, therefore, an additional source of potassium compounds in Lavras, such as biomass burning. Because of the ambiguity of sources in this factor, it was characterized by crustal processes and fires.

Factor 3, classified as fertilizer production and application, explained 17% of the ionic compounds and was dominated by NH_4^+ (85%) and Mg^{2+} (76%). Mg^{2+} originates naturally from marine aerosols and/or crustal particles, and its anthropogenic sources can be associated with cement industries and fertilizer production. NH_4^+ can be directly attributed to an input of NH_3 in the atmosphere, mainly due to farming and nitrogen fertilizer production and

application (Zeng et al., 2020). This profile corroborates with the agricultural background of the study region, where an average nitrogen and phosphor synthetic fertilizers application rate was estimated at 194 $kgha^{-1}year^{-1}$ (IBGE, 2014). In addition, there are agro-industrial sources inside the county air basin.

In order to estimate the variability in the PMF solution, 100 bootstrap runs with a minimum correlation of 0.6 were performed. For all factors, more than 90% of the bootstrap profiles showed a minimum correlation of 0.6 with their respective base profiles. In addition, less than 1% of the factors were unmapped. Concerning DISP analyses, no swap between factors was observed.

CONCLUSION

We assessed bulk atmospheric deposition in a Brazilian agricultural region and observed that the pH mean was 5.99, and most deposition samples (~98%) were alkaline (pH > 5.60). This pattern was corroborated by the higher abundance of Ca^{2+} (33%) among all ions measured, which is an important neutralizing agent of sulfuric and nitric acids. The PMF analysis resulted in three factors, which demonstrated the influence of anthropogenic and natural sources, of which neutralization processes was the major source (44% of the total), following by crustal processes and fires (34%) and fertilizer production and application (17%).

The atmospheric deposition systemic analysis allowed us to monitor and evaluate the chemical transformation processes and to identify the polluting sources. From that, it is possible to develop emission reduction strategies, as effectively done in the previous decades for acid deposition. Given this perspective, our findings are useful to understand the majority of atmospheric species sources in the Southern Minas Gerais, Brazil.

ACKNOWLEDGEMENTS

This study was financed in part by the Coordenação de Aperfeiçoamento de Pessoal de Nível Superior – Brasil (CAPES) – Finance Code 001.

REFERENCES

Akpo, A.B., Galy-Lacaux, C., Laouali, D., Delon, C., Liousse, C., Adon, M., Gardrat, E., Mariscal, A., Darakpa, C., 2015. Precipitation chemistry and wet deposition in a remote wet savanna site in West Africa: Djougou (Benin). Atmos. Environ. 115, 110–123. https://doi.org/10.1016/j.atmosenv.2015.04.064

Almaraz, M., Bai, E., Wang, C., Trousdell, J., Conley, S., Faloona, I., Houlton, B.Z., 2018. Erratum: Agriculture is a major source of NOx pollution in California. Sci. Adv. 4, 1–9. https://doi.org/10.1126/SCIADV.AAU2561

Almeida, G.L.M.D., Ferreira, E.C. da M., Mendes, D.J. da S., Gomes, B.A.B., Souza, F. do N., Silva, J. do N., Dos Santos, S.A., Teixeira, P.B., 2017. Estudo sobre as regiões de planejamento de Minas Gerais: Sul de Minas Gerais. Belo Horizonte.

Alves, D.D., Backes, E., Rocha-Uriartt, L., Riegel, R.P., de Quevedo, D.M., Schmitt, J.L., da Costa, G.M., Osório, D.M.M., 2018. Chemical composition of rainwater in the Sinos River Basin, Southern Brazil: a source apportionment study. Environ. Sci. Pollut. Res. 25, 24150–24161. https://doi.org/10.1007/s11356-018-2505-1

Anil, I., Alagha, O., Karaca, F., 2017. Effects of transport patterns on chemical composition of sequential rain samples: trajectory clustering and principal component analysis approach. Air Qual. Atmos. Heal. 10. https://doi.org/10.1007/s11869-017-0504-x

Arana, A.A., 2014. Aerossóis Atmosféricos na Amazônia : Composição elementar orgânica e inorgânica em regiões com diferentes usos do solo .

Araujo, T.G., Souza, M.F.L., De Mello, W.Z., Da Silva, D.M.L., 2015. Bulk Atmospheric Deposition of Major Ions and Dissolved Organic Nitrogen in the Lower Course of a Tropical River Basin, Southern Bahia, Brazil. J. Braz. Chem. Soc. 26, 1692–1701. https://doi.org/10.5935/0103-5053.20150143

Bakayoko, A., Galy-Lacaux, C., Yoboué, V., Hickman, J.E., Roux, F., Gardrat, E., Julien, F., Delon, C., 2021. Dominant contribution of nitrogen compounds in precipitation chemistry in the Lake Victoria catchment (East Africa). Environ. Res. Lett. 16. https://doi.org/10.1088/1748-9326/abe25c

DENATRAN, 2019. Frota de Veículos - 2019 [WWW Document]. Ministério da Infraestrutura. URL https://infraestrutura.gov.br/component/content/article/115-portal-denatran/8559-frota-de-veiculos-2019.html (accessed 7.4.20).

Deusdará, K.R.L., Forti, M.C., Borma, L.S., Menezes, R.S.C., Lima, J.R.S., Ometto, J.P.H.B., 2017. Rainwater chemistry and bulk atmospheric deposition in a tropical semiarid ecosystem: the Brazilian Caatinga. J. Atmos. Chem. 74, 71–85. https://doi.org/10.1007/s10874-016-9341-9

Duan, L., Chen, X., Ma, X., Zhao, B., Larssen, T., Wang, S., Ye, Z., 2016. Atmospheric S and N deposition relates to increasing riverine transport of S and N in southwest China: Implications for soil acidification. Environ. Pollut. 218, 1191–1199. https://doi.org/10.1016/j.envpol.2016.08.075

EMBRAPA, 2006. Levantamento de Reconhecimento de Média Intensidade dos Solos da Zona Campos das Vertentes - MG. https://doi.org/1678-0892

Garaga, R., Chakraborty, S., Zhang, H., Gokhale, S., Xue, Q., Kota, S.H., 2020. Influence of anthropogenic emissions on wet deposition of pollutants and rainwater acidity in Guwahati, a UNESCO heritage city in Northeast India. Atmos. Res. 232, 104683. https://doi.org/10.1016/j.atmosres.2019.104683

IBGE, 2019. Produção Agrícola Municipal [WWW Document]. URL https://sidra.ibge.gov.br/Tabela/5457 (accessed 6.3.21).

IBGE, 2018. Cidades e Estados: Lavras [WWW Document]. URL https://cidades.ibge.gov.br/brasil/mg/lavras (accessed 6.1.19).

IBGE, 2014. Aplicação de Fertilizantes Nitrogenados por Unidades da Federação [WWW Document].

INMET, 2019a. Normais Climatológicas do Brasil [WWW Document]. Ministério da Agric. Pecuária e Abast. URL https://portal.inmet.gov.br/normais (accessed 9.15.19).

INMET, 2019b. Banco de Dados Meteorológicos para Ensino e Pesquisa

[WWW Document]. Ministério da Agric. Pecuária e Abast. URL https://bdmep.inmet.gov.br/ (accessed 5.2.20).

Izquierdo, R., Avila, A., 2012. Comparison of collection methods to determine atmospheric deposition in a rural Mediterranean site (NE Spain). J. Atmos. Chem. 69, 351–368. https://doi.org/10.1007/s10874-012-9246-1

Kamani, H., Hoseini, M., 2014. Study of trace elements in wet atmospheric precipitation in Tehran , Iran. https://doi.org/10.1007/s10661-014-3759-9

Khan, M.F., Latif, M.T., Saw, W.H., Amil, N., Nadzir, M.S.M., Sahani, M., Tahir, N.M., Chung, J.X., 2016. Fine particulate matter in the tropical environment: Monsoonal effects, source apportionment, and health risk assessment. Atmos. Chem. Phys. 16, 597–617. https://doi.org/10.5194/acp-16-597-2016

Kuzu, S.L., Saral, A., 2017. The effect of meteorological conditions on aerosol size distribution in Istanbul. Air Qual. Atmos. Heal. 10, 1029–1038. https://doi.org/10.1007/s11869-017-0491-y

Lara, L.B.L.S., Artaxo, P., Martinelli, L.A., Victoria, R.L., Camargo, P.B., Krusche, A., Ayers, G.P., Ferraz, E.S.B., Ballester, M. V., 2001. Chemical composition of rainwater and anthropogenic influences in the Piracicaba River Basin, Southeast Brazil. Atmos. Environ. 35, 4937–4945. https://doi.org/10.1016/S1352-2310(01)00198-4

Meng, Y., Zhao, Y., Li, R., Li, J., Cui, L., Kong, L., Fu, H., 2019. Characterization of inorganic ions in rainwater in the megacity of Shanghai: Spatiotemporal variations and source apportionment. Atmos. Res. 222, 12–24. https://doi.org/10.1016/j.atmosres.2019.01.023

Moreda-Piñeiro, J., Alonso-Rodríguez, E., Moscoso-Pérez, C., Blanco-Heras, G., Turnes-Carou, I., López-Mahía, P., Muniategui-Lorenzo, S., Prada-Rodríguez, D., 2014. Influence of marine, terrestrial and anthropogenic sources on ionic and metallic composition of rainwater at a suburban site (northwest coast of Spain). Atmos. Environ. 88, 30–38. https://doi.org/10.1016/j.atmosenv.2014.01.067

Niu, H., He, Y., Zhu, G., Xin, H., Du, J., Pu, T., Lu, X., Zhao, G., 2013. Environmental implications of the snow chemistry from Mt. Yulong, southeastern Tibetan Plateau. Quat. Int. 313–314, 168–178. https://doi.org/10.1016/j.quaint.2012.11.019

Paatero, P., 1997. Least squares formulation of robust non-negative factor analysis. Chemom. Intell. Lab. Syst. 37, 23–35. https://doi.org/10.1016/S0169-7439(96)00044-5

Paatero, P., Tapper, U., 1994. Positive matrix factorization: A non-negative factor model with optimal utilization of error estimates of data values. Environmetrics 5, 111–126. https://doi.org/10.1002/env.3170050203

Pereira, J.N., Fornaro, A., Vieira-Filho, M., 2021. Atmospheric Deposition Chemistry in a Brazilian Rural Area: Alkaline Species Behavior and Agricultural Inputs. Environ. Sci. Pollut. Res. 28, 23448–23458. https://doi.org/https://doi.org/10.1007/s11356-020-12317-3

Qiao, X., Xiao, W., Jaffe, D., Kota, S.H., Ying, Q., Tang, Y., 2015. Atmospheric wet deposition of sulfur and nitrogen in Jiuzhaigou National Nature Reserve, Sichuan Province, China. Sci. Total Environ. 511, 28–36. https://doi.org/10.1016/j.scitotenv.2014.12.028

Rastegari Mehr, M., Keshavarzi, B., Sorooshian, A., 2019. Influence of natural and urban emissions on rainwater chemistry at a southwestern Iran coastal site. Sci. Total Environ. 668. https://doi.org/10.1016/j.scitotenv.2019.03.082

Reff, A., Eberly, S.I., Bhave, P. V., 2007. Receptor modeling of ambient particulate matter data using positive matrix factorization: Review of existing methods. J. Air Waste Manag. Assoc. 57, 146–154. https://doi.org/10.1080/10473289.2007.10465319

Roy, A., Chatterjee, A., Tiwari, S., Sarkar, C., Das, S.K., Ghosh, S.K., Raha, S., 2016. Precipitation chemistry over urban, rural and high altitude Himalayan stations in eastern India. Atmos. Res. 181, 44–53. https://doi.org/10.1016/j.atmosres.2016.06.005

Schaug, J., Semb, A., Hjellbrekke, A.-G., Hanssen, J.., Pedersen, A., 1997. Data quality and quality assurance report. Kjeller, Norway.

Sofowote, U.M., Su, Y., Dabek-Zlotorzynska, E., Rastogi, A.K., Brook, J., Hopke, P.K., 2015. Sources and temporal variations of constrained PMF factors obtained from multiple-year receptor modeling of ambient PM2.5 data from five speciation sites in Ontario, Canada. Atmos. Environ. 108, 140–150. https://doi.org/10.1016/j.atmosenv.2015.02.055

Sun, X., Wang, Y., Li, H., Yang, X., Sun, L., Wang, X., Wang, T., Wang, W., 2016. Organic acids in cloud water and rainwater at a mountain site in acid rain areas of South China. Environ. Sci. Pollut. Res. 23, 9529–9539. https://doi.org/10.1007/s11356-016-6038-1

Szép, R., Bodor, Z., Miklóssy, I., Niță, I.A., Oprea, O.A., Keresztesi, Á., 2019. Influence of peat fires on the rainwater chemistry in intra-mountain basins with specific atmospheric circulations (Eastern Carpathians, Romania). Sci. Total Environ. 647, 275–289. https://doi.org/10.1016/j.scitotenv.2018.07.462

US-EPA, 2018. Positive Matrix Factorization Model.

US-EPA, 2014. EPA Positive Matrix Factorization (PMF) 5.0 - Fundamentals and User Guide. Environ. Prot. Agency Off. Researc Dev. Publushing House Whashington, DC 20460.

WMO, 2004. Manual for the Gaw Precipitation Chemistry Programme: Guidelines, Data Quality Objectives and Standard Operating Procedures.

Xing, J., Song, J., Yuan, H., Li, X., Li, N., Duan, L., Kang, X., Wang, Q., 2017. Fluxes, seasonal patterns and sources of various nutrient species (nitrogen, phosphorus and silicon) in atmospheric wet deposition and their ecological effects on Jiaozhou Bay, North China. Sci. Total Environ. 576, 617–627. https://doi.org/10.1016/j.scitotenv.2016.10.134

Yatkin, S., Adali, M., Bayram, A., 2016. A study on the precipitation in Izmir, Turkey: chemical composition and source apportionment by receptor models. J. Atmos. Chem. 73, 241–259. https://doi.org/10.1007/s10874-015-9325-1

Ye, L., Huang, M., Zhong, B., Wang, X., Tu, Q., Sun, H., Wang, C., Wu, L., Chang, M., 2018. Wet and dry deposition fluxes of heavy metals in Pearl River Delta Region (China): Characteristics, ecological risk assessment, and source apportionment. J. Environ. Sci. (China) 70, 106–123. https://doi.org/10.1016/j.jes.2017.11.019

Zeng, J., Han, G., Wu, Q., Tang, Y., 2020. Effects of agricultural alkaline substances on reducing the rainwater acidification: Insight from chemical compositions and calcium isotopes in a karst forests area. Agric. Ecosyst. Environ. 290, 106782. https://doi.org/10.1016/j.agee.2019.106782

Zhang, N., Cao, J., He, Y., Xiao, S., 2014. Chemical composition of rainwater at Lijiang on the Southeast Tibetan Plateau: Influences from various air mass sources. J. Atmos. Chem. 71, 157–174. https://doi.org/10.1007/s10874-014-9288-7

Zhou, X., Xu, Z., Liu, W., Wu, Y., Zhao, T., Jiang, H., Zhang, X., Zhang, J., Zhou, L.,

Wang, Y., 2019. Chemical composition of precipitation in Shenzhen, a coastal mega-city in South China: Influence of urbanization and anthropogenic activities on acidity and ionic composition. Sci. Total Environ. 662, 218–226. https://doi.org/10.1016/j.scitotenv.2019.01.096

3. ARTIGO III - NITROGEN ATMOSPHERIC DEPOSITION DRIVEN BY SEASONAL PROCESSES IN A BRAZILIAN REGION WITH AGRICULTURAL BACKGROUND

Nitrogen atmospheric deposition driven by seasonal processes in a Brazilian region with agricultural background

Jaqueline Natiele Pereira[a], Vanessa Alves Mantovani[b], Carlos Rogério de Mello[b], Adalgiza Fornaro[b], Marcelo Vieira-Filho*[a]

a Departamento de Engenharia Ambiental, Universidade Federal de Lavras, Campus da UFLA, 37200-000, Lavras, Minas Gerais, Brazil

b Departamento de Recursos Hídricos, Universidade Federal de Lavras, Campus da UFLA, 372000-000, Lavras, Minas Gerais, Brazil

c Departamento de Ciências Atmosféricas, Instituto de Astronomia, Geofísica e Ciências, Atmosféricas da Universidade de São Paulo, Rua do Matão, 1226, 05508-090, Cidade, Universitária, São Paulo, SP, Brazil

*e-mail marcelo.filho@ufla.br, phone: (+55)11-9 8598 6567

Abstract

Understanding the seasonal patterns and influencing factors of nitrogen atmospheric deposition is essential to evaluate human impacts on the air quality and nitrogen biogeochemical cycle. However, evaluation of the nitrogen deposition flux, especially in South America agricultural regions, has not been fully investigated. In this paper, we quantified the atmospheric wet deposition fluxes of total dissolved nitrogen (TDN), dissolved organic nitrogen (DON) and dissolved inorganic nitrogen (DIN, including NH_4^+ and NO_3^-), in a region with agricultural and livestock predominance in the Southern Minas Gerais region, Brazil, from May 2018 to April 2019. The annual fluxes of DON, NO_3^- and NH_4^+ were 11.3, 4.04 and 1.41 kg.ha^{-1}.yr^{-1}, respectively, with a TDN flux of 16.7 kg.ha^{-1}.yr^{-1}. DON was dominant, accounting for 68% of TDN, and its role in atmospheric wet deposition could not be neglected. Deposition fluxes of nitrogen species in the wet season (October – March) were on average 4.8 fold higher than dry season, which revealed significant seasonal variations (ANOVA test; p-value < 0.05) driven largely by the seasonality of agricultural operations and by rainfall pattern. We also found high NO_3^-/NH_4^+ ratios (average = 8.25), with higher values in dry season (NO_3^-/NH_4^+ = 12.8) in comparison with wet season (NO_3^-/NH_4^+ = 4.48), which revealed a higher relative contribution of NO_x emissions from traffic sources in dry season. In addition, moderate correlations between DON and NH_4^+ and between DON and NO_3^- (**ρ** = 0.67, **ρ** = 0.55, respectively) indicated that DON was partially derived from other sources, such as soil dust, biomass burning and industrial emissions. We also estimated the influence of atmospheric deposition of inorganic nitrogen (N-DIN) on environmental ecosystems, being 2.01 kgNha^{-1}yr^{-1} with potential risk of acidification and eutrophication of 30%. Therefore, attention should be paid to the role of wet atmospheric deposition of nitrogen as a source of nitrogen environmental pollution in agricultural regions.

Keywords Atmospheric wet deposition fluxes; Total dissolved nitrogen; Dissolved organic nitrogen; NO_3^-/NH_4^+ ratio; Agricultural sources; Seasonality.

INTRODUCTION

The nitrogen cycle is essential to living organisms and triggers several natural reservoirs processes, and in the last centuries such processes have been changed ascribed to anthropogenic sources inputs (Jaffe and Weiss-Penzias, 2003). From the local to global scale, several activities, such as fossil fuel combustion, mobile exhaust engines and agricultural activities including fertilizer use and livestock husbandry account to specific variations and the increase of atmospheric reactive nitrogen (Nr) emissions (Liu et al., 2013; Xing et al., 2018). Galloway et al. (2004) estimated that global atmospheric Nr emissions (NO_x and NH_3) will increase from 23 $TgNyr^{-1}$ in 1860 to 189 $TgNyr^{-1}$ in 2050. The main forms of Nr in the atmosphere are divided among: (i) the inorganic reduced forms of nitrogen (e.g., NH_3, NH_4^+); (ii) inorganic oxidized forms (e.g., NO_x, HNO_3, N_2O, NO_3^-), and; (iii) organic compounds (e.g., urea, amines, proteins, nucleic acids) (Galloway et al., 2004; Xing et al., 2018; Zeng et al., 2020). These species may be considerably modified by (photo)chemical reactions and enter into biogeochemical cycles of terrestrial and aquatic ecosystems (Qiao et al., 2018).

The nitrogen species analysis through wet, dry or bulk deposition are a key process in better understanding the human impacts on the nitrogen biogeochemical cycle (Song et al., 2017; Souza et al., 2020; Wang et al., 2013). Since net primary production of most terrestrial ecosystems is limited by nitrogen availability, deposition of reactive nitrogen becomes a source of nutrients in these sites and could improve productivity (Dentener et al., 2006; Vet et al., 2014; Xu et al., 2020). In contrast, the excessive nitrogen input may cause acidification of forest soils, eutrophication, unbalance and decreases in biodiversity, and enhanced greenhouse gas emissions (Bobbink et al., 2010; Stevens et al., 2018; Wang et al., 2018).

During the wet atmospheric deposition, nitrogen is supplied in soluble form (total dissolved nitrogen – TDN), which encompasses dissolved inorganic (DIN: $NH_4^+ + NO_3^-$) and organic nitrogen (DON) (González Benítez et al., 2009; Rasse et al., 2018; Violaki et al., 2010). TDN atmospheric deposition has been extensively investigated worldwide (Hofhansl et al., 2011; Matsumoto et al., 2020; Violaki et al., 2010; Zamora et al., 2011; Zhang et al., 2008). Cui et al. (2014)

and Tu et al. (2013) reported that wet deposition fluxes of TDN in agricultural and forest ecosystems in China ranged from 37.37 $kgNha^{-1}yr^{-1}$ to 113.8 $kgNha^{-1}yr^{-1}$, respectively, with DON accounting for approximately 26% of TDN. In Brazil, studies have shown that both urban and forest regions receive a considerable TDN deposition (5 – 18 $kgNha^{-1}yr^{-1}$) by bulk deposition (Araujo et al., 2015; de Souza et al., 2015; Parron et al., 2011; Schroth et al., 2001). According to these sites, DON deposition ranged between 30 and 58 % of TDN, highlighting its potential importance to N cycling in different ecosystems. DON contribution to TDN varies due to local sources, seasonal patterns and mixed sources, thus it is desirable to evaluate the partition from natural to anthropogenic sources and their environmental impacts. Moreover, studies from 2010's highlighted some of these mechanisms, and pointed out the ubiquitous role of DON in atmospheric deposition (Rasse et al., 2018; Song et al., 2017; Xing et al., 2017).

Despite nitrogen atmospheric deposition has been adequately estimated in Asia, Europe and North America through monitoring networks (Wang et al., 2018), available data for many Southern hemisphere developing countries are either scarce or non-existent (Vet et al., 2014). As it pertains to Brazil, nitrogen atmospheric deposition data comes from private and isolated initiatives or from research groups limited to specific regions for restricted periods, which impoverishes the global analysis of the nitrogen input impacts in ecosystems of said country (Araujo et al., 2015; de Souza et al., 2015; Parron et al., 2011; Vieira-Filho et al., 2016). In this perspective, we evaluated and quantified the atmospheric deposition fluxes of TDN, DIN and DON in a region with agricultural influence in the Southern Minas Gerais region, Brazil.

METHODOLOGY

Sampling Site

The state of Minas Gerais is located in the Southeastern region of Brazil, where the largest metropolitan regions of the country are located, e.g., São Paulo, Rio de Janeiro and Belo Horizonte (Fig. 1). The major atmospheric pollutant emissions in this region are related to transport, farming, biomass burning and industrial activities such as mining, metallurgical, agro-industrial and chemical facilities (IBGE, 2021). This study was conducted in the Southern Minas Gerais state region, which

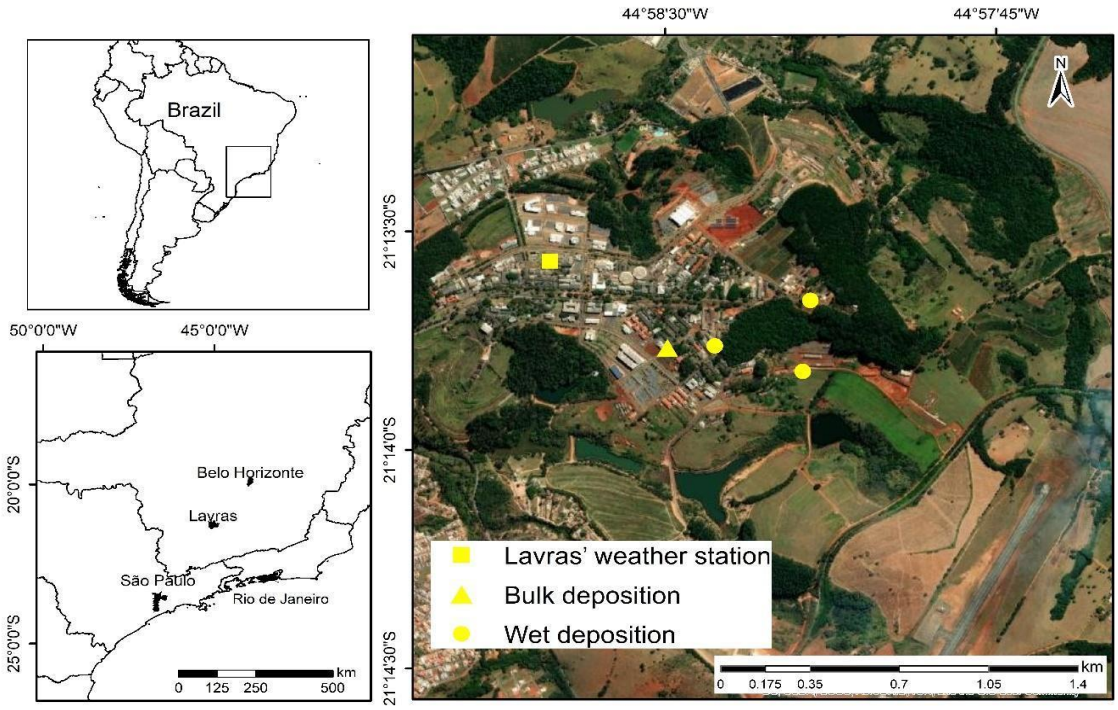

Fig.1 Location of sampling points and of the weather station in Lavras city, Southern Minas Gerais region, Brazil. Bulk and wet deposition samplers are depicted in yellow

encompasses 21.8% of agricultural commodities (mainly from coffee crop production), and accounts for 12% of the state's Gross Domestic Product (Almeida et al., 2017).

The sampling collection was conducted specifically in Lavras city (21° 13' 45.3"S and 44° 58' 32.4"W), 241 km from the Atlantic Ocean (Fig.1). Lavras has an area of 564.744 km², 919 m of altitude and a population of 102,728 inhabitants, occupying the fifth place among the most populous cities in the Southern region of Minas Gerais (IBGE, 2018). Approximately 19% (107 km^2) of the total area of Lavras is associated with agricultural activities, mainly coffee production (IBGE, 2019). IBGE (2014) estimated an average synthetic nitrogen fertilizers application rate in Minas Gerais as approximately 110.4 kg $ha^{-1}yr^{-1}$. Lavras city vehicular fleet counts approximately 50 thousand light-duty vehicles, comprising 54% automobiles and 26% motorcycles. Moreover, its vehicle fleet is about 15 years old on average, with 62% of its passenger cars produced before 2010 and 14% before 1990 (DENATRAN, 2018).

The Köppen-type climate of the region is subtropical Cwa with well-defined seasons, and rainfall concentrated in Summer (Junqueira Junior et al., 2019). Long-term average annual precipitation (1981-2010) is 1462 mm, and 85% of the rainfall occurs in the wet period (October to March). The mean annual temperature is 20.3ºC ranging from 16.9ºC to 22.5ºC (INMET, 2019a).

Sampling Campaign

From May 2018 until April 2019 wet deposition samples were collected after each rainfall event (daily at 9:00 AM local time) using 3 *Ville de Paris*-type rain gauges. Moreover, 61 different rainfall events were collected with at least 5 mm (critical volume necessary for laboratory analysis). In addition, monthly samples were analyzed, adding an aliquot of each rain-gauge in the same flask. Regarding preservation procedures and analytical methodologies, we followed the criteria adopted by *Standard Methods for Examination of Water and Wastewater* (APHA/AWWA/WEF, 2014).

In the same period (May 2018 – April 2019), we also collected 36 bulk deposition samples through a high-density polyethylene bucket (NALGON) of 10L with a collecting area of 439 cm^2. To prevent sunlight effects and reduce litter fall in samples, the collector was placed inside a sun-protective PVC structure and covered with a nylon mesh. In this case, the sampling period was around 7 days. In the absence of precipitation, 50 mL of deionized water was added in order to analyze soluble species. It is important to note that the sampling collector was installed 1.5 m above ground level and rinsed several times with ultrapure water Milli-Q (Millipore, electrical resistivity 18 MΩ) in order to follow GAW´s sampling procedures (WMO, 2004). In addition, blank sample analyses were carried out throughout the experimental campaign.

Analytical Procedures

Total Kjeldahl nitrogen (TKN) was determined according to the macro-Kjeldahl method (ABNT, 1997) for monthly ammonium and organic nitrogen quantification in the wet deposition samples. The process for TKN analysis consists in converting organic nitrogen to ammoniacal nitrogen by acid digestion, and thereafter the sample pH is raised for the ammoniacal nitrogen distillation, lastly the nitrogen was quantified by titrimetric method. For TKN analysis the detection limit was calculated as 0.36 mgL^{-1}.

We measured pH and DIN concentrations from bulk deposition samples. The pH measurements were obtained by using pHmeter (AKSO AK model 151), calibrated with buffer solutions (pH 4.0 and 7.0). In order to quantify nitrogen inorganic species (NH_4^+ and NO_3^-), one sample aliquot was filtered with a 0.22 μm diameter membrane (Millex), stored in conditioned polyethylene bottles kept at -18 ºC prior to ion chromatography (IC) analysis (Metrohm model 851) with anionic column (Metrosep ASupp5 - 250 mm x 4 mm) and cationic column (Metrosep C2 150 - 150 x 4 mm). Analytical quantification was performed using an external calibration curve from the standard concentrations for each ion. We calculated detection limits (DL) values from the parameters obtained from the analysis, by the method of the least squares, from the calibration curve (y = a + bx) and corresponded to the white sign (or linear coefficient) plus 3 times the standard deviation (sd) of the angular coefficient ($sd_{y/x}$), that is, DL = a + 3 $sd_{y/x}$. Both NH_4^+ and NO_3^- species presented DL less than 0.01 mgL^{-1}.

Blank samples concentrations were quantified and subtracted by 0.36, 0.05 and 0.15 mgL^{-1} for TKN, NH_4^+ and NO_3^-, respectively.

Flux Calculations and Statistical Analyses

We estimated nitrogen inputs as the product between concentrations of TKN, NH_4^+ and NO_3^- species and collected rainfall amount. The monthly and annual nitrogen deposition flux was expressed using equation 1 (Song et al., 2017; Zhang et al., 2020).

$$I = 0.01 \sum_{i=1}^{n} C_i \left(\frac{V_i}{A}\right) \text{ (Eq.1)}$$

where I represents the input ($kg.ha^{-1}.month^{-1}$ or $kg.ha^{-1}.yr^{-1}$), C represents the nitrogen specie concentration ($mg.L^{-1}$), V represents the volume sample (L), A represents the collector area (m^2), i refers to the number of sample and n is the amount of samples at the corresponding monthly or annual scale. For bulk deposition samples in which we added 50 mL of deionized water due to rainfall absence, we considered this volume for calculations.

From wet deposition inputs, we calculated DON by determining the difference between TKN and NH_4^+ (DON = TKN - NH_4^+) and calculated TDN by adding the deposition fluxes of DON, NH_4^+ and NO_3^- (TDN = DON + NH_4^+ + NO_3^-). It is valuable to report that, for bulk

deposition samples, we estimated wet deposition inputs according to Filoso et al. (2003), in which N inputs from wet deposition were considered 50% of bulk deposition. This study was conducted in the countryside of Brazil's Southeastern region, where ~31% of the area is associated with agricultural activities.

We carried out parametric and non-parametric statistical tests accordingly, following the Shapiro–Wilk test (Shapiro and Wilk, 1965). Thus, a one-way analysis of variance (ANOVA) and Kruskal-Wallis test were performed to detect differences in rainfall and in deposition fluxes of the nitrogen species among the wet and dry seasons (Liu et al., 2021; Romero Orué et al., 2019). In addition, a correlation analysis was applied to identify associations between the different nitrogen forms (de Souza et al., 2015; Rasse et al., 2018; Xing et al., 2018). We emphasize that all statistical analysis and data processing were performed in the R programming environment, through which we applied several functions pertaining to the *stats* and *ggplot2* packages (R Core Team, 2019; Wickham, 2016).

RESULTS AND DISCUSSION

Atmospheric Deposition Seasonal Patterns

From May 2018 until April 2019, the total rainfall collected by wet deposition (Fig.1) was 1524.6 mm, which represents 99% of the total rainfall reported by Lavras' weather station for the same period (INMET, 2019b). In comparison with climatological values, the sampling period showed a surplus of 63 mm (rainfall positive anomaly) in comparison with climatological values, such differences represent almost 5% above long-term annual average rainfall (1981-2010). Approximately 85% of the rainfall occurred in the wet season (October to March) (Fig. 2a), which is in accordance with the expected pattern of the region. Regarding the atmospheric bulk deposition, the total rainfall collected in the sampling period was 1050.4 mm, which in comparison with Lavras' weather station represents 68%. In addition, such differences were expected due to wet and bulk deposition collection methods, moreover sample loss by evaporation is inherent to atmospheric deposition sampling. Conversely, we can assume that most of the atmospheric processes were represented by both atmospheric deposition samples collected.

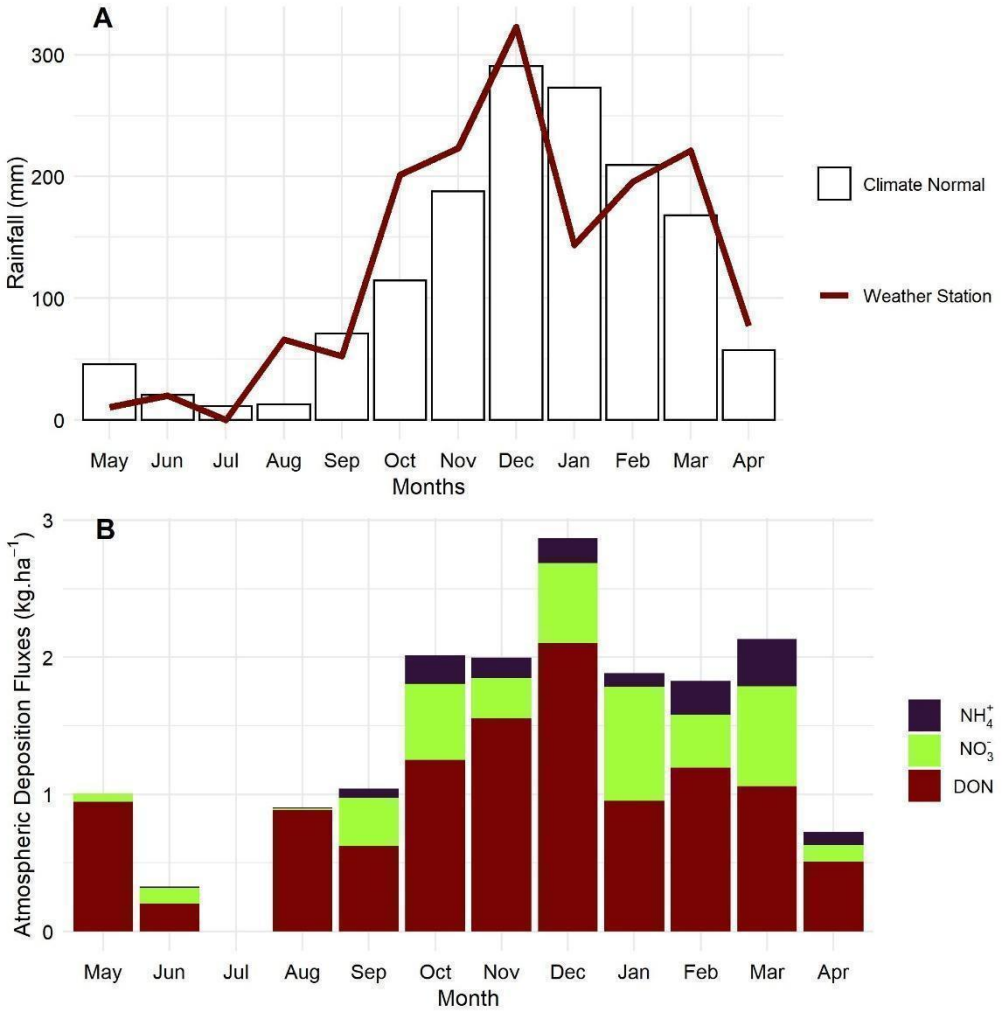

Fig. 2 (A) Comparison between long-term annual rainfall (1981-2010) and rainfall reported by Lavras' weather station from March 2018 until April 2019 (in units of mm); (B) Wet deposition fluxes of nitrogen species (NH_4^+, NO_3^- and DON) in kg.ha^{-1} from samples collect in Lavras, Brazil from May 2018 until April 2019. TDN is represented as the accumulated fluxes of NH_4^+, NO_3^- and DON in kg.ha^{-1}

Total Dissolved Nitrogen (TDN)

Deposition flux of TDN ranged from 0.328 to 2.869 kg.ha^{-1}.month^{-1} in June and December, respectively (Fig.2b). According to the climatological normal for Lavras, December regularly presents the most rainfall and as expected, the highest rainfall amount collected. Alternatively, rainfall in June was 22 times lower than December in 2018. Moreover, TDN fluxes showed significant correlation (p-value < 0.05) with rainfall reported by Lavras weather station in the study period (r = 0.95). Thus, this pattern suggests that monthly variability of TDN deposition was influenced by the rainfall distribution

pattern. Similar results were observed in the Northern Indo Gangetic Plain, Nepal (Bhattarai et al., 2021), in the Sichuan province, southwest China (Deng et al., 2018) and in Lagos Lagoon basin, Nigeria (Oladosu et al., 2017), where wet deposition flux of nitrogen increased with the increase in precipitation volume.

We calculated an annual TDN atmospheric deposition of 16.73 $kg.ha^{-1}.yr^{-1}$, which was comparable with the global estimates higher than 8 $kg.ha^{-1}.yr^{-1}$ at sites like eastern North America, Southern Brazil, Europe and Asia (Vet et al., 2014). In this perspective, Souza et al. (2015) (n = 40) reported a similar TDN bulk atmospheric deposition ranging from 12.1 to 17.2$kg.ha^{-1}.yr^{-1}$ in a forest area and a coastal urban area in the Southeast region of Brazil, where the increase in the TDN deposition was not related to increases in the annual rainfall, but due to the proximity of the Rio de Janeiro metropolitan region. In contrast, Araujo et al. (2015) (n = 20) monitored an urban area in the Northeast region of Brazil, with similar annual average precipitation (1500 mm) in comparison with our study region, however, the bulk TDN deposition was four times lower (4.32 $kg.ha^{-1}.yr^{-1}$). The results reported in the cited studies suggest that other factors control TDN fluxes besides rainfall, suggesting that agricultural sources are main drivers for nitrogen fluxes in the studied site.

Dissolved Inorganic and Organic Nitrogen (DIN and DON)

In the sampling campaign, NO_3^- fluxes ranged from 0.011 (August) to 0.831 $kg.ha^{-1}.month^{-1}$ (January), while NH_4^+ deposition varied from 0.003 $kg.ha^{-1}.month^{-1}$ in May to 0.343 $kg.ha^{-1}.month^{-1}$ in March. The combined deposition flux of DIN (NO_3^- + NH_4^+) ranged between 0.016 (August) and 1.074 $kg.ha^{-1}.month^{-1}$ (March), with NO_3^- contributing more than 56% of DIN throughout the study period. Regarding organic nitrogen, DON deposition fluxes ranged from 0.203 to 2.103 $kg.ha^{-1}.month^{-1}$ in June and December, respectively. In this sense, DON was the predominant nitrogen species throughout the sampling campaign, with a monthly contribution relative to TDN ranging from 50% to 98%. In addition, same as that of TDN, the monthly deposition fluxes of inorganic and organic nitrogen species were controlled by the precipitation, since NO_3^-, NH_4^+ and DON presented strong and significant correlations (p-value <0.05)

with rainfall (r = 0.68, r = 0.79 and 0.87, respectively).

In order to characterize the seasonal variability, monthly deposition fluxes of NO_3^-, NH_4^+ and DON were combined according to seasons: the wet season (October – March) and the dry season (April – September). Nitrogen deposition fluxes in the wet season reached values of 3.38, 1.23 and 8.11 $kg.ha^{-1}$ for NO_3^-, NH_4^+ and DON respectively, which were 5.15, 6.74 and 2.56 times higher than deposition fluxes of these species in the dry season, revealing a significant distinct seasonal pattern (ANOVA test; p-value < 0.05). It is important to note that the highest deposition fluxes for both inorganic and organic nitrogen species occurred in the months that concentrate the fertilizers application period in coffee crop plantations (October - March) (Freitas, 2017), suggesting that agricultural emissions induce strong seasonal variations in the deposition fluxes, driven largely by the seasonality of agricultural operations.

Based on the monthly deposition flux data, we found a strong positive correlation between NH_4^+ and NO_3^- (ρ = 0.78; p < 0.05), indicating likely sources, mainly agricultural production, suggesting NH_4NO_3 formation. Among the inorganic species, NH_4^+ had a higher rate of increase when comparing the dry and wet seasons (574%), also a higher correlation with rainfall (r = 0.79) than NO_3^- (r = 0.68). This behavior emphasizes the influence of fertilizer application and rainfall on NH_4^+ deposition and reveals a slight presence of non-agricultural factors in NO_3^- deposition, likely fossil fuel combustion sources.

It should be noted that DON is constitutive of a variety of organic compounds, of which many originate from diverse natural and anthropogenic sources (Cape et al., 2011). In this sense, previous studies carried out in agricultural regions indicated that DON in the atmosphere may be related with the application of urea and organic fertilizers as livestock manure (Ham and Tamiya, 2006; Zhang et al., 2012). Figure 2B shows DON inputs with the lowest rate of increase across both seasons (156 %), and the highest correlation with rainfall (r = 0.87), suggesting that DON is more influenced by rainfall and other mixed sources, such as litterfall and biomass burning. Moreover, the moderate correlations between DON and NH_4^+ (ρ = 0.67; p <

0.05) and between DON and NO_3^- (ρ = 0.55; $p < 0.10$) suggest that DON also may be partially derived from other sources, such as soil dust, biological emissions, biomass burning and industrial emissions. Although the Southern Minas Gerais region could not be described as an industrialized area, Pereira et al. (2021) showed that cement manufacturing and forest fires influenced atmospheric deposition chemistry in the region.

NO_3^-/NH_4^+ ratio & pH

Several studies have been using the NO_3^-/NH_4^+ ratio as a reliable proxy for assessing the relative contributions of oxidized and reduced nitrogen species in the atmospheric deposition (Hunová et al., 2017; Xing et al., 2017; Zheng et al., 2020). In our study, the monthly mean values of NO_3^-/NH_4^+ ratios varied between 1.36 in April and 33.7 in May, with an annual average of 8.25 (Fig.3). This pattern reveals monthly NO_3^-/NH_4^+ ratios > 1 for the entire study period, thereby indicating that oxidized nitrogen played a more important role for the nitrogen deposition flux. It is noteworthy that pH values were lower in May (pH = 5.75) than April (pH = 6.03), which was expected, since NO_3^- is well recognized as an acidity proxy, whereas NH_4^+ is associated with NH_3 gas (Seinfeld and Pandis, 1998). In addition, despite NO_3^-/NH_4^+ ratios > 1, none of the samples presented pH values below the limit of 5.60, a critical value for determining acid rain samples. Thus, all samples were alkaline with an average pH of 5.99 (5.73 – 6.19).

Aiming to identify seasonal patterns, we calculated an average NO_3^-/NH_4^+ ratio of 12.8 and 4.48 in the dry and wet period, respectively. In general, NH_4^+ can be directly attributed to ammonia (NH_3) emissions, mainly due to agricultural activities, such as fertilizer application and livestock production (Zheng et al., 2020), and to a lesser extent due to the combustion of fossil fuels (Liu et al., 2016). Regarding the driving factors of NO_3^-, although it is linked to high NO_x emissions mainly from vehicle exhaust systems in large urban centers (Cui et al., 2014; Wu et al., 2018), recent findings identified soil emissions as a significant origin of high emissions of NO_x in agricultural regions (Almaraz et al., 2018; Molina-Herrera et al., 2017). In this sense, the decrease of the NO_3^-/NH_4^+ ratio in the wet season implies an increase of NH_3 emission in the wet season. In another perspective, the NO_3^-/NH_4^+ ratio closer to

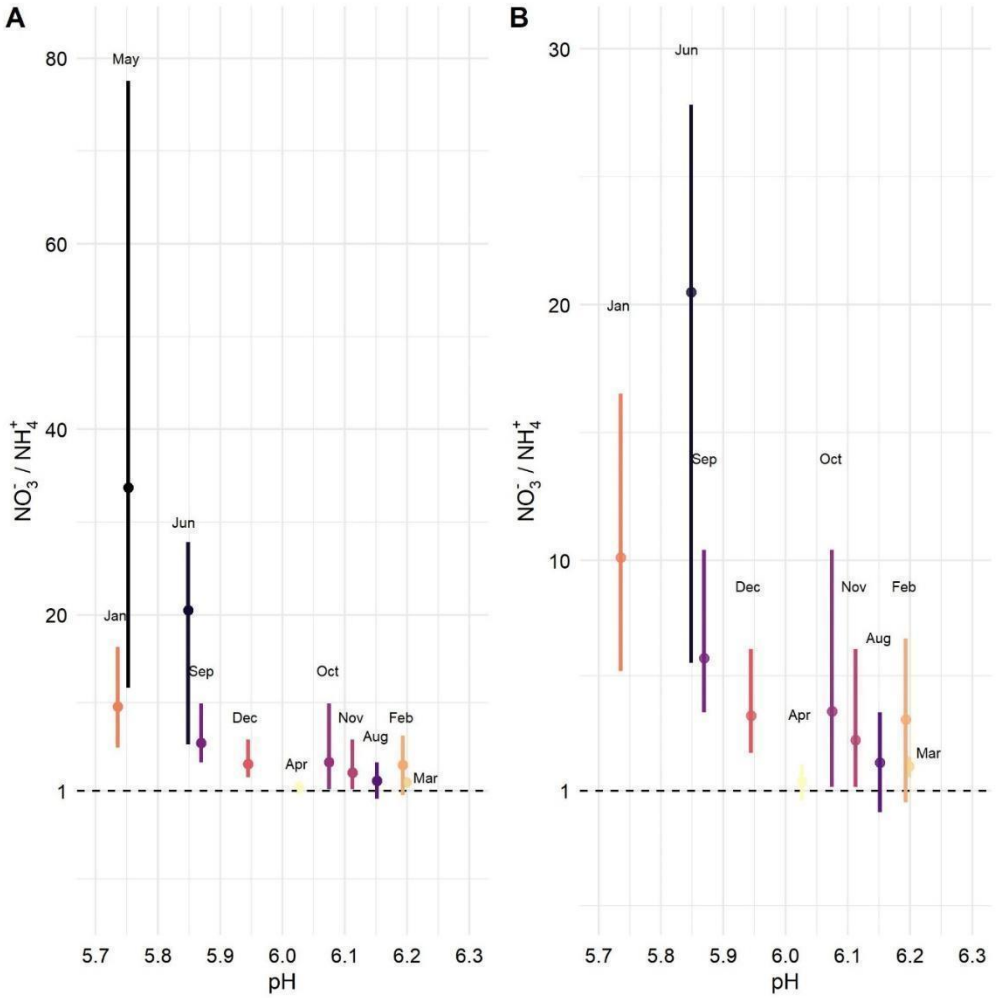

Fig 3. Inorganic ratio between NO_3^- and NH_4^+ as function of pH values from: (A) March 2018 until April 2019; (B) same period, excluding May 2018. The ratio equals unity is depicted as a dashed line.

the unit also shows the importance of NO_x emissions from the fertilized soil. This behavior suggests a strong seasonality of agricultural activities in the studied region, due to nitrogen fertilizers application.

Moreover, fertilization coupled with heavy rain and high temperature promote strong volatility of NH_3 and NO_x, which could lead to volatilization rates of 8% and 11%, respectively (Calvo-Fernández et al., 2017; Freitas, 2017; Kurvits and Matta, 1998). By contrast, the higher NO_3^-/NH_4^+ ratio in the dry season reflects the NO_x emissions from anthropogenic sources, as well as the lower temperatures and higher relative humidity contributes to higher formation of nitrate due to gas-particles reactions (Dong et al., 2020). It is valuable to note that NO_3^-/NH_4^+ ratios displayed

statistically non-significant differences between the dry and wet seasons, which may be associated with high ratio values in January (10.1) and low values in August (2.10). This non-seasonal behavior of nitrogen species could be associated with the negative rainfall anomaly in January (-129 mm) and positive in August (+53 mm).

Worldwide deposition comparisons

On an annual basis, NO_3^- and NH_4^+ deposition fluxes were 4.04 and 1.41 $kg.ha^{-1}.year^{-1}$, accounting for 24% and 8% of the TDN, respectively. The NO_3^- deposition flux was similar to reported by Souza et al. (2015) in a coastal urban area in Brazil and 2.6 fold lower than reported in urban and agricultural areas in China (Cui et al., 2014; Deng et al., 2018), Table 1. Same as NO_3^-, the NH_4^+ deposition flux was lower than reported in agricultural and urban areas in China (Cui et al., 2014; Deng et al., 2018). In addition, it agrees with Ounissi et al. (2021), Cao et al. (2019) and by Izquieta-Rojano et al. (2016) in Algeria coastal, Japanese forest and Iberian Peninsula urban areas, respectively.

Regarding DON, the annual deposition flux was of 11.3 $kg.ha^{-1}.year^{-1}$, which is similar to areas with agricultural background in the Iberian Peninsula and China (Cui et al., 2014; Deng et al., 2018; Izquieta-Rojano et al., 2016), as well as urban areas in Brazil and China (de Souza et al., 2015; Deng et al., 2018). Moreover, DON deposition flux was about 5 fold higher than reported by Schroth et al. (2001) in forest areas. DON represented the major fraction of the TDN (68%), similar to Cao et al. (2019) in a forest area in Japan. Such high relative contributions also were reported in Chinese inland regions (Liu et al., 2016; Wu et al., 2018) and are reasonable due to fertilizer application in croplands.

In general, NH_4^+ showed the lowest values when comparing with all locations, whereas NO_3^- levels in the studied region were similar to urban zones and DON has values comparable to urban and agricultural areas. In addition, when comparing all agricultural background locations (Table 1), one can assume that nitrogen deposition in this study is within the levels estimated by other studies, thereby indicating that agricultural regions, especially Lavras, are hotspots of nitrogen deposition.

Table 1. Worldwide comparison of nitrogen species in atmospheric deposition in $kgha^{-1}yr^{-1}$.

Reference	TDN	DON	NO_3^-	NH_4^+	Localization	Background	Period
This study	16.7	11.3	4.04	1.41	Lavras, Minas Gerais - Brazil	Agricultural	May 2018 to Apr 2019
Schroth et al. (2001)	5.5	2.3	1.4	1.8	Central Amazonia - Brazil	Forest/Agricultural	Apr 1996 to Mar 1997
Souza et al. (2015)	12.1	4.0	5.0	3.1	Rio de Janeiro, Brazil	Forest	Aug 2008 to Aug 2009
	17.2	9.9	3.9	3.4		Coastal urban area	
Tu et al. (2013)	114	26.9	24.9	61.9	Liujiang, Sichuan, China	Forest	Jan to Dec 2009
Izquieta-Rojano et al. (2016)	7.96	3.17	2.9	1.89	Iberian Peninsula	Urban	Jun to May (2012-2013)
	9.23	3.11	3.54	2.58		Background plot	
	22	12.27	3.18	6.55		Agricultural	
	2.84	1.08	1.08	0.68		Urban	
Parron et al. (2011)	12.6	3.8	1.4	7.4	Brasília in the Federal District, Brazil	Forest	Apr 18, 2011 to May 28, 2002
Decina et al. (2018)	8.88	3.65	1.22	4.01	Boston, Massachusetts, USA.	Urban	May to Oct 2015
Cao et al. (2019)	11.09	7.9	1.53	1.66	Mt. Norikura, central Japan	Forest	May 2015 to Apr 2018
Deng et al. (2018)	37.1	10.8	10.4	16	Sichuan Agriculture University Far, China	Urban	Jan 2015 to Dec 2016
	36.6	9.14	8.71	18.8		Intensive agricultural area	
	27.9	7.52	7.04	13.3		Agricultural	
Ounissi et al. (2021)	2.30-3.36	0.48-0.89	0.94-1.32	0.65-1.36	Annaba, Algeria	Coastal	2012 to 2017
Cui et al. (2014)	30.5-37.4	5.71-10.6	7.42-10.4	16.3-17.3	Southeastern China	Agricultural	Jan 2011 to Dec 2012

Ecological Effects of Wet Nitrogen Deposition

Due to TDN values observed in our study, we suggest that nitrogen supply via wet deposition should be considered when calculating optimum nitrogen fertilizer application rates, since the study region has a rural background, mostly

agricultural. Moreover, nitrogen species deposition by wet deposition provided 16.73 $kgha^{-1}yr^{-1}$, which is about 15% of the annual nitrogen fertilizer application in the region, suggesting a major input of nitrogen species, specifically in the wet season.

Regarding N-DIN species, the annual value observed (2.011 $kgNha^{-1}yr^{-1}$) via wet deposition was lower than the empirical critical nitrogen load proposed by Pardo et al. (2011) for tropical and subtropical humid forests (5–10 $kgNha^{-1}yr^{-1}$). However, such value does not account for N-DON nitrogen inputs that would surpass such critical range. The excesses of nitrogen deposition over critical loads could lead to environmental impacts in the region, such as soil acidification, which has implications for the chemical availability of metals and other nutrients, influencing plants nutritional status (Stevens et al., 2018).

Excess nitrogen may also cause damage in freshwater aquatic ecosystems (Chen et al., 2018; Clark et al., 2018). Baron et al. (2011) estimated an acidification critical load of 8.0 $kgNha^{-1}yr^{-1}$ and an even lower nutrient enrichment critical load, ranging from 3.5 to 6.0 $kgNha^{-1}yr^{-1}$, for lakes of the northeastern United States. Thus, our results showed that nitrogen atmospheric deposition of N-DIN (2.011 $kgNha^{-1}yr^{-1}$) has the potential to increase acidification and eutrophication in water bodies in the studied region by atmospheric input by 25% and 33%, respectively.

CONCLUSION

We assessed the wet atmospheric deposition fluxes of TDN, DON and DIN (NO_3^- + NH_4^+) for one year (March 2018 - April 2019), as well the factors controlling its seasonal variations in the Southern Minas Gerais region, Brazil, an area with agricultural background. TDN annual flux was 16.73 $kg.ha^{-1}.yr^{-1}$, with a dominant contribution of DON (68%), followed by NO_3^- (24%) and NH_4^+ (8%). These results showed that TDN deposition should be included in the calculation of optimum nitrogen fertilizer application rates, since they provided 15% of the annual nitrogen fertilizer application in Lavras. Moreover, the N-DIN fluxes (2.011 $kgNha^{-1}yr^{-1}$) presented potential to increase acidification and eutrophication in Lavras water bodies by about 30%. Because such value does not account for N-DON fluxes, the TDN inputs would increase even more the nitrogen pollution in the environment.

We observed considerable seasonal variations (ANOVA test; p-value<0.05), since that all nitrogen species presented higher fluxes in wet season (NO_3^- = 3.38, NH_4^+ = 1.23 and DON = 8.11 $kg.ha^{-1}$), induced by rainfall and agricultural emissions. In another hand, moderate correlations between DON and NH_4^+ and between DON and NO_3^- (**ρ** = 0.67, **ρ** = 0.55, respectively) indicated that DON was partially derived from other sources, such as soil dust, biomass burning and industrial emissions. We also found high NO_3^-/NH_4^+ ratio (average = 8.25), with lower values in the wet season (NO_3^-/NH_4^+ = 4.48) and higher values in dry season (NO_3^-/NH_4^+ = 12.8). This behavior revealed a higher relative contribution of NO_x emissions from traffic sources in the dry season and corroborated with the increase of NH_3 emissions from agricultural sources during wet season. Therefore, our study sheds light on the importance of agricultural activity as a driver of nitrogen wet deposition coupled with its potential to change biogeochemical cycles.

ACKNOWLEDGMENTS

The authors thank to Conselho Nacional de Desenvolvimento Científico e Tecnológico (CNPq), Coordenação de Aperfeiçoamento de Pessoal de Nível Superior (CAPES), Fundação de Amparo à Pesquisa do Estado de Minas Gerais (FAPEMIG) for the Graduate and Undergraduate Scholarships. Special thanks go to "Laboratório de Análise de Água da Universidade 18 Federal de Lavras (LAADEG-UFLA)" and "Laboratório de Processos Atmosféricos da Universidade de São Paulo (LAPAt-IAG-USP)" for the facilities and equipments used in this study.

REFERENCES

ABNT, 1997. Água - Determinação de nitrogênio orgânico, Kjeldahl e total - Métodos macro e semimicro Kjeldahl.

Almaraz, M., Bai, E., Wang, C., Trousdell, J., Conley, S., Faloona, I., Houlton, B.Z., 2018. Erratum: Agriculture is a major source of NOx pollution in California. Sci. Adv. 4, 1–9. https://doi.org/10.1126/SCIADV.AAU2561

Almeida, G.L.M.D., Ferreira, E.C. da M., Mendes, D.J. da S., Gomes, B.A.B., Souza, F. do N., Silva, J. do N., Dos Santos, S.A., Teixeira, P.B., 2017. Estudo sobre as regiões de planejamento de Minas Gerais: Sul de Minas Gerais. Belo Horizonte.

APHA/AWWA/WEF, 2014. Standard Methods for the Examination of Water and Wastewater, 22nd ed. American Public Health Association, Washington, D.C.

Araujo, T.G., Souza, M.F.L., De Mello, W.Z., Da Silva, D.M.L., 2015. Bulk Atmospheric Deposition of Major Ions and Dissolved Organic Nitrogen in the Lower Course of a Tropical River Basin,

Southern Bahia, Brazil. J. Braz. Chem. Soc. 26, 1692–1701. https://doi.org/10.5935/0103-5053.20150143

Baron, J.S., Driscoll, C.T., Stoddard, J.L., Richer, E.E., 2011. Empirical critical loads of atmospheric nitrogen deposition for nutrient enrichment and acidification of sensitive US lakes. Bioscience 61, 602–613. https://doi.org/10.1525/bio.2011.61.8.6

Bhattarai, H., Tripathee, L., Kang, S., Sharma, C.M., Chen, P., Guo, J., Ghimire, P.S., 2021. Concentration, sources and wet deposition of dissolved nitrogen and organic carbon in the Northern Indo-Gangetic Plain during monsoon. J. Environ. Sci. 102, 37–52. https://doi.org/10.1016/j.jes.2020.09.011

Bobbink, R., Hicks, K., Galloway, J., Spranger, T., Alkemade, R., Ashmore, M., Cinderby, S., Davidson, E., Dentener, F., Emmett, B., Erisman, J., Fenn, M., Nordin, A., Pardo, L., Vries, W. De, Bobbink, R., Hicks, K., Galloway, J., Spranger, T., Alkemade, R., Ashmore, M., Bustamante, M., 2010. Global assessment of nitrogen deposition effects on terrestrial plant diversity : a synthesis. Ecol. Appl. 20, 30–59.

Calvo-Fernández, J., Marcos, E., Calvo, L., 2017. Bulk deposition of atmospheric inorganic nitrogen in mountainous heathland ecosystems in North-Western Spain. Atmos. Res. 183, 237–244. https://doi.org/10.1016/j.atmosres.2016.09.006

Cao, R., Chen, S., Yoshitake, S., Ohtsuka, T., 2019. Nitrogen deposition and responses of forest structure to nitrogen deposition in a cool-temperate deciduous forest. Forests 10, 631. https://doi.org/10.3390/f10080631

Cape, J.N., Cornell, S.E., Jickells, T.D., Nemitz, E., 2011. Organic nitrogen in the atmosphere - Where does it come from? A review of sources and methods. Atmos. Res. 102, 30–48. https://doi.org/10.1016/j.atmosres.2011.07.009

Chen, X., Wang, Y.H., Ye, C., Zhou, W., Cai, Z.C., Yang, H., Han, X., 2018. Atmospheric Nitrogen Deposition Associated with the Eutrophication of Taihu Lake. J. Chem. 2018, 10. https://doi.org/10.1155/2018/4017107

Clark, C.M., Phelan, J., Doraiswamy, P., Buckley, J., Cajka, J.C., Dennis, R.L., Lynch, J., Nolte, C.G., Spero, T.L., 2018. Atmospheric deposition and exceedances of critical loads from 1800−2025 for the conterminous United States. Ecol. Appl. 28, 978–1002. https://doi.org/10.1002/eap.1703

Cui, J., Zhou, J., Peng, Y., He, Y., Yang, H., Mao, J., Zhang, M., Wang, Y., Wang, S., 2014. Atmospheric wet deposition of nitrogen and sulfur in the agroecosystem in developing and developed areas of Southeastern China. Atmos. Environ. 89, 102–108. https://doi.org/10.1016/j.atmosenv.2014.02.007

de Souza, P.A., Ponette-González, A.G., de Mello, W.Z., Weathers, K.C., Santos, I.A., 2015. Atmospheric organic and inorganic nitrogen inputs to coastal urban and montane Atlantic Forest sites in southeastern Brazil. Atmos. Res. 160, 126–137. https://doi.org/10.1016/j.atmosres.2015.03.011

Decina, S.M., Templer, P.H., Hutyra, L.R., 2018. Atmospheric Inputs of Nitrogen, Carbon, and Phosphorus across an Urban Area: Unaccounted Fluxes and Canopy Influences. Earth's Futur. 6, 134–148. https://doi.org/10.1002/2017EF000653

DENATRAN, 2018. Frota de Veículos - 2018 [WWW Document]. Ministério da Infraestrutura. URL https://www.gov.br/infraestrutura/pt-br/assuntos/transito/conteudo-denatran/frota-de-veiculos-2018 (accessed 6.1.19).

Deng, O., Zhang, S., Deng, L., Zhang, C., Fei, J., 2018. Wet nitrogen deposition across the urban-intensive agricultural–rural transect of a small urban area in southwest China. Environ. Sci. Pollut. Res. 25, 7866–7874.

https://doi.org/10.1007/s11356-017-1082-z

Dentener, F., Drevet, J., Lamarque, J.F., Bey, I., Eickhout, B., Fiore, A.M., Hauglustaine, D., Horowitz, L.W., Krol, M., Kulshrestha, U.C., Lawrence, M., Galy-Lacaux, C., Rast, S., Shindell, D., Stevenson, D., Van Noije, T., Atherton, C., Bell, N., Bergman, D., Butler, T., Cofala, J., Collins, B., Doherty, R., Ellingsen, K., Galloway, J., Gauss, M., Montanaro, V., Müller, J.F., Pitari, G., Rodriguez, J., Sanderson, M., Solmon, F., Strahan, S., Schultz, M., Sudo, K., Szopa, S., Wild, O., 2006. Nitrogen and sulfur deposition on regional and global scales: A multimodel evaluation. Global Biogeochem. Cycles 20. https://doi.org/10.1029/2005GB002672

Dong, X., Guo, Q., Han, X., Wei, R., Tao, Z., 2020. The isotopic patterns and source apportionment of nitrate and ammonium in atmospheric aerosol. J. Geophys. Res. Atmos. 1–24. https://doi.org/https://doi.org/10.1002/essoar.10504598.1

Filoso, S., Martinelli, L.A., Williams, M.R., Lara, L.B., Krusche, A., Ballester, M.V., Victoria, R., De Camargo, P.B., 2003. Land use and nitrogen export in the Piracicaba River basin, Southeast Brazil. Biogeochemistry 65, 275–294. https://doi.org/10.1023/A:1026259929269

Freitas, T., 2017. Fertilizantes Nitrogenados Convencionais, Estabilizados, de Libertação Lenta ou Controlada na Cultura do Cafeeiro: Eficiência e Custos. Universidade Federal de Lavras.

Galloway, J.N., Dentener, F.J., Capone, D.G., Boyer, E.W., Howarth, R.W., Seitzinger, S.P., Asner, G.P., Cleveland, C.C., Green, P.A., Holland, E.A., Karl, D.M., Michaels, A.F., Porter, J.H., Townsend, A.R., Vorosmarty, C.J., 2004. Nitrogen cycles: past, present, and future. Biogeochemistry 70, 153–226. https://doi.org/10.1007/s10533-004-0370-0

González Benítez, J.M., Cape, J.N., Heal, M.R., van Dijk, N., Díez, A.V., 2009. Atmospheric nitrogen deposition in south-east Scotland: Quantification of the organic nitrogen fraction in wet, dry and bulk deposition. Atmos. Environ. 43, 4087–4094. https://doi.org/10.1016/j.atmosenv.2009.04.061

Ham, Y.S., Tamiya, S., 2006. Contribution of dissolved organic nitrogen deposition to total dissolved nitrogen deposition under intensive agricultural activities. Water. Air. Soil Pollut. 178, 5–13. https://doi.org/10.1007/s11270-006-9109-y

Hofhansl, F., Wanek, W., Drage, S., Huber, W., Weissenhofer, A., Richter, A., 2011. Topography strongly affects atmospheric deposition and canopy exchange processes in different types of wet lowland rainforest, Southwest Costa Rica. Biogeochemistry 106, 371–396. https://doi.org/10.1007/s10533-010-9517-3

Hunová, I., Kurfürst, P., Stráník, V., Modlík, M., 2017. Nitrogen deposition to forest ecosystems with focus on its different forms. Sci. Total Environ. 575, 791–798. https://doi.org/10.1016/j.scitotenv.2016.09.140

IBGE, 2021. Pesquisa Industrial Mensal [WWW Document]. SIDRA Banco de Tabelas Estatísticas. URL https://sidra.ibge.gov.br/home/pimpfrg/minas-gerais (accessed 6.30.21).

IBGE, 2019. Produção Agrícola Municipal [WWW Document]. URL https://sidra.ibge.gov.br/Tabela/5457 (accessed 6.3.21).

IBGE, 2018. Cidades e Estados: Lavras [WWW Document]. URL https://cidades.ibge.gov.br/brasil/mg/lavras (accessed 6.1.19).

IBGE, 2014. Aplicação de Fertilizantes Nitrogenados por Unidades da Federação [WWW Document].

INMET, 2019a. Normais Climatológicas do Brasil [WWW Document]. Ministério da Agric. Pecuária e Abast. URL https://portal.inmet.gov.br/normais (accessed 9.15.19).

INMET, 2019b. Banco de Dados

Meteorológicos para Ensino e Pesquisa [WWW Document]. Ministério da Agric. Pecuária e Abast. URL https://bdmep.inmet.gov.br/ (accessed 5.2.20).

Izquieta-Rojano, S., García-Gomez, H., Aguillaume, L., Santamaría, J.M., Tang, Y.S., Santamaría, C., Valiño, F., Lasheras, E., Alonso, R., Àvila, A., Cape, J.N., Elustondo, D., 2016. Throughfall and bulk deposition of dissolved organic nitrogen to holm oak forests in the Iberian Peninsula: Flux estimation and identification of potential sources. Environ. Pollut. 210, 104–112. https://doi.org/10.1016/j.envpol.2015.12.002

Jaffe, D.A., Weiss-Penzias, P.S., 2003. Biogeochemical Cycles / Nitrogen Cycle, in: Holton, J.R. (Ed.), Encyclopedia of Atmospheric Sciences. Academic Press, Bothell, WA, USA, pp. 205–213. https://doi.org/10.1016/b0-12-227090-8/00016-6

Junqueira Junior, J.A., de Mello, C.R., de Mello, J.M., Scolforo, H.F., Beskow, S., McCarter, J., 2019. Rainfall partitioning measurement and rainfall interception modelling in a tropical semi-deciduous Atlantic forest remnant. Agric. For. Meteorol. 275, 170–183. https://doi.org/10.1016/j.agrformet.2019.05.016

Kurvits, T., Matta, T., 1998. Agricultural NH_3 and NO_x emissions in Canada. Environ. Pollut. 102, 187–194. https://doi.org/10.1016/S0269-7491(98)80032-8

Liu, L., Zhang, X., Wang, S., Lu, X., Ouyang, X., 2016. A review of spatial variation of inorganic nitrogen (N) wet deposition in China. PLoS One 11, 1–17. https://doi.org/10.1371/journal.pone.0146051

Liu, Q., Liu, Y., Zhao, Q., Zhang, T., Schauer, J.J., 2021. Increases in the formation of water soluble organic nitrogen during Asian dust storm episodes. Atmos. Res. 253, 105486. https://doi.org/10.1016/j.atmosres.2021.105486

Liu, X., Zhang, Y., Han, W., Tang, A., Shen, J., Cui, Z., Vitousek, P., Erisman, J.W., Goulding, K., Christie, P., Fangmeier, A., Zhang, F., 2013. Enhanced nitrogen deposition over China. Nature 494, 459–462. https://doi.org/10.1038/nature11917

Matsumoto, K., Ogawa, T., Ishikawa, M., Hirai, A., Watanabe, Y., Nakano, T., 2020. Organic and inorganic nitrogen deposition on the red pine forests at the northern foot of Mt. Fuji, Japan. Atmos. Environ. 237, 117676. https://doi.org/10.1016/j.atmosenv.2020.117676

Molina-Herrera, S., Haas, E., Grote, R., Kiese, R., Klatt, S., Kraus, D., Butterbach-Bahl, K., Kampffmeyer, T., Friedrich, R., Andreae, H., Loubet, B., Ammann, C., Horváth, L., Larsen, K., Gruening, C., Frumau, A., Butterbach-Bahl, K., 2017. Importance of soil NO emissions for the total atmospheric NOxbudget of Saxony, Germany. Atmos. Environ. 152, 61–76. https://doi.org/10.1016/j.atmosenv.2016.12.022

Oladosu, N.O., Abayomi, A.A., Olayinka, K.O., Alo, B.I., 2017. Wet nitrogen and phosphorus deposition in the eutrophication of the Lagos Lagoon , Nigeria. Environ. Sci. Pollut. Res. 24, 8645–8657. https://doi.org/10.1007/s11356-017-8479-6

Ounissi, M., Laskri, H., Ziouch, O.R., Justić, D., 2021. Riverine and wet atmospheric nutrient inputs to the Southwestern Mediterranean region of North Africa. Mar. Chem. 228, 103915. https://doi.org/10.1016/j.marchem.2020.103915

Pardo, L.H., Fenn, M.E., Goodale, C.L., Geiser, L.H., Driscoll, C.T., Allen, E.B., Baron, J.S., Bobbink, R., Bowman, W.D., Clark, C.M., Emmett, B., Gilliam, F.S., Greaver, T.L., Hall, S.J., Lilleskov, E.A., Liu, L., Lynch, J.A., Nadelhoffer, K.J., Perakis, S.S., Robin-Abbott, M.J., Stoddard, J.L., Weathers, K.C., Dennis, R.L., 2011. Effects of nitrogen deposition and empirical nitrogen critical

loads for ecoregions of the United States. Ecol. Appl. 21, 3049–3082. https://doi.org/10.1890/10-2341.1

Parron, L.M., Bustamante, M.M.C., Markewitz, D., 2011. Fluxes of nitrogen and phosphorus in a gallery forest in the Cerrado of central Brazil. Biogeochemistry 105, 89–104. https://doi.org/10.1007/s10533-010-9537-z

Pereira, J.N., Fornaro, A., Vieira-Filho, M., 2021. Atmospheric Deposition Chemistry in a Brazilian Rural Area: Alkaline Species Behavior and Agricultural Inputs. Environ. Sci. Pollut. Res. 28, 23448–23458. https://doi.org/https://doi.org/10.1007/s11356-020-12317-3

Qiao, X., Du, J., Kota, S.H., Ying, Q., Xiao, W., Tang, Y., 2018. Wet deposition of sulfur and nitrogen in Jiuzhaigou National Nature Reserve, Sichuan, China during 2015–2016: Possible effects from regional emission reduction and local tourist activities. Environ. Pollut. 233, 267–277. https://doi.org/10.1016/j.envpol.2017.08.041

R Core Team, 2019. R: A Language and Environment for Statistical Computing.

Rasse, R., Pérez, T., Giuliante, A., Donoso, L., 2018. Total dissolved atmospheric nitrogen deposition in the anoxic Cariaco basin. Atmos. Environ. 179, 118–131. https://doi.org/10.1016/j.atmosenv.2018.02.007

Romero Orué, M., Gaiero, D., Kirschbaum, A., 2019. Seasonal characteristics of the chemical composition of rainwaters from Salta city, NW Argentina. Environ. Earth Sci. 78. https://doi.org/10.1007/s12665-018-8007-0

Schroth, G., Elias, M.E.A., Uguen, K., Seixas, R., Zech, W., 2001. Nutrient fluxes in rainfall, throughfall and stemflow in tree-based land use systems and spontaneous tree vegetation of central Amazonia. Agric. Ecosyst. Environ. 87, 37–49. https://doi.org/10.1016/S0167-8809(00)00294-2

Seinfeld, J.H., Pandis, S.N., 1998. Atmospheric Chemistry and Physics: From Air Pollution to Climate Change, 2nd ed, Physics Today. John Wiley & Sons, Inc., Hoboken, New Jersey. https://doi.org/10.1063/1.882420

Shapiro, A.S.S., Wilk, M.B., 1965. An Analysis of Variance Test for Normality (Complete Samples). Biometrika 52, 591–611.

Song, L., Kuang, F., Skiba, U., Zhu, B., Liu, X., Levy, P., Dore, A., Fowler, D., 2017. Bulk deposition of organic and inorganic nitrogen in southwest China from 2008 to 2013. Environ. Pollut. 227, 157–166. https://doi.org/10.1016/j.envpol.2017.04.031

Souza, M. de A., Pacheco, F.S., Palandi, J.A. de L., Forti, M.C., Campos, M.L.A.M., Ometto, J.P.H.B., Reis, D.C.O., de Carvalho Junior, J.A., 2020. Atmospheric concentrations and dry deposition of reactive nitrogen in the state of São Paulo, Brazil. Atmos. Environ. 230, 117502. https://doi.org/10.1016/j.atmosenv.2020.117502

Stevens, C.J., David, T.I., Storkey, J., 2018. Atmospheric nitrogen deposition in terrestrial ecosystems: Its impact on plant communities and consequences across trophic levels. Funct. Ecol. 32, 1757–1769. https://doi.org/10.1111/1365-2435.13063

Tu, L. hua, Hu, T. xing, Zhang, J., Huang, L. hua, Xiao, Y. long, Chen, G., Hu, H. ling, Liu, L., Zheng, J. kun, Xu, Z. feng, Chen, L. hua, 2013. Nitrogen Distribution and Cycling through Water Flows in a Subtropical Bamboo Forest under High Level of Atmospheric Deposition. PLoS One 8, 2–12. https://doi.org/10.1371/journal.pone.0075862

Vet, R., Artz, R.S., Carou, S., Shaw, M., Ro, C.U., Aas, W., Baker, A., Bowersox, V.C., Dentener, F., Galy-Lacaux, C., Hou, A., Pienaar, J.J., Gillett, R., Forti, M.C., Gromov, S., Hara, H., Khodzher, T., Mahowald, N.M., Nickovic, S., Rao, P.S.P., Reid, N.W., 2014. A global

assessment of precipitation chemistry and deposition of sulfur, nitrogen, sea salt, base cations, organic acids, acidity and pH, and phosphorus. Atmos. Environ. 93, 3–100. https://doi.org/10.1016/j.atmosenv.2013.10.060

Vieira-Filho, M.S., Ito, D.T., Pedrotti, J.J., Coelho, L.H.G., Fornaro, A., 2016. Gas-phase ammonia and water-soluble ions in particulate matter analysis in an urban vehicular tunnel. Environ. Sci. Pollut. Res. 23, 19876–19886. https://doi.org/10.1007/s11356-016-7177-0

Violaki, K., Zarbas, P., Mihalopoulos, N., 2010. Long-term measurements of dissolved organic nitrogen (DON) in atmospheric deposition in the Eastern Mediterranean: Fluxes, origin and biogeochemical implications. Mar. Chem. 120, 179–186. https://doi.org/10.1016/j.marchem.2009.08.004

Wang, H., Shi, G., Tian, M., Chen, Y., Qiao, B., Zhang, Liuyi, Yang, F., Zhang, Leiming, Luo, Q., 2018. Wet deposition and sources of inorganic nitrogen in the Three Gorges Reservoir Region, China. Environ. Pollut. 233, 520–528. https://doi.org/10.1016/j.envpol.2017.10.085

Wang, X., Wu, Z., Shao, M., Fang, Y., Zhang, L., Chen, F., Chan, P.W., Fan, Q., Wang, Q., Zhu, S., Bao, R., 2013. Atmospheric nitrogen deposition to forest and estuary environments in the Pearl River Delta region, southern China. Tellus, Ser. B Chem. Phys. Meteorol. 65, 1–13. https://doi.org/10.3402/tellusb.v65i0.20480

Wickham, H., 2016. ggplot2: Elegant Graphics for Data Analysis. https://doi.org/978-3-319-24277-4

WMO, 2004. Manual for the Gaw Precipitation Chemistry Programme: Guidelines, Data Quality Objectives and Standard Operating Procedures.

Wu, Y., Zhang, J., Liu, S., Jiang, Z., Arbi, I., Huang, X., Macreadie, P.I., 2018. Nitrogen deposition in precipitation to a monsoon-affected eutrophic embayment: Fluxes, sources, and processes. Atmos. Environ. 182, 75–86. https://doi.org/10.1016/j.atmosenv.2018.03.037

Xing, J., Song, J., Yuan, H., Li, X., Li, N., Duan, L., Kang, X., Wang, Q., 2017. Fluxes, seasonal patterns and sources of various nutrient species (nitrogen, phosphorus and silicon) in atmospheric wet deposition and their ecological effects on Jiaozhou Bay, North China. Sci. Total Environ. 576, 617–627. https://doi.org/10.1016/j.scitotenv.2016.10.134

Xing, J., Song, J., Yuan, H., Wang, Q., Li, X., Li, N., Duan, L., Qu, B., 2018. Water-soluble nitrogen and phosphorus in aerosols and dry deposition in Jiaozhou Bay, North China: Deposition velocities, origins and biogeochemical implications. Atmos. Res. 207, 90–99. https://doi.org/10.1016/j.atmosres.2018.03.001

Xu, W., Wen, Z., Shang, B., Dore, A.J., Tang, A., Xia, X., Zheng, A., Han, M., Zhang, L., Zhao, Y., Zhang, G., Feng, Z., Liu, X., Zhang, F., 2020. Precipitation chemistry and atmospheric nitrogen deposition at a rural site in Beijing, China. Atmos. Environ. 223, 117253. https://doi.org/10.1016/j.atmosenv.2019.117253

Zamora, L.M., Prospero, J.M., Hansell, D.A., 2011. Organic nitrogen in aerosols and precipitation at Barbados and Miami: Implications regarding sources, transport and deposition to the western subtropical North Atlantic. J. Geophys. Res. 116, 1–17. https://doi.org/10.1029/2011JD015660

Zeng, J., Yue, F.J., Li, S.L., Wang, Z.J., Qin, C.Q., Wu, Q.X., Xu, S., 2020. Agriculture driven nitrogen wet deposition in a karst catchment in southwest China. Agric. Ecosyst. Environ. 294, 106883. https://doi.org/10.1016/j.agee.2020.106883

Zhang, Y., Cao, Y., Tang, Y., Ying, Q., Hopke, P.K., Zeng, Y., Xu, X., Xia, Z.,

Qiao, X., 2020. Wet deposition of sulfur and nitrogen at Mt. Emei in the West China Rain Zone, southwestern China: Status, inter-annual changes, and sources. Sci. Total Environ. 713, 136676. https://doi.org/10.1016/j.scitotenv.2020.136676

Zhang, Y., Song, L., Liu, X.J., Li, W.Q., Lü, S.H., Zheng, L.X., Bai, Z.C., Cai, G.Y., Zhang, F.S., 2012. Atmospheric organic nitrogen deposition in China. Atmos. Environ. 46, 195–204. https://doi.org/10.1016/j.atmosenv.2011.09.080

Zhang, Y., Zheng, L., Liu, X., Jickells, T., Neil Cape, J., Goulding, K., Fangmeier, A., Zhang, F., 2008. Evidence for organic N deposition and its anthropogenic sources in China. Atmos. Environ. 42, 1035–1041. https://doi.org/10.1016/j.atmosenv.2007.12.015

Zheng, L., Chen, W., Jia, S., Wu, L., Zhong, B., Liao, W., Chang, M., Wang, W., Wang, X., 2020. Temporal and spatial patterns of nitrogen wet deposition in different weather types in the Pearl River Delta (PRD), China. Sci. Total Environ. 740, 139936. https://doi.org/10.1016/j.scitotenv.2020.139936

TERCEIRA PARTE

1. CONSIDERAÇÕES FINAIS

Esse estudo avaliou química da deposição atmosférica total em Lavras, uma região agrícola no Sul de Minas Gerais. De forma geral, observou-se uma tendência alcalina nas amostras de deposição, uma vez que o pH médio foi em torno de 5,95 e mais de 90% do conjunto de dados apresentou valores de pH maiores que 5,60. Esse padrão foi corroborado pela maior abundância de Ca^{2+} (~37%) entre todos os íons medidos, indicando neutralização da acidez por compostos de $CaCO_3$. Ressalta-se que o modelo EPA PMF 5.0 foi aplicado para avaliação da contribuição de fontes dos compostos presentes na deposição atmosférica, e esse processo de neutralização atmosférica foi identificado como fonte majoritária, correspondendo a 44% do total de fontes. Além disso, o modelo também identificou como fontes processos crustais e incêndios (34%) e produção e aplicação de fertilizantes (17%). Por fim, esse estudo também avaliou os fluxos de deposição atmosférica úmida para espécies de nitrogênio e foi observado um fluxo dominante de espécies de nitrogênio orgânico dissolvido (11,4 $kg.ha^{-1}.ano^{-1}$; 68% do nitrogênio total dissolvido) e o fluxo de nitrogênio inorgânico dissolvido (5,3 $kg.ha^{-1}.ano^{-1}$) apresentou potencial de causar acidificação e eutrofização nos ecossistemas ambientais da região de estudo.

Com base no exposto, a análise sistêmica da deposição atmosférica permitiu monitorar e avaliar os processos de transformação química, identificar as fontes poluidoras e os possíveis impactos ambientais causados. Diante dessa perspectiva, nossos resultados são úteis para entender a ciclagem de nutrientes e poluentes entre os ecossistemas ambientais na Região Sul de Minas Gerais e podem auxiliar no desenvolvimento de estratégias que visem a redução das emissões de poluentes.

2. SUGESTÕES DE TRABALHOS FUTUROS

Como sugestões de trabalhos futuros, insere-se a continuidade da coleta de amostras de deposição atmosférica total para identificar tendências de longo prazo. Além disso, também se destaca a importância da implantação de um sistema de coleta de deposição atmosférica úmida, a fim de se obter as contribuições segregadas da água de chuva e da deposição seca.